Echahid Cheikh Larbi Tebessi University

Tebessa

Faculty of Sciences and Technology

Electrical Engineering Department

PhD THESIS

With a view to obtaining the LMD 3rd cycle doctoral degree

Option: Automatic **Speciality:** Industrial Electrotechnics

LABGET Laboratory

TOWARDS OPTIMAL CONTROL OF A HYBRID SYSTEM WITH STORAGE FOR EFFICIENT MANAGEMENT OF ELECTRICAL ENERGY

Presented by :

SAADI Moufida

Publicly supported on: ../../2024 before the jury composed of:

Jury Member	**Grade**	**Designation**	**University**
Meraoumia Abdallah	Professor	Presedent	University of Tebessa
Dib Djalel	Professor	Supervisor	University of Tebessa
Magheni Billel	Professor	Co-supervisor	University of Annaba
Ghoudelbourk Sihem	Docteur	Examiner	University of Annaba
Aouiche Abdelaziz	Docteur	Examiner	University of Tebessa
Rahmani Lazhar	Professor	Examiner	University of Setif
Boukadoum Aziz	Professor	Examiner	University of Tebessa

Année universitaire 2024-2025

Contents

List of Figures **iv**

List of Tables **vii**

1 Literature Review on multi-source renewable energy systems **8**

1.1 Introduction 8

1.2 Renewable Energy Systems overview 8

1.2.1 Photovoltaic Solar systems 9

1.2.2 The Wind Turbines 9

1.2.3 Energy Storage 12

1.3 hybrid energy systems 15

1.3.1 Configurations of hybrid systems 17

1.4 Some Issues with Hybrid Systems 19

1.4.1 Hybrid Systems with Conventional Energy Source 19

1.4.2 Hybrid Systems without Conventional Source 20

1.5 Energy Management and Control 21

1.5.1 Centralized Control System Configuration 23

1.5.2 Distributed Control system Configuration 23

1.5.3 Hybrid Arrangement of Centralized and Distributed Control 24

1.6 Energy Management Systems (EMS) 25

1.7 Conclusion 27

2 Multi-Source System: Modeling and Optimization **28**

2.1 Introduction 28

2.2 Photovoltaic Sources 29

2.2.1 Components of Photovoltaic Systems 29

2.2.2 Equivalent Electrical Circuits and Mathematical Modeling of PV Devices (Cells, Modules and Arrays) 30

2.2.3 The One-Diode Model with Series and Shunt Resistances 4 and 5 Parameter Model 30

2.2.4 The Dual-Diode Model 33

2.2.5 Characterization of Photovoltaic Systems 34

2.2.6 MPPT Techniques for PV Systems 35

2.3 Global modeling of the variable speed wind system 49

2.4 Description of the wind turbine system 50

2.4.1 Wind Modeling 51

2.4.2 Wind System Modeling 52

2.4.3 MPPT control of variable speed wind turbines 62

2.4.4 Wind turbine operating zones 63

2.5 Battery modeling 65

2.5.1 Thevenin model 66

2.5.2 Thevenin Model Including Hysteresis Effect 67

2.5.3 Dynamic model including the polarization effect 68

2.5.4 2nd Thevenin model including the polarization effect 69

2.5.5 Model including the "EDL" electrical double layer phenomenon . . . 71

2.6 Deferent Types of batteries 73

2.7 Conclusion 74

3 Management and Sizing of Multi-Source Systems **75**

3.1 Introduction 75

3.2 Sizing Methodologies 76
3.2.1 Criteria for Sizing 76
3.2.2 Sizing Methods 77
3.2.3 Simulation Tools for Sizing Multi-Source Renewable Energy Systems 81
3.3 Energy Management Systems (EMS) 81
3.3.1 Key Techniques and Technologies in EMS 82
3.3.2 Management Strategies for Hybrid Renewable Energy Systems 83
3.4 Case Studies and Applications 86
3.4.1 Sizing hybrid system based on Monthly average method 88
3.4.2 Energy Management System Based on ANN Model 92
3.5 Challenges and Future Perspectives 95

4 Results, Analysis, and Discussion **97**
4.1 Introduction 97
4.2 Evaluation of DL-GA Based MPPT Technique 98
4.2.1 Methodology and results 98
4.3 Power Curve Analysis of the Standalone System 104
4.4 Overall System Performance and Efficiency 108
4.5 Conclusion 110

Bibliography **115**

List of Figures

1.1 Variation in global installed PV capacity (MW) between 2010 and 2020. . . 10

1.2 Wind Turbine. 11

1.3 Types of Energy storage system 15

1.4 Hybrid system classification 16

1.5 Basic components of hybrid system 18

1.6 Energy flow management in IRES 22

1.7 Centralized Control System Configuration 23

1.8 Distributed Control system Configuration 24

1.9 Hybrid Arrangement of Centralized and Distributed Control 25

2.1 Layout and Structure of Photovoltaic Components: Single Cell (a), Series String of Cells (b), Module (c), and PV Array (d). 29

2.2 Electrical Circuit Representations for Photovoltaic Cells: (a) Ideal Model; (b) Single Diode with Series Resistance (4-Parameter Model); (c) Single Diode with Both Series and Shunt Resistance (5-Parameter Model); and (d) Dual Diode Model (7-Parameter Model) 31

2.3 I-V Characteristic Curve of a PV Module Highlighting Three Key Points . . 35

2.4 General scheme of a PV with an MPPT system 36

2.5 MPPT General Classification 38

2.6 flowchart of Perturb & Observe (P&O) 39

2.7 flowchart of Incremental Conductance (INC) 41
2.8 Basic structure of MLFFNN 43
2.9 Basic structure of ANFIS 45
2.10 A typical structure of the fuzzy system 47
2.11 wind turbine system Description 51
2.12 wind speed curve 52
2.13 Wind System Modeling 53
2.14 The Power Coefficient for Different Pitch Angles 55
2.15 Wind Turbine Shaft Model 58
2.16 Strategy for Controlling Wind Turbines Across Four Wind Speed Zones . . . 64
2.17 Optimal Torque MPPT Algorithm for Wind Energy Conversion Systems . . 65
2.18 Thevenin's electric model for battery 67
2.19 Thevenin model including the charge/discharge hysteresis effect 68
2.20 Dynamic Model 70
2.21 Model "2" representing the polarization effect 71
2.22 Model including the double electrical layer EDL 72

3.1 Schematic representation of a hybrid renewable energy system with energy management 84
3.2 Renewable energy system with power converters and control algorithms for enhanced reliability and stability 86
3.3 System components and description. 88
3.4 Performance of ANN, training, tasting, and validation 94
3.5 The Best validation Perfermance 95

4.1 The Dynamic training of varions ANN architectures 102
4.2 profile of a PV power in the 12 hours 103
4.3 profile of a Battery power in the 12 hours 104

4.4 System components and description 105
4.5 Historical data Wind speed, ambient temperature, and solar insolation in one year 105
4.6 Profile of a typical day corresponding to each Month in year 105
4.7 PV and Wind Load Powers Profile 106
4.8 Various power outputs were obtained 106
4.9 State of charge profile 107
4.10 Voltage of battery in 24 h 107
4.11 Profile of Voltage DC bus in 24 h 108

List of Tables

2.1 Comparative Table of DFIGs and PMSGs 50

2.2 Comparative Table of Rechargeable Batteries 73

3.1 Tool Comparison for Renewable Energy System Design 81

3.2 Compact Comparison of Hybrid System Integration Techniques 85

3.3 Comparison of Control Algorithms for Renewable Energy Systems 87

3.4 Compact Comparison Table for KPERC and Energy Parameters 91

3.5 The Number of Wind Turbines and Panels Determined Through Calculation 92

4.1 Comparison of ANN Architectures' Performance 101

4.2 the performance comparison of DLGA, DL, ANN, and P&O 109

4.3 Power and Energy Metrics for PV, Wind, Load, and SOC 110

Abstract

اللخص تركز هذه الدراسة على تحسين الكفاءة والموثوقية والأداء لأنظمة الطاقة المتجددة، وخاصة في التكوينات المستقلة والهجينة. باستخدام استراتيجيات تحكم متقدمة، بما في ذلك الشبكات العصبية الاصطناعية وتقنيات تتبع نقطة القدرة القصوى ، تعالج الدراسة التحديات الرئيسية في إدارة الطاقة وتحسين التخزين وتحديد حجم الأنظمة.تطوّر هذه الدراسة استراتيجيات إدارة ذكية للطاقة باستخدام الشبكات العصبية الاصطناعية لتحسين استغلال أنظمة تخزين الطاقة في الأنظمة الهجينة، مما يضمن تدفقات طاقة فعالة وأداءً محسّنًا للنظام. كما تقارن الدراسة بين تقنيات المختلفة لتحديد الطريقة الأكثر فعالية لزيادة إنتاج الطاقة في الأنظمة الفوتوفولتية تحت ظروف بيئية متغيرة.تستكشف الدراسة أيضًا دمج مصادر متعددة للطاقة المتجددة، مثل الطاقة الشمسية والرياح، في الأنظمة الهجينة، وتحقق في استراتيجيات التحكم وتحديد الحجم لضمان تشغيل مستقر وفعّال من حيث التكلفة. تم تقييم الاستراتيجيات المقترحة من خلال محاكاة پاڤـا وتم التحقق من صحتها باستخدام بيانات تجريبية، مما يوضح قابليتها للتطبيق في سيناريوهات واقعية.بشكل عام، تساهم هذه الدراسة بشكل كبير في مجال الطاقة المتجددة من خلال تقديم حلول مبتكرة لتحسين إدارة الأنظمة المتجددة، ودعم الانتقال نحو طاقة مستدامة، وتوجيه التطورات المستقبلية في تقنيات وممارسات إدارة الطاقة المتجددة.

Abstract This research focuses on enhancing the efficiency, reliability, and performance of renewable energy systems, particularly in standalone and hybrid configurations. Using advanced control strategies, including Artificial Neural Networks (ANN) and Maximum Power Point Tracking (MPPT) techniques, the study addresses key challenges in energy management, storage optimization, and system sizing. The research develops intelligent energy management strategies with ANN to optimize energy storage in hybrid setups, ensuring ef-

ficient energy flow and system performance. It also compares various MPPT techniques to identify the most effective method for maximizing power output in photovoltaic (PV) systems under changing environmental conditions. The study further explores the integration of multiple renewable energy sources, like PV and wind, in hybrid systems, investigating control and sizing strategies to ensure stable and cost-effective operation. The proposed strategies are evaluated through MATLAB/Simulink simulations and validated with experimental data, demonstrating their applicability in real-world scenarios.

Abstract Cette recherche se concentre sur l'amélioration de l'efficacité, de la fiabilité et des performances des systèmes d'énergie renouvelable, en particulier dans les configurations autonomes et hybrides. En utilisant des stratégies de contrôle avancées, y compris les réseaux de neurones artificiels (ANN) et les techniques de suivi du point de puissance maximale (MPPT), l'étude aborde les principaux défis de la gestion de l'énergie, de l'optimisation du stockage et du dimensionnement des systèmes. La recherche développe des stratégies de gestion intelligente de l'énergie avec les ANN pour optimiser le stockage d'énergie dans les configurations hybrides, garantissant ainsi des flux d'énergie efficaces et des performances optimales du système. Elle compare également diverses techniques de MPPT pour identifier la méthode la plus efficace pour maximiser la production d'énergie dans les systèmes photovoltaïques (PV) sous des conditions environnementales changeantes. L'étude explore également l'intégration de plusieurs sources d'énergie renouvelable, telles que le PV et l'éolien, dans les systèmes hybrides, en investiguant des stratégies de contrôle et de dimensionnement pour assurer une exploitation stable et rentable. Les stratégies proposées sont évaluées à travers des simulations MATLAB/Simulink et validées par des données expérimentales, démontrant leur applicabilité dans des scénarios réels. En somme, ce travail contribue au domaine des énergies renouvelables en proposant des solutions innovantes pour optimiser les systèmes énergétiques, soutenir les transitions énergétiques durables et orienter les futurs développements des technologies et des pratiques de gestion de l'énergie renouvelable.

Acknowledgements

I would first like to express my deepest gratitude to my thesis supervisor, Professor Djalel DIB from the University of Tebessa, for his invaluable guidance, unwavering support, and insightful feedback throughout this research work. His expertise, patience, and encouragement were essential in shaping both the direction and the quality of this thesis. I would also like to thank Mr. Kadir Erkan, Professor at Yildiz Technical University in Turkey, and Ms. Djamila Rekioua, Professor at the University of Béjaïa in Algeria. I had the opportunity to complete two short internships with them, and I truly appreciate these invaluable opportunities.

I would like to extend my thanks to Pr. Abdellah Meraoumia from the University of Tebessa for agreeing to chair my thesis jury. My heartfelt thanks also go to Dr. Abdelaziz Aouich and Pr. Bougadoum Aziz from the University of Tebessa for the honor of reviewing this work. Additionally, I would like to thank Pr.Lazhar Rahmani from the University of Sétif, and Dr. Sihem Ghoudelbourk from the University of Annaba, for their participation in the jury. I am sincerely grateful to all the members of the jury for the time and effort they devoted to reading and correcting my dissertation.

Finally, these acknowledgments would not be complete without a special mention to my heroes: My mother, My father, My sisters (Wiam, Assala and Habala), and My four brothers, especially Amir. Their presence and encouragement have been the foundational pillars of who I am and everything I do.

General introuction

The global energy landscape is undergoing a significant transformation as nations strive to mitigate the impacts of climate change, reduce reliance on fossil fuels, and ensure long-term energy security. According to the International Energy Agency (IEA), global CO2 emissions from energy reached 33.9 gigatons in 2021, necessitating urgent action to transition to low-carbon energy sources [1]. This shift towards sustainable energy has placed renewable energy at the forefront of global strategies, with countries setting ambitious targets to reduce greenhouse gas emissions. For instance, the European Union aims to cut emissions by 55% by 2030 and achieve net-zero emissions by 2050, while the United States has pledged to achieve a 50-52% reduction in greenhouse gas emissions by 2030 [2]. Among the various renewable energy options, solar and wind energy have emerged as the most viable and widely adopted technologies, owing to their abundant availability and the rapid advancements in their respective technologies. As of 2021, solar and wind power accounted for over 10% of global electricity generation, with solar PV capacity growing by nearly 22% and wind capacity increasing by 14% annually [3].

The global installed capacity of solar PV reached approximately 942 gigawatts (GW) by the end of 2021, while wind energy capacity surpassed 837 GW, making them the fastest-growing sources of electricity generation [4]. Solar energy generation is highly dependent on sunlight, which varies throughout the day and across seasons. For example, the capacity factor for solar PV, which measures the actual output as a percentage of its theoretical maximum, typically ranges between 10% to 25%, depending on geographic location and weather

conditions [5]. On the other hand, wind energy is influenced by changing wind patterns, with capacity factors ranging from 20% to 40%, depending on turbine technology and site location [6]. These fluctuations in solar and wind energy production can lead to periods of excess generation, particularly during sunny or windy conditions, followed by periods of shortfall when the weather is less favorable[7].

To address these challenges, it is essential to develop advanced energy management and storage solutions that can effectively harness and optimize the use of renewable energy. Traditional energy management systems are often inadequate in dealing with the complexities introduced by renewable energy sources, leading to inefficiencies and potential energy losses. As a result, there is a growing need for innovative control strategies that can dynamically manage the generation, storage, and distribution of energy in systems that incorporate renewable sources.

The global transition towards renewable energy sources has underscored significant challenges in integrating these technologies into existing energy systems, particularly when addressing the intermittent nature of solar and wind resources. Unlike fossil fuels, which provide a stable and predictable energy output, renewable sources such as solar and wind are inherently variable. Solar power generation fluctuates based on daylight hours, weather conditions, and seasonal changes, while wind energy is subject to unpredictable wind patterns. This intermittency can lead to periods of overproduction followed by periods of low or no production, complicating efforts to maintain a consistent energy supply. For example, studies have shown that in regions with high solar penetration, grid operators may need to curtail up to 7% of the generated solar energy to avoid overloading the grid during periods of low demand [8].

Traditional energy management systems, which were primarily designed for the steady output of fossil fuel-based generation, often prove inadequate when applied to renewable energy systems. These systems typically lack the flexibility and responsiveness needed to handle the rapid fluctuations in energy generation that characterize solar and wind power. As a

result, inefficiencies arise in energy capture, storage, and utilization. For instance, in many solar PV systems, without adequate storage or real-time demand response, excess energy generated during peak sunlight hours is wasted, leading to an overall reduction in the system's efficiency[9]. One of the most pressing challenges in renewable energy systems is the effective management of energy storage. Battery energy storage systems (BESS) are crucial for balancing supply and demand in both standalone and hybrid renewable systems. However, these systems often operate below optimal efficiency due to the lack of advanced management strategies. Traditional energy storage management approaches, such as basic charge-discharge cycles, do not fully exploit the capabilities of modern storage technologies like lithium-ion batteries. These batteries can degrade faster or operate less efficiently if not managed correctly, leading to increased operational costs and shorter lifespans. In fact, research indicates that poor battery management can reduce the efficiency of a storage system by up to 20%, contributing to higher energy costs and lower system reliability [10].

Moreover, the efficiency of photovoltaic (PV) systems is heavily dependent on the ability to operate at the Maximum Power Point (MPP), which is the point at which the system produces its highest power output. This MPP varies with environmental conditions such as sunlight intensity and temperature. Existing Maximum Power Point Tracking (MPPT) techniques are widely used to ensure that PV systems operate at this optimal point. However, these techniques often struggle in rapidly changing conditions, such as passing clouds or sudden temperature shifts, leading to suboptimal power output and reduced overall system efficiency. Studies have shown that in some cases, inefficiencies in MPPT can lead to a loss of up to 15% of the potential energy output of a PV system [11]. Proper sizing of hybrid renewable energy systems is critical to ensuring that each component, such as PV panels, wind turbines, and batteries, has the appropriate capacity to meet energy demands reliably. Incorrect sizing can lead to significant issues: underperformance, where the system fails to meet energy needs, or over-dimensioning, where the system is unnecessarily large and expensive. Advanced sizing methodologies that take into account the variability of renewable

sources and the dynamic interaction between them are essential for optimizing both performance and cost-effectiveness. Research has shown that optimized sizing and management strategies can improve the efficiency of hybrid systems by up to 25%, making them more practical and viable for widespread adoption [12].

In addition to sizing, the integration of a hybrid system, introduces further complexity in energy management. The variability of each energy source demands a sophisticated control strategy to ensure that the hybrid system operates efficiently and reliably under different environmental conditions. For example, a hybrid system might generate excess energy during periods of simultaneous high wind and solar availability, which, without adequate storage or grid integration, could lead to overproduction and potential system instability. Conversely, during periods of low wind and solar availability, the system might fail to meet energy demand, resulting in underperformance. This complexity often necessitates costly overdimensioning of system components to ensure reliability, potentially increasing the overall cost of the system by as much as 30% [13].

One of the significant contributions of this study is the development of advanced energy management strategies using Artificial Neural Networks (ANN). By improving the management of energy storage systems, especially in standalone PV configurations, this research seeks to enhance the efficiency and reliability of renewable energy systems . Effective energy management is crucial for ensuring that renewable systems can consistently meet energy demands, even in the face of variability in energy generation. The outcomes of this research have the potential to reduce energy losses, optimize battery usage, and ultimately lower the operational costs of renewable energy systems [14]. Another key contribution is the evaluation and optimization of Maximum Power Point Tracking (MPPT) techniques. Given the critical role that MPPT plays in maximizing the energy harvested from PV systems, this research compares traditional methods with ANN-based approaches to determine the most effective techniques under varying environmental conditions . The findings from this evaluation are expected to provide valuable insights into how to maximize the performance

of PV systems, contributing to more efficient and reliable renewable energy generation[15]. The study also addresses the challenge of integrating multiple renewable energy sources, particularly in hybrid systems that combine PV and wind energy. By developing methodologies for the effective management and sizing of these systems, the research aims to ensure that hybrid configurations can operate efficiently and cost-effectively [16].

Proper sizing is essential for avoiding over-dimensioning, which can lead to unnecessary expenses, while ensuring that the system can meet energy demands . The strategies developed in this research could serve as a guide for future projects involving hybrid renewable energy systems, helping to optimize their design and operation [17]. Furthermore, this study contributes to the practical implementation of renewable energy technologies by validating the proposed energy management, sizing, and MPPT strategies through simulations and real-world scenarios. By demonstrating the effectiveness of these strategies in actual applications, the research bridges the gap between theoretical models and practical deployment, offering actionable solutions for improving renewable energy systems' performance [18].

The thesis is structured into four comprehensive chapters, each designed to build upon the previous one, offering a thorough exploration of multi-source renewable energy systems.

Chapter 1 begins by introducing the critical concepts and significance of renewable energy, particularly focusing on standalone and hybrid configurations. This chapter delves deeply into the current state of photovoltaic (PV) solar systems, wind energy technologies, and the pivotal role of battery storage in enhancing the efficiency and reliability of these renewable energy sources. By analyzing the operational principles, advantages, and challenges associated with each technology, the chapter constructs a nuanced understanding of how these systems are integrated to foster a sustainable and resilient energy future. Furthermore, it highlights the latest advancements in these technologies and identifies potential areas for further research and development.

Chapter two, moves the discussion forward by focusing on the modeling and optimization of multi-source renewable energy systems. This chapter emphasizes the growing importance

of these systems in meeting the increasing global demand for sustainable and reliable energy. It discusses the complexities involved in modeling systems that combine various energy sources, such as solar, wind, and energy storage technologies, and explores the optimization techniques necessary to enhance their performance. Advanced methodologies, including the use of Artificial Neural Networks (ANN), are explored as tools for optimizing the configuration of these systems, ensuring that they meet specific energy demands in a reliable and cost-effective manner.

Following the discussion on modeling and optimization, Chapter 3 examines the crucial aspects of sizing and managing these complex energy systems. Proper sizing of the system components—such as PV panels, wind turbines, and batteries—is essential for ensuring that the system operates efficiently without unnecessary over-dimensioning, which can lead to increased costs. The chapter discusses the methodologies used to determine the optimal capacity of each component and explores management strategies that are vital for coordinating the operation of these components in real-time, adapting to varying conditions, and maximizing overall system performance. Intelligent control algorithms, including those based on ANN, are highlighted for their role in enhancing the flexibility and efficiency of these systems. The chapter also reviews emerging trends in the sizing and management of multi-source systems, providing a forward-looking perspective on sustainable energy management.

Chapter 4 presents the findings from the research, including data and insights gained from the modeling, optimization, and management strategies discussed in the previous chapters. This chapter offers a detailed analysis of the results, comparing the performance of different system configurations and management strategies, and evaluates their effectiveness in enhancing the efficiency, reliability, and cost-effectiveness of multi-source renewable energy systems. The discussion also synthesizes the key findings, relating them back to the research objectives and the broader literature reviewed in Chapter I. The implications of these findings for future research and practical applications are thoroughly examined, providing a

critical evaluation of the study's contributions to the field of renewable energy. The chapter concludes with a reflection on the overall significance of the research and its potential impact on the future development of renewable energy technologies.

Chapter 1

Literature Review on multi-source renewable energy systems

1.1 Introduction

This chapter embarks on a comprehensive literature review of renewable energy systems, with a particular focus on the exploration and analysis of standalone and hybrid configurations. It delves into the intricacies of photovoltaic (PV) solar systems, wind energy technologies, and the critical role of battery storage in enhancing the efficiency and reliability of renewable energy sources. By dissecting the operational principles, advantages, and challenges associated with each technology, this review aims to construct a nuanced understanding of the current state of renewable energy systems. It underscores the significance of integrating these technologies to foster a sustainable and resilient energy future, highlighting the latest advancements and identifying potential areas for further research and development.

1.2 Renewable Energy Systems overview

Provide an overview of standalone and hybrid renewable energy systems, focusing on PV, Wind, and battery storage technologies.

1.2.1 Photovoltaic Solar systems

Photovoltaic solar systems use cells to convert sunlight into electricity. The PV cell consists of one or two layers of a semiconductor material, usually silicon. When light illuminates the cell, it creates an electric field across the layers, resulting in a flow of electricity. The higher the intensity of the light, the greater the flow of electricity. Photovoltaic cells are designated based on the peak power they generate under ideal sunlight and temperature conditions, referred to as peak kilowatts (kW). PV cells are wired together to form a PV module. PV modules collect solar energy from sunlight and convert it into direct electric current. PV modules are connected to form a PV solar panel system. An inverter is usually linked to the PV solar panel system. The main purpose of the solar inverter is to convert direct current into alternating current so that it can be used in a standalone power supply system or by the public distribution network [19]. As a cornerstone of renewable energy, PV technology offers a sustainable and limitless source of power. These systems can range from small, rooftop installations to large, utility-scale power plants, providing versatility in application. The efficiency and cost-effectiveness of PV systems have improved over time, making solar energy increasingly accessible and a vital component in the global transition towards cleaner energy sources. Figure 1.1 illustrates the dramatic growth in global installed solar photovoltaic (PV) capacity over the last decade, as reported by the International Renewable Energy Agency (IRENA). This period, spanning from 2010 to 2020, witnessed an exponential increase in PV installations, reflecting a significant shift towards sustainable energy adoption. The rise in solar PV capacity underscores a global commitment to sustainable energy practices, highlighting the role of solar power as a pivotal element in the transition to a more sustainable and secure energy future.

1.2.2 The Wind Turbines

The concept of harnessing wind energy dates back millennia. As early as 5000 BC, the Egyptians used wind energy to propel boats on the Nile. Others used windmills to grind

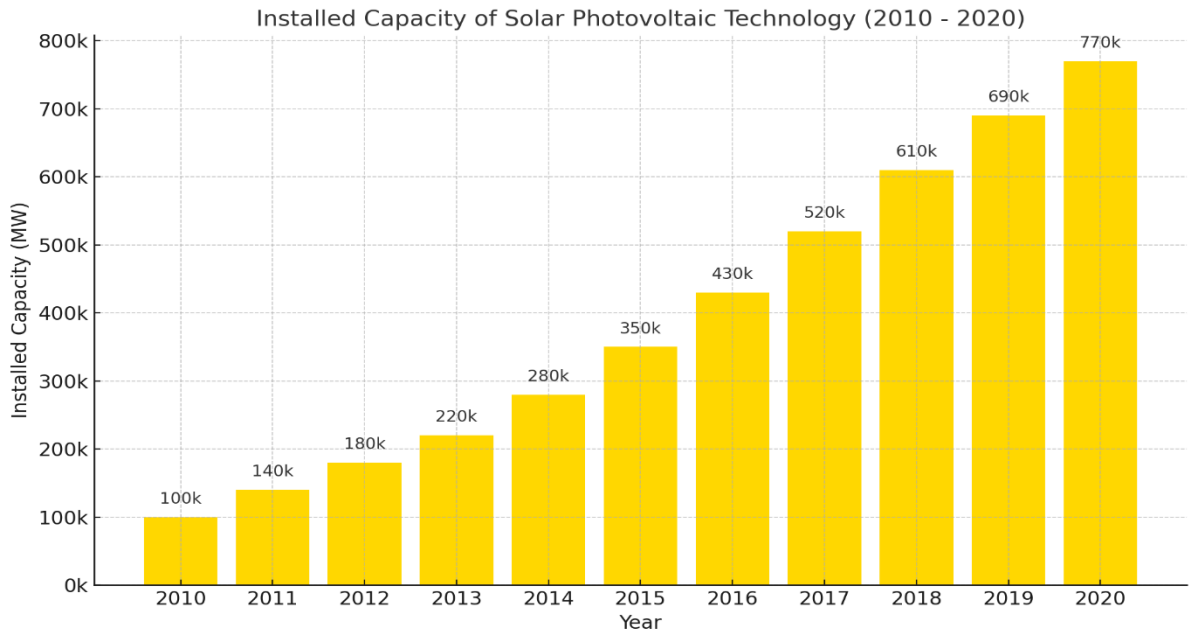


Figure 1.1: Variation in global installed PV capacity (MW) between 2010 and 2020.

grain, pump water, and cut wood in sawmills [20]. Today's wind turbines are the modern equivalent of the windmill: they convert the kinetic energy of the wind into clean and renewable electricity. Today, wind energy typically comes in two different types: onshore wind farms, which are large wind turbine installations located on land, and offshore wind farms, which are installations located off the coast in marine environments. Onshore wind farms are the most popular type of wind farm in the world, but several countries, especially in Europe, are increasingly interested in the construction of offshore wind farms. The 20th century saw significant advancements, particularly in Denmark and the United States, with the technology evolving from small-scale generators to the large, highly efficient turbines used today. The oil crisis of the 1970s sparked renewed interest in wind power as a sustainable energy source, leading to rapid technological improvements and widespread adoption worldwide [21]. Wind turbines operate on a simple principle. The energy of the wind turns two or three propeller-like blades around a rotor. The rotor is connected to the main shaft, which spins a generator to produce electricity. A wind turbine consists of three parts (see Figure 1.2): upstream, a turbine absorbs the mechanical power Pwind, supplied by the



Figure 1.2: Wind Turbine.

wind of speed Vwind passing through the surface S = 2RH (R being the radius of the blades and H the height covered by its blades). The turbine then generates a torque Twind) which drives the rotor of a rotating machine at the angular velocity m. This machine transforms the absorbed mechanical power into usable electrical power. The generator will produce in reaction, both a resisting electromagnetic torque Tem, and three phase currents [Ia, Ib, Ic] T. In the literature, the Permanent Magnet Synchronous Machine (PMSM) is the most used because it can operate at various speeds up to a halt without stalling, does not require rotor excitation, requires little maintenance, and can be manufactured with a significant number of poles, which avoids the use of a speed multiplier [22].

1.2.3 Energy Storage

Energy storage plays a crucial role in the expansion of renewable energy (RE), especially for intermittent sources in remote locations not connected to the grid. As new energy markets emerge, integrating decentralized, intermittent renewables can cause network instability. Energy Storage Systems (ESSs) and effective resource management are vital for addressing these challenges. Energy can be stored in various forms, including mechanical, electrochemical, electromagnetic, and thermal, each classified by duration into long, medium, and short-term storage technologies. Energy storage technologies can be broadly classified into several types, each with unique characteristics and applications. Here's a comprehensive overview of all major types of energy storage [23]:

Mechanical Energy Storage

1. Pumped Hydroelectric Storage (PHS): Uses electricity to pump water uphill to a reservoir; energy is recovered when water flows back downhill through a turbine.

2. Compressed Air Energy Storage (CAES): Stores energy by compressing air in underground caverns; released air is used to generate electricity.

3. Flywheels: Store kinetic energy in a rotating mass; energy is released by slowing down the rotation.

4. Gravitational Energy Storage: Involves elevating a mass and releasing it to generate energy, including newer concepts like elevated mass storage systems.

Elector-Chemical Energy Storage

1. Batteries: Store energy through chemical reactions in cells; includes Lithium-ion, Lead-acid, Nickel-cadmium, and more.

2. Flow Batteries: Elector-chemical storage where chemicals are stored externally and pumped through a reactor to produce electricity.

Electromagnetic Energy Storage

1. Supercapacitors (Ultracapacitors): Store energy using electric fields, allowing for rapid charging and discharging.

2. Inductive Energy Storage: Utilizes magnetic fields in superconducting coils to store and release energy.

Thermal Energy Storage

1. Molten Salt Storage: Stores heat in molten salts, commonly used in concentrated solar power plants.

2. Ice Storage: Freezes water to ice during off-peak hours and uses it for cooling during peak demand.

3. Phase Change Materials (PCMs): Store and release heat or cold through materials that change phase (e.g., melting and solidifying).

Chemical Energy Storage

1. Hydrogen Storage: Stores energy in the form of hydrogen gas, produced via electrolysis; hydrogen is used in fuel cells or burned to generate energy.

2. Synthetic Natural Gas (SNG): Converts surplus electricity into methane, which can be stored and used in gas networks.

Biological Energy Storage

1. Bioenergy with Carbon Capture and Storage (BECCS): Captures CO2 from bioenergy processes and stores it underground.

2. Biogas: Produced from the anaerobic digestion of organic materials, which can be stored and used for heating, electricity, or as vehicle fuel.

Other Innovative and Emerging Technologies

1. Underwater Compressed Air Energy Storage: Stores compressed air in underwater balloons or tanks.

2. Liquid Air Energy Storage (LAES): Stores energy by cooling air into a liquid state, which is vaporized to drive a turbine when energy is needed.

3. Kinetic Energy Recovery Systems (KERS): Captures and stores kinetic energy (typically in vehicles), for example, using flywheels or ultracapacitors.

These diverse energy storage technologies offer various solutions for managing energy supply and demand, improving energy system flexibility and reliability, and facilitating the integration of renewable energy sources. Hybrid energy storage systems (HESS) combine two or more types of energy storage technologies to leverage the strengths and mitigate the weaknesses of each individual system, resulting in improved performance, efficiency, and reliability. For instance, integrating batteries with supercapacitors in electric vehicles and renewable energy setups allows the system to capitalize on the high energy density of batteries for sustained power delivery and the high-power density of supercapacitors for rapid energy bursts. This enhances the overall efficiency and lifespan of the storage system. Similarly, combining flywheels with batteries in uninterruptible power supplies (UPS) offers a robust solution where flywheels provide immediate response to power fluctuations for short-term surges, while batteries ensure longer-duration power stability. On a larger scale, pairing pumped hydro storage with batteries for grid applications marries the large-scale, long-term storage capabilities of pumped hydro with the quick discharge and charge capabilities of batteries, offering a flexible solution to grid management and load balancing. Such hybrid systems not only optimize for both short-term power fluctuations and long-term energy

storage needs but also promise cost efficiency and increased reliability, making them particularly suitable for a wide range of applications, from electric vehicles to grid stabilization and renewable energy integration Figure 1.3 [24].

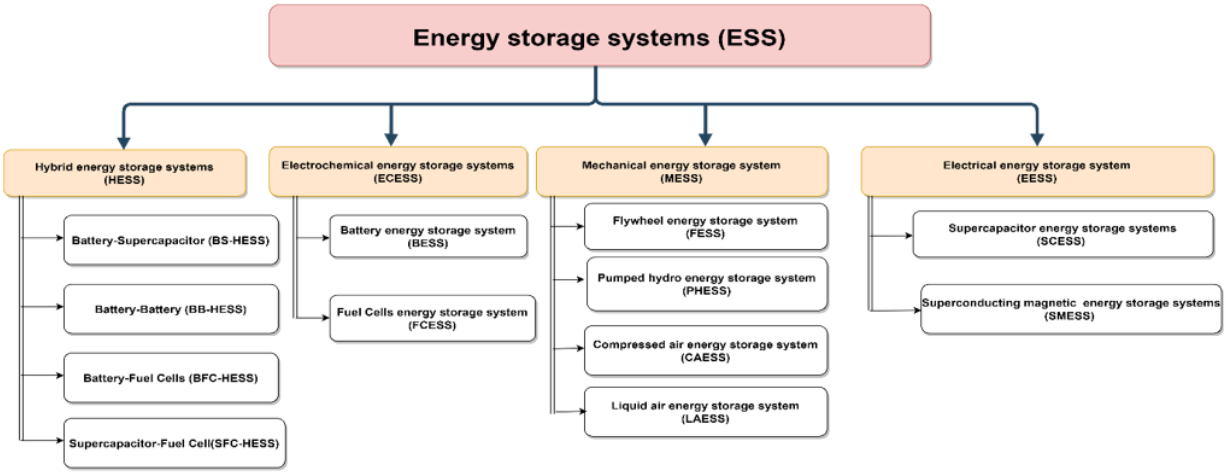


Figure 1.3: Types of Energy storage system

1.3 hybrid energy systems

The term "Hybrid Energy System" refers to multi-source electric power generation systems. These are complex systems that combine different renewable sources of different natures or are combined with conventional sources (nuclear power plants, diesel generators, etc.), storage elements, and loads. They compensate for the intermittent nature of renewable sources and offer higher overall energy efficiency. Their essential interest is the possibility of energy autonomy they allow since they do not depend on a single source. They can solve, to a great extent, the problem of energy availability. There are several configurations of multi-source electrical systems in the literature. Hybrid systems can be classified into two groups. In the first group, there are hybrid systems that work in parallel with the electrical grid, also called Grid-connected. These systems contribute to meeting the load demand. The hybrid systems of the second group operate in an isolated regime or in autonomous mode. They must meet the needs of consumers located in sites remote from the electrical grid: mountain

shelters, islands, isolated villages, road signage panels, etc. The structure of a hybrid energy system typically integrates multiple components to harness and utilize energy from various sources efficiently and three criteria can be considered in classifying hybrid systems based on the system's structure. The first criterion is the presence or absence of a conventional energy source. This conventional source can be a diesel generator, a micro gas turbine, or an entire power plant in the case of a complete electrical grid. A second possible criterion is the presence or absence of a storage device. The presence of an energy storage device ensures better satisfaction of electrical loads during periods when a primary resource is unavailable for conversion to electricity. Storage devices can be rechargeable batteries, supercapacitors, electrolyzes with hydrogen tanks, flywheels, etc. The last possible classification relates to the type of renewable energy sources used. The system structure can contain a photovoltaic system, a wind turbine, a hydraulic energy converter (hydroelectric power stations or wave use), or a combination of these sources. An important criterion for selecting the used source is the available energy potential, which depends on the hybrid system's installation location. Another determining factor is the electrical consumer being powered. Its significance determines the need for an additional source, a storage device, and/or a conventional source, etc. A generalization of the described classification is illustrated in Figure 1.4 [25].

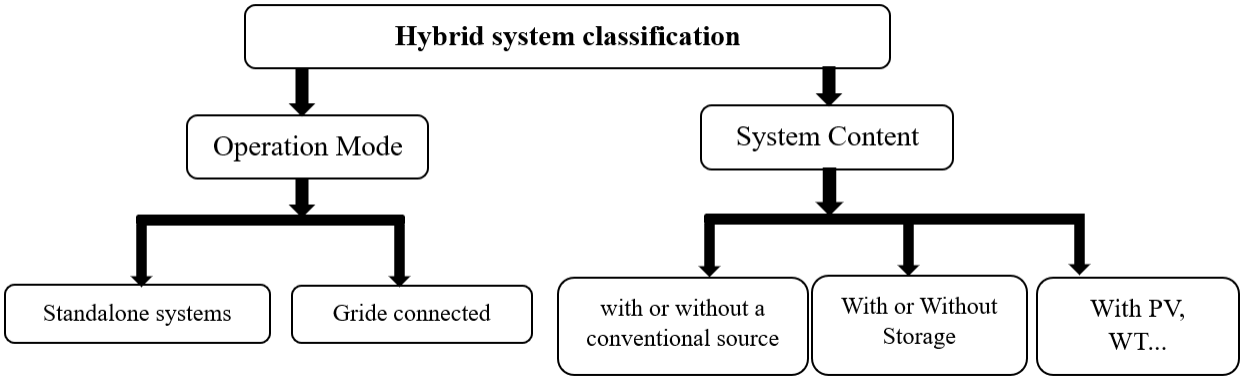


Figure 1.4: Hybrid system classification

1.3.1 Configurations of hybrid systems

Hybrid power generation systems intelligently combine various energy sources to enhance efficiency, reliability, and flexibility. These systems can be configured in several ways, each with unique advantages and considerations. Let's delve deeper into the configurations you mentioned [26]:

AC Bus Configuration (AC-Coupled Hybrid Power Generators)

In an AC-coupled configuration, all energy sources are connected to a main alternating current (AC) bus. This setup allows for the integration of multiple sources into a unified system, potentially including the utility grid as part of the AC bus. The key advantage of this configuration is its flexibility in source location, allowing energy sources to be spread across vast distances. However, this setup demands meticulous control over the voltage and frequency of the main AC bus to ensure stable operation of the distributed sources and their compatibility with the electrical grid. This ensures that regardless of the diversity and distribution of energy sources, the system maintains harmony and stability, crucial for both operational efficiency and grid compliance.

DC Bus Configuration (DC-Coupled Hybrid Power Generators)

In contrast, a DC-coupled configuration connects all sources to a main direct current (DC) bus, which is then linked to the grid through a central inverter. This approach decouples the network's voltage and frequency from the energy sources, providing a more straightforward management of the power flow. A significant advantage of the DC-coupled system is its ability to easily integrate storage solutions, such as batteries or supercapacitors, via a DC/DC converter. This converter facilitates an optimized charging and discharging regime, enhancing the system's overall efficiency and responsiveness. Furthermore, both conventional (e.g., nuclear, diesel) and decentralized (e.g., wind, PV) energy sources can be seamlessly integrated into the DC bus through power electronics converters, offering a versatile and efficient

energy solution.

Mixed Configuration

A mixed configuration combines elements of both AC and DC coupling, aiming to leverage the benefits of each. This hybrid approach allows for a flexible and scalable system design, where the number and type of energy sources, as well as their operational modes, can be tailored to specific requirements. The mixed configuration stands out for its adaptability, enabling the integration of a wide range of energy sources without being constrained by the grid's frequency or the voltage of the DC bus. Static converters are used to manage the discrepancies between the network voltage, the DC bus voltage, and the voltage levels of the individual sources, ensuring a smooth and efficient energy transfer within the hybrid power generation system. Each configuration presents a distinct approach to managing and

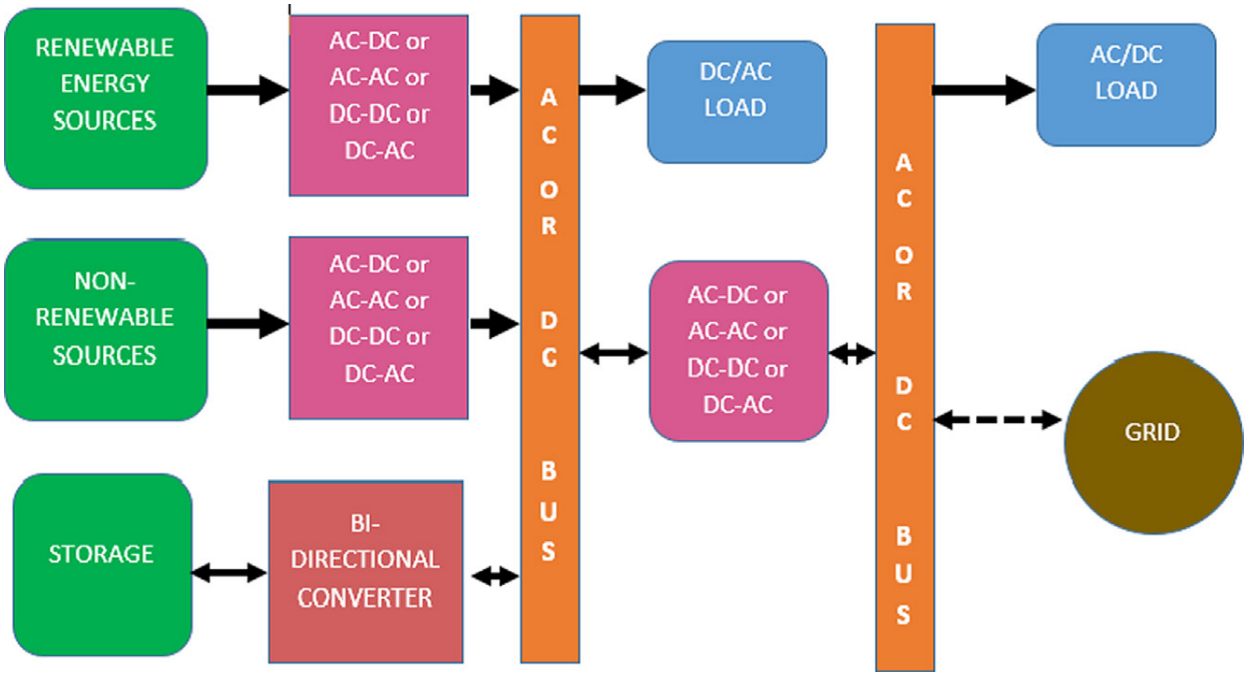


Figure 1.5: Basic components of hybrid system

integrating diverse energy sources within a hybrid system, catering to different operational needs and objectives. The choice between AC, DC, and mixed configurations depends on factors such as the geographical distribution of energy sources, the types of sources involved,

the integration of storage solutions, and specific system requirements for efficiency, flexibility, and grid compatibility.

1.4 Some Issues with Hybrid Systems

1.4.1 Hybrid Systems with Conventional Energy Source

1. Photovoltaic/Conventional Source Systems:This type of system, aims to provide uninterrupted power when operating in autonomous mode, whether to a house, a residential or administrative building, or a village. Other systems power research centers or are also connected to the electrical grid and/or storage devices. Batteries and the photovoltaic field produce direct current. However, diesel engines can drive either direct or alternating current generators. Consumers most often require alternating current. Therefore, two system structures are distinguished according to the type of electric machine coupled with the diesel engine[27],[28].

2. Wind/Conventional Source Systems: Research on hybrid wind/diesel systems is different from studies on photovoltaic hybrid systems because wind turbines are capable of producing alternating current similar to that produced by a diesel generator. Thus, there is not a wide diversity of hybrid system configurations. These systems are more common on islands, where sea breezes and wind favor the use of wind energy for electricity production [29]. This type of system is also studied in [30], where a Ni–MH type storage system was integrated, contributing to the stability, reliability, and safety of the overall system.

3. Photovoltaic/Wind/Diesel Systems:This type of system has been studied in previous work at GREAH [31],[32],[33],[34],[35],[36]. In [31] and [32], to optimize costs and life cycle performance, a method based on an estimation of the storage units' lifespan was proposed. Indeed, a Rainflow counting method is applied to size the storage units, tak-

ing into account the actual operating conditions of the system. In [33],[34], a method focused on energy management based on the frequency approach using wind/load power fluctuation sharing and polynomial controllers is developed. This method first reduces the impacts of micro-cycles on the battery and micro-grid due to wind/load power fluctuations. Secondly, it allows for a proper estimation of energy storage capacity without overflow. Another system with the same structure is developed in [37], where the authors present an experimental implementation of an autonomous microgrid topology based on a two-level voltage source converter associated with PV, wind, a diesel group, and batteries. The proposed topology has the advantage of having reduced switching devices and simple control. The implementation of such a system aims to diversify renewable energy sources. This leads to a more significant reduction in the amount of fuel consumed since renewable sources can complement each other and provide a greater quantity of energy. There are also studies on the interconnection of systems in the electrical grid, in the State of New York. Storage can be in the form of batteries, a hydrogen reservoir with electrolyzer and fuel cell, or a combination of the two.

1.4.2 Hybrid Systems without Conventional Source

These hybrid systems primarily operate in autonomous mode in sites where diesel fuel supply or grid connection is difficult or even impossible. Hybrid Systems without Conventional Source The photovoltaic installation must be connected with another energy source to satisfy the load during the night or cloudy weather. This type of system is described in [38], where an energy management strategy for a residential photovoltaic solar unit with an energy storage unit via two-level static converters is proposed. It is an efficient solution to integrate storage and renewable energy sources, such as photovoltaic solar energy, into the conventional grid to improve the reliability and efficiency of the electrical system and reduce the total cost of electricity for the consumer. These systems power either homes or villages.

1. Photovoltaic/Storage Hybrid Systems:Coupling a storage device with a wind generator can have two objectives. The first is based on a buffering role when the system is coupled with the electrical grid; the device then allows smoothing the rapid variations of electric power from the wind turbine. The second is based on a role of longer-term storage, in autonomous mode to supply the consumer during periods of low wind speed, [39]. Other authors [40]studied this system in which an energy management algorithm is proposed for hybrid energy storage based on batteries and supercapacitors to improve the performance of battery storage.

2. Wind/Storage Hybrid System: The major drawback of the two previously described hybrid systems is the lack of diversity in supply because the primary resource used is unique. This leads to several disadvantages, such as the oversizing of elements aimed at ensuring a continuous supply, which will translate into a high initial investment (thus limiting the development of these systems) and an increase in the cost per kWh produced. These disadvantages can be limited or even eliminated by adding a second energy source. An example of this configuration is given in [41]. Storage devices are most often batteries; sometimes supercapacitors are used as a storage solution [42].

1.5 Energy Management and Control

In Integrated Renewable Energy Systems (IRES) and Hybrid Power Systems (HPS) that combine multiple Renewable Energy (RE) sources with conventional Distributed Generation (DG) and energy storage, managing the energy flow is paramount for ensuring a continuous and reliable power supply to meet demand. An effective energy management strategy is crucial for creating a cost-efficient, reliable, and highly efficient system. The interaction between renewable energy sources and demand introduces stability and power quality challenges, such as frequency and voltage regulation issues, necessitating stringent control and monitoring of the system to address transient responses in the energy distribution network.

Forecasting for all energy sources and demand is a preliminary step, followed by the optimization of energy sources, demand, and the scheduling of these sources along with storage devices to guarantee optimal energy flow. This process involves allocating active and reactive power output from each source while keeping output voltage and frequency within desired parameters, as depicted in energy flow management examples in IRES and illustrated for HPS in Figure 1.6. Control systems, essential for adjusting power to meet load demands, fall into centralized, distributed, and hybrid paradigms, with each energy source equipped with a local controller for optimal operation based on current data. Typically, the control

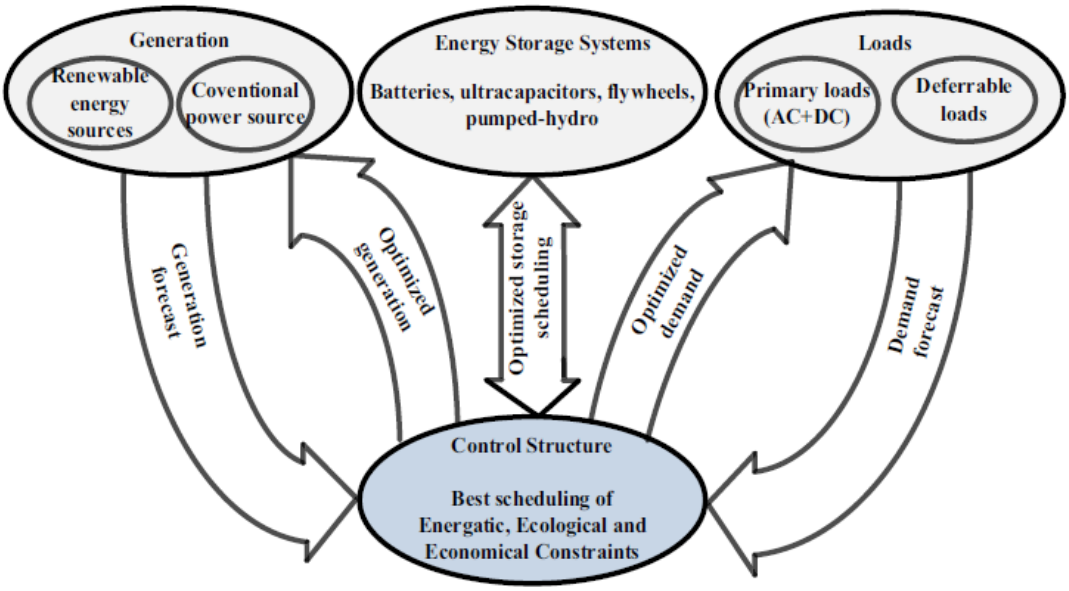


Figure 1.6: Energy flow management in IRES

framework for managing energy flow in Integrated Renewable Energy Systems (IRES) is divided into three main categories: centralized control systems, distributed control systems, and a hybrid approach combining centralized and distributed control mechanisms. Within each of these categories, every renewable energy source is equipped with its local controller (a slave controller), which is responsible for determining the most efficient operation of the unit based on real-time data [43].

1.5.1 Centralized Control System Configuration

In a centralized control setup, the system is managed by one main controller (the centralized controller), along with numerous subordinate controllers for different renewable energy resources and energy storage systems. This central controller coordinates closely with all energy resources and their respective subordinate controllers. It receives measurement signals from all energy sources within the group, as depicted in Figure 1.7. Acting as the system's energy supervisor, the central controller determines control actions based on these signals, adhering to a set of predefined objectives and constraints. It assesses resource availability and load demand to allocate and regulate energy flow across the various renewable sources within the integrated system efficiently. This centralized approach is particularly effective for multi-objective energy management in IRES, aiming for global optimum outcomes based on current data. Nonetheless, this control structure may encounter drawbacks, such as extensive computational demands and potential vulnerability to single points of failure.

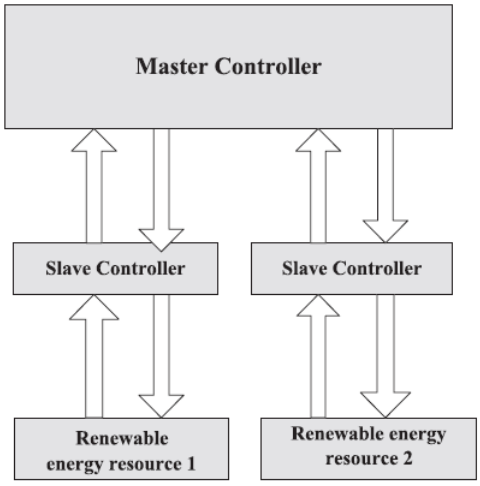


Figure 1.7: Centralized Control System Configuration

1.5.2 Distributed Control system Configuration

In a distributed control setup, each energy source transmits measurement signals to its respective local controller, as illustrated in Figure 1.8. These local controllers then collaborate

to make decisions aimed at achieving global optimization. This arrangement significantly lowers the computational load on each controller and eliminates the risk of a single point of failure. However, the downside to this approach is the complexity of the communication network required among the local controllers. To address these challenges, artificial intelligence algorithms such as fuzzy logic, artificial neural networks, genetic algorithms, and their combined forms are viable solutions for enhancing the distributed control scheme's effectiveness. One of the most promising methods for implementing distributed control is through a Multi-Agent System (MAS), which has been widely applied for the integration of energy sources, system restoration and reconfiguration, and energy management within an integrated system.

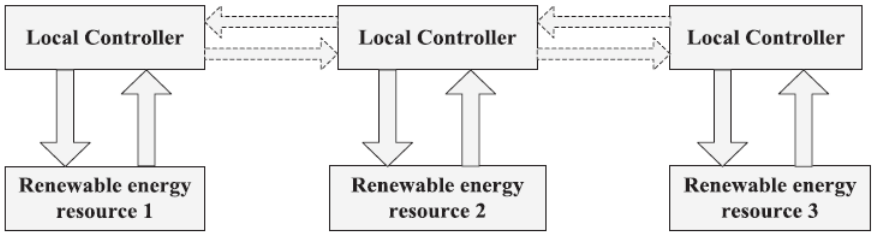


Figure 1.8: Distributed Control system Configuration

1.5.3 Hybrid Arrangement of Centralized and Distributed Control

The hybrid control arrangement merges the elements of both centralized and distributed control schemes within an integrated renewable energy system. In this model, renewable energy sources are organized into groups, where a centralized control method is implemented within each group, and a distributed control approach is employed to manage coordination between these groups. This hybrid structure facilitates local optimization within each group via centralized control, while global optimization across various groups is achieved through distributed control. This strategy reduces the computational load on both the master controller and the local controllers, diminishing the risk of single-point failures within

the integrated energy system. An illustration of the hybrid control scheme is provided in Figure 1.9.

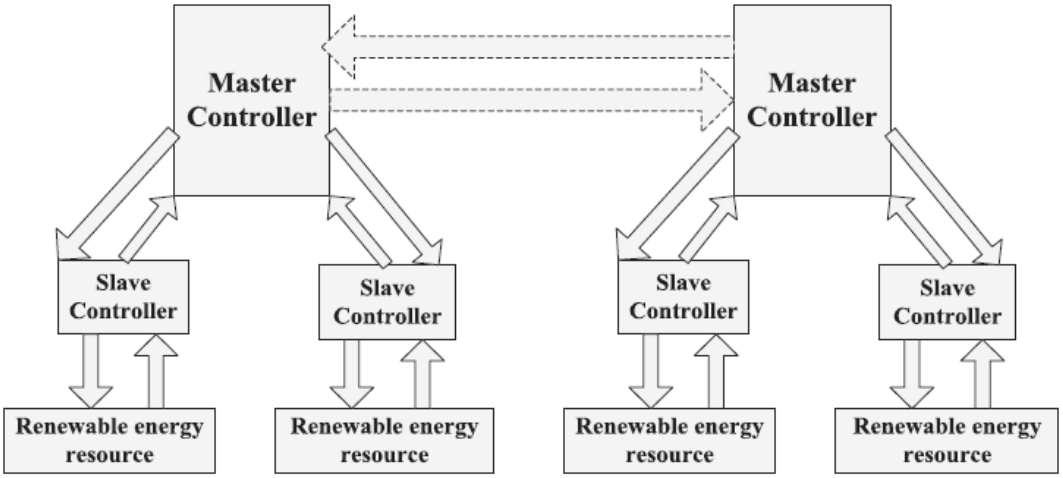


Figure 1.9: Hybrid Arrangement of Centralized and Distributed Control

1.6 Energy Management Systems (EMS)

Energy Management Systems (EMS) are instrumental in optimizing the operation of hybrid energy systems, offering a full array of capabilities for overseeing, directing, and refining energy flows. These systems integrate functionalities such as live data gathering, analysis of energy usage, and forward-looking modeling, aiding in knowledgeable decision-making and boosting system efficacy. EMS's core functionalities encompass [44]:

- Live Monitoring and Adjustment: EMS persistently tracks the functioning status of the entire hybrid system's components, from energy generation units and storage mechanisms to consumption trends. This feature facilitates immediate modifications to control parameters to hone performance and adapt to changes in the system.

- Forward-looking Analysis: Leveraging historical data alongside predictive algorithms, EMS can project forthcoming energy needs and generation potentials, enabling pre-

emptive adjustments to operational plans for ideal alignment of energy provision with demand.

- Efficiency Algorithms: Sophisticated algorithms are deployed by EMS to identify the most efficient methods for energy distribution and use, taking into account factors like energy pricing, the availability of renewables, and operational limits to diminish energy wastage and curtail expenses.

- Demand Response Handling: Through analyzing usage patterns and forecasting peak demand intervals, EMS can execute demand response initiatives, modifying consumption behaviors or activating alternative energy sources to mitigate system strain during high-demand instances. Adaptive and predictive control strategies further elevate the agility and performance of hybrid systems by dynamically modulating control parameters in response to evolving conditions and anticipating future states of the system. These strategies are pivotal in managing the variability and unpredictability associated with renewable energy sources, encompassing [45]:

- Adaptive Control: This strategy dynamically adjusts control parameters based on real-time system performance and feedback, allowing for compensation for fluctuations in renewable energy supply, demand shifts, and external perturbations to maintain steady system operations.

- Predictive Control: Utilizing models to anticipate future states of the system, such as demand or renewable generation levels, predictive control enables early adjustments to control settings, optimizing energy flows and preempting potential challenges.

- Machine Learning and AI: The adoption of machine learning and AI technologies facilitates the creation of sophisticated predictive models for energy patterns, enabling the identification of optimal control strategies and continual enhancement of predictive accuracy through learning from historical data.

- Integration with Renewable Forecasting: These control strategies are closely intertwined with predictive tools for weather and renewable energy, where accurate forecasts of solar irradiance, wind speed, and other environmental variables are crucial for optimizing the performance of renewable energy sources within the hybrid setup.

Simultaneously, EMS strategies encompass load forecasting, demand management, renewable energy integration, energy storage optimization, real-time monitoring, grid interaction, energy efficiency measures, and economic and environmental optimization. These strategies involve utilizing predictive analytics, integrating renewables efficiently, optimizing energy storage, employing real-time control systems, contributing to grid management, implementing energy-saving measures, minimizing costs and environmental impacts, and leveraging advanced analytics and machine learning for predictive maintenance and system optimization. Collectively, EMS and adaptive/predictive control strategies form the backbone of modern hybrid energy system management, ensuring efficient, reliable, and sustainable operations. By intelligently coordinating system components and anticipating future scenarios, these technologies equip hybrid systems to navigate today's complex energy landscape, fulfilling consumer needs economically, sustainably, and with future adaptability.

1.7 Conclusion

This chapter highlights the significant advancements and growing role of standalone and hybrid renewable energy systems, emphasizing solar, wind, and battery technologies. It stresses the need for ongoing innovation, supportive policies, and interdisciplinary research to overcome existing challenges. Key future directions include optimizing technology integration, improving efficiency, and addressing socio-economic and environmental impacts, ultimately supporting the global transition to sustainable and secure energy.

Chapter 2

Multi-Source System: Modeling and Optimization

2.1 Introduction

In this chapter, we explore the intricate dynamics of modeling and optimizing a hybrid energy system that synergizes the strengths of photovoltaic (PV) panels and wind turbines (WT), supplemented by Modeling of Battery storage. Crucial to the efficacy of such hybrid systems is the deployment of Maximum Power Point Tracking (MPPT) techniques, which serve as the cornerstone for optimizing energy harvest from fluctuating renewable sources. We delve into the mathematical models that simulate the behavior of these complex systems, considering the variable nature of solar irradiance and wind speed. By integrating storage, we add a layer of stability and reliability, ensuring that the generated energy can be efficiently used to meet demand patterns. The optimization strategies By MPPT aim to maximize efficiency, minimize costs, and ensure the seamless operation of this multi-faceted energy system, paving the way for smarter, greener energy solutions.

2.2 Photovoltaic Sources

2.2.1 Components of Photovoltaic Systems

The foundational component of a photovoltaic (PV) system is the PV cell, which is a semiconductor device capable of converting sunlight directly into electricity, as depicted in Figure 2.1. Multiple PV cells are linked together in series to form what is known as a cell series string, effectively increasing the electrical output through cumulative voltage. These series strings are then encapsulated within a protective frame to create a PV module, designed for durability and ease of installation. To further amplify the system voltage, several modules are connected in series, forming a module string. To achieve a higher current output, a PV array is constructed by connecting multiple module strings in parallel. This configuration allows for the scalable generation of electricity, catering to various power requirements. The collective DC power generated by the PV array is then converted into AC power through a solar inverter. This conversion is crucial for making the electricity suitable for everyday consumption by electrical loads and for safe integration into the electrical grid.[46]

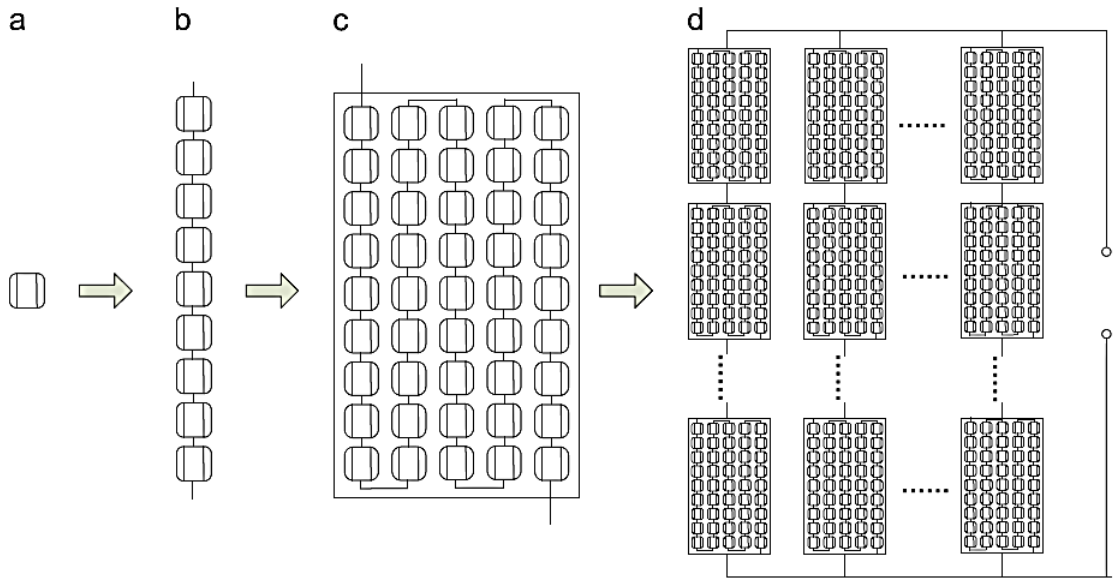


Figure 2.1: Layout and Structure of Photovoltaic Components: Single Cell (a), Series String of Cells (b), Module (c), and PV Array (d).

2.2.2 Equivalent Electrical Circuits and Mathematical Modeling of PV Devices (Cells, Modules and Arrays)

The accurate modeling of photovoltaic (PV) device outputs plays a crucial role in evaluating the overall performance of PV systems. Typically, a PV cell is represented through an equivalent electrical circuit model, which integrates a current source alongside one or two anti-parallel diodes (D). This setup may also incorporate an internal series resistance (Rs) and a parallel or shunt resistance (Rp), depending on the complexity and fidelity of the model. Three predominant models— the ideal, one-diode, and two-diode models—offer varying levels of detail and accuracy, as depicted in Figure 2.2. These models have been extensively discussed and validated in existing literature, highlighting their relevance and application in understanding PV cell behaviors [47]. Among these, the circuit representation shown in Figure 2c gains particular emphasis due to its widespread adoption in academic and practical scenarios. This preference is attributed to its balance between simplicity and precision, allowing for effective simulation of PV cell electrical characteristics. These models generate crucial current (I) and voltage (V) data points, which are instrumental in constructing the I–V characteristic curve (illustrated in Figure 2.3). A fundamental goal of this research involves aligning the theoretical I–V curves with those obtained from real-world experiments, focusing on three pivotal points: the short-circuit condition (0, Isc), the maximum power point (MPP) (Vm, Im), and the open-circuit situation (Voc, 0).

2.2.3 The One-Diode Model with Series and Shunt Resistances 4 and 5 Parameter Model

Figure 2b presents the electrical circuit representation of a PV cell tailored for scenarios involving series resistance, known as the four-parameter (4-p) model [48]. In this model, the parallel (shunt) resistance is assumed to be infinitely large, rendering its influence negligible. Reference [49] introduced the 4-p PV model and integrated it into the TRNSYS simulation

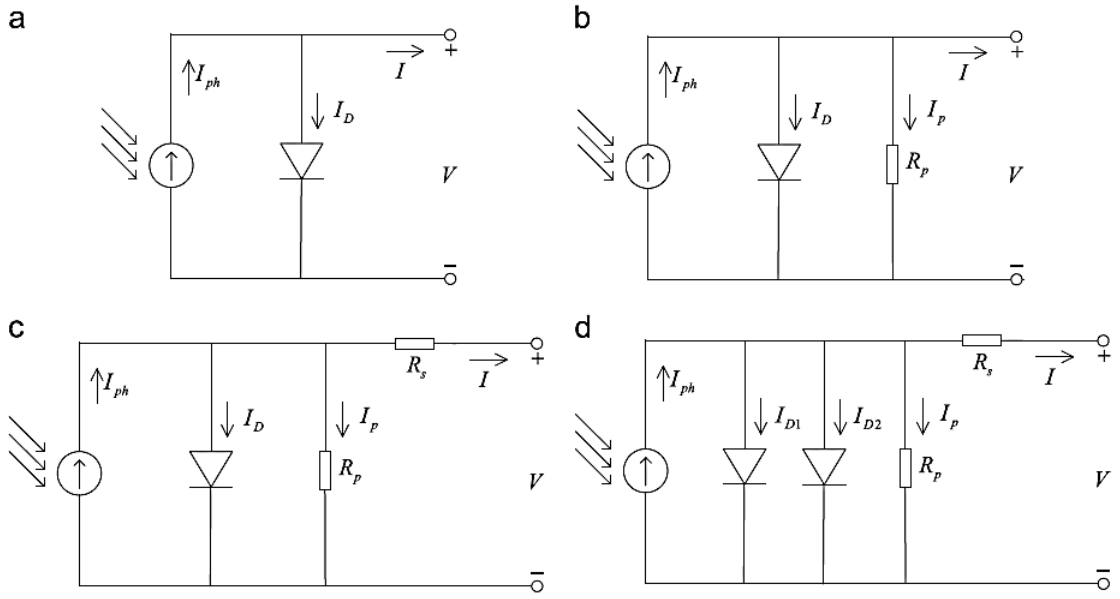


Figure 2.2: Electrical Circuit Representations for Photovoltaic Cells: (a) Ideal Model; (b) Single Diode with Series Resistance (4-Parameter Model); (c) Single Diode with Both Series and Shunt Resistance (5-Parameter Model); and (d) Dual Diode Model (7-Parameter Model)

software, aiming to enhance the analysis and optimization of PV-powered pumping system installations. This particular model, grounded in four distinct parameters, facilitated simulations across three unique types of PV panels: thin film, polycrystalline silicon, and monocrystalline silicon, each varying in construction and material properties[50]. Despite its applications, recent researchers have highlighted the limitations of the 4-p model, especially its omission of shunt resistance effects, proving it insufficient for accurately fitting experimental current-voltage (I–V) and power-voltage (P–V) data during current-source operations. Comparative studies between the four-parameter and the more comprehensive five-parameter PV models reveal that the former falls short in accurately capturing the impact of elevated temperatures on electrical current. This leads to predictions of current that are less precise than those derived from the five-parameter model [51], underscoring the necessity for models that can more faithfully represent PV cell behavior under a broader range of conditions.

Enhancing the precision of simulation models necessitates the inclusion of parallel (shunt)

resistance alongside series resistance in the one-diode framework. This approach culminates in the creation of the five-parameter (5-p) model, illustrated in Figure 2c and mathematically formulated in Equation (3). This model is celebrated for its ability to provide a more accurate representation of PV device behavior by accounting for both series (Rs) and parallel (Rp) resistances, which are pivotal in shaping the current voltage (I–V) characteristics of PV devices. Specifically, Rp tends to diminish the electrical current that can be harnessed, whereas Rs influences the output voltage.

$$I = I_{\text{ph}} - I_D - I_p = I_{\text{ph}} - I_0 \left(e^{\frac{V+IR_s}{V_t}} - 1 \right) - \frac{V + IR_s}{R_p} \tag{2.1}$$

Where:

- I_{ph} represents the photocurrent (A),
- I_D denotes the diode current,
- I_p denotes the parasitic current,
- I_0 is the diode's saturation current (A),
- R_s is the series resistance,
- R_p is the parallel (shunt) resistance,
- $V_t = \frac{nKT}{q}$ is the thermal voltage of the diode, where n is the ideality factor, k is Boltzmann's constant, q is the elementary charge, and T is the cell temperature.

Recent advancements in this area include innovative methodologies for deriving the five critical parameters of this model, pioneered by researchers such as Bai et al[52]. The efficacy of the 5-p model has been validated through practical assessments, including the analysis of a 3.2 kW photovoltaic system's dynamic performance under real-world conditions, and the modeling of output from PV modules under partial shading scenarios [53]. A thorough examination of the 5-p model has been undertaken in recent literature, discussing the

model's foundational mathematics, the techniques for parameter extraction, and the core assumptions and simplifications employed [54]. The collective findings from these studies underscore the extensive research dedicated to refining the 5-p model, offering insights for its enhancement or simplification. These efforts have led to the identification of the five essential parameters (IL, I0, Vt, Rs, Rp) required for the model, with the resultant models achieving commendable levels of accuracy and reliability in simulating PV system performance [55] [56] [57].

2.2.4 The Dual-Diode Model

While the widely adopted single-diode model offers a reasonable degree of precision in simulating photovoltaic (PV) cell behavior, it simplifies the complexity of the saturation current, which arises from the combined effects of charge diffusion and recombination within the space-charge layer[58]. Essentially, the saturation current is influenced by two distinct processes, each analogous to a Shockley diode, leading to the conceptualization of the dual-diode model, also referred to as the double-diode model . This model integrates both processes into its framework, aiming to enhance the accuracy of PV cell simulations. Figure 2d showcases the schematic representation of this more sophisticated electrical circuit, and the corresponding mathematical model is articulated, capturing the nuanced dynamics of PV cell operation more effectively.

$$I = I_{\text{ph}} - I_{D1} - I_{D2} - I_P = I_{\text{ph}} - I_{01}\left(e^{\frac{V+IR_s}{V_{t1}}}\right) - I_{02}\left(e^{\frac{V+IR_s}{V_{t2}}} - 1\right) - \frac{V+IR_s}{R_P} \qquad (2.2)$$

In the two-diode model, ID1 and ID2 represent the currents flowing through each of the two diodes, respectively. This model, akin to the five-parameter model that incorporates series (Rs) and shunt (Rp) resistances, shows how these resistances influence the PV device's output in terms of voltage and current. Notably, the dual-diode approach excels in precision, especially under conditions of low sunlight exposure and during instances of par-

tial shading . However, the addition of a second diode introduces complexity by increasing the total count of parameters needed for computation. Equation 2.2 highlights the model's complexity, featuring a nonlinear equation with two exponential terms and as many as seven variables, thereby extending the computational duration . Moreover, the model's intricacy is further amplified by the introduction of additional coefficients, escalating the computational demands [59]. Efforts to streamline the computational process of the two-diode model have largely fallen short of significantly reducing its complexity . A common simplification involves setting the diode ideality factors at n1=1 and n2=2, approximating the Shockley-Read-Hall recombination within the space charge region of the photodiode [60]. Despite its frequent application, this assumption does not universally apply, leading to potential inaccuracies [61]. An enhanced version of the two-diode model was proposed, which simplifies the current equation to rely on only four parameters, requiring ID1 and ID2 to be equal in magnitude. This adjustment, while expedient, may compromise the model's accuracy in favor of reduced computational time. The higher accuracy of the two-diode model in depicting PV cell behavior is acknowledged, yet it was not chosen for this study due to two main reasons. Firstly, the additional recombination effects modeled by the second diode are predominantly relevant at low voltages and under low irradiance conditions [62]—scenarios not typically prioritized in simulation studies. Secondly, the determination of parameters becomes exceedingly complex with the incorporation of an extra diode. This complexity, alongside the specific focus and scope of the study, led to the decision against employing the two-diode model, despite its potential for enhanced accuracy in certain applications.

2.2.5 Characterization of Photovoltaic Systems

The I-V characteristic curve of a photovoltaic (PV) module is pivotal for delineating its electrical performance under varying irradiance and temperature conditions, serving as a critical indicator of efficiency, maximum power output, and environmental adaptability. This curve is instrumental in optimizing PV system design and deployment to maximize

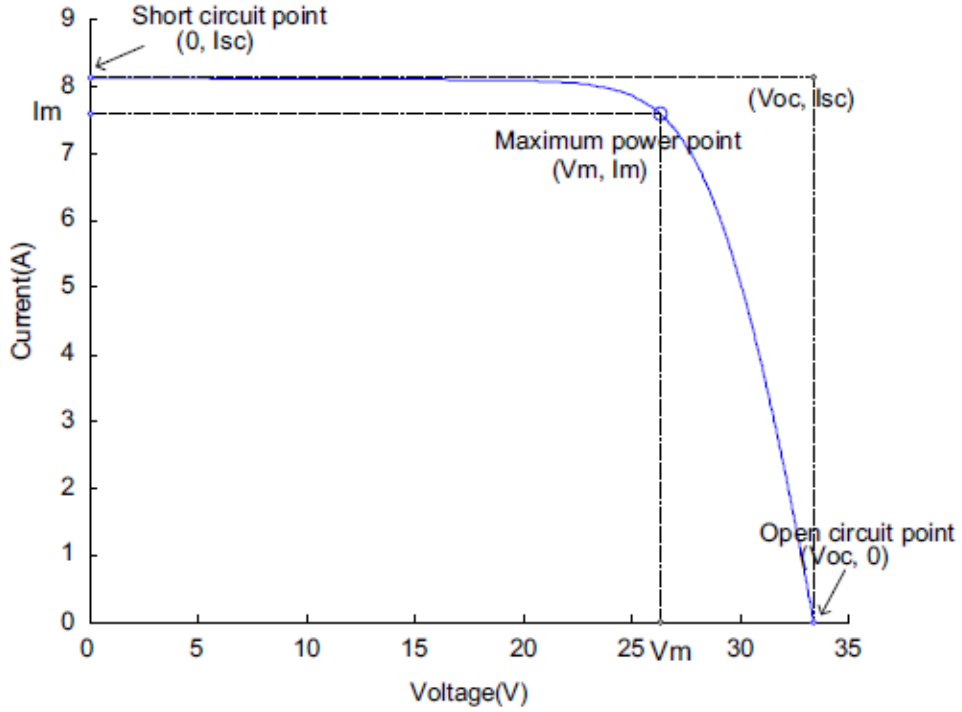


Figure 2.3: I-V Characteristic Curve of a PV Module Highlighting Three Key Points

energy production. It features three essential points for evaluating module performance: the open-circuit voltage (Voc), indicative of the highest voltage output without load; the short-circuit current (Isc), representing the peak current when terminals are shorted; and the maximum power point (MPP), where current and voltage product peaks, marking the optimal power output. These points, affected by factors like cell technology, temperature, and irradiance, are key to system efficiency, guiding performance analysis, system design, and quality assurance. Understanding and leveraging the I-V curve ensures PV systems are designed and operated for optimal efficiency and reliability.[63]

2.2.6 MPPT Techniques for PV Systems

Tracking the Maximum Power Point (MPP) is a critical component of photovoltaic (PV) systems, essential for optimizing energy production, especially under consistent irradiance. This topic has been extensively explored for scenarios with a singular MPP in the power-

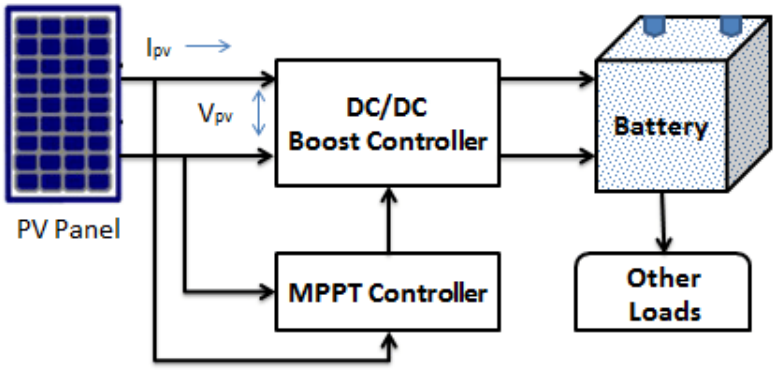


Figure 2.4: General scheme of a PV with an MPPT system

voltage (P-V) curve. Challenges arise, however, with varying solar irradiance due to factors like partial shading from clouds, obstructions, or debris, leading to multiple peaks within the P-V curve. Consequently, an MPPT algorithm must identify the global MPP amidst several local maxima, necessitating a versatile approach as no single MPPT method guarantees optimal performance across all conditions for a PV generator. Selecting an MPPT solution for a specific PV setup involves considering various factors to meet the system's unique requirements. Ideally, an effective MPPT technique should: accurately pinpoint the global MPP in shaded conditions, adapt swiftly to changes in weather, operate independently of the PV array configuration, maintain stability and robustness against environmental and panel parameter fluctuations, and be straightforward to implement, minimizing computational demands and costs. Implementing MPPT in PV systems necessitates both hardware and software components. The software encompasses the MPPT algorithm and a closed-loop controller, which utilizes a reference signal (such as voltage or duty ratio) generated by the MPPT algorithm. This signal guides the controller to adjust the PV array's terminal voltage towards the Maximum Power Point (MPP), typically by modulating the duty ratio of a Pulse Width Modulation (PWM) signal directed to the power switches in the inverter/converter. Grid-connected PV systems predominantly employ either a single-stage or two-stage inverter structure. The single-stage inverter combines MPPT and grid power

control into one operation, whereas the two-stage structure separates these controls. Various power conversion structures detailed in the literature impact power quality aspects like system stability and dynamic response but do not influence the system's ability to reach the global MPP, a task determined by the MPPT algorithm.The initial PV system employing MPPT technology debuted in 1968 for space applications. Since then, the development of MPPT controllers has surged, enhancing their reliability, accuracy, tracking speed, efficiency, and ease of use. An ideal MPPT algorithm is characterized by its quick response time and minimal oscillation around the PPP, making it adept at adapting to swift changes in output power. To date, a vast array of MPPT control techniques have been implemented, designed to either navigate towards the MPP under consistent irradiance conditions or to manage PV systems characterized by multiple maximum power points (MMPP). Various classifications of MPPT controllers have been introduced, typically dividing them into conventional methods and advanced (soft computing) methods. Conventional MPPT techniques, established quite sometimes ago, are widely recognized for their simplicity and straightforward implementation, primarily suited for tracking a single MPP under uniform irradiance conditions. On the other hand, advanced MPPT strategies, often referred to as soft computing, bio-inspired (BI), or artificial intelligence (AI) methods, present a more complex approach but offer enhanced tracking performance compared to their conventional counterparts.[64](See figure Figure 2.4)

Conventional MPPT Methods

Two traditional MPPT algorithms stand out for their widespread adoption in commercial applications, are known for their effectiveness, and are often integrated with more sophisticated techniques to enhance tracking precision and speed. These algorithms are Perturb & Observe (P&O) and Incremental Conductance (INC).

1. Perturb & Observe (P&O):The Perturb & Observe (P&O) method, also known as hill climbing, operates by periodically adjusting (either increasing or decreasing) the

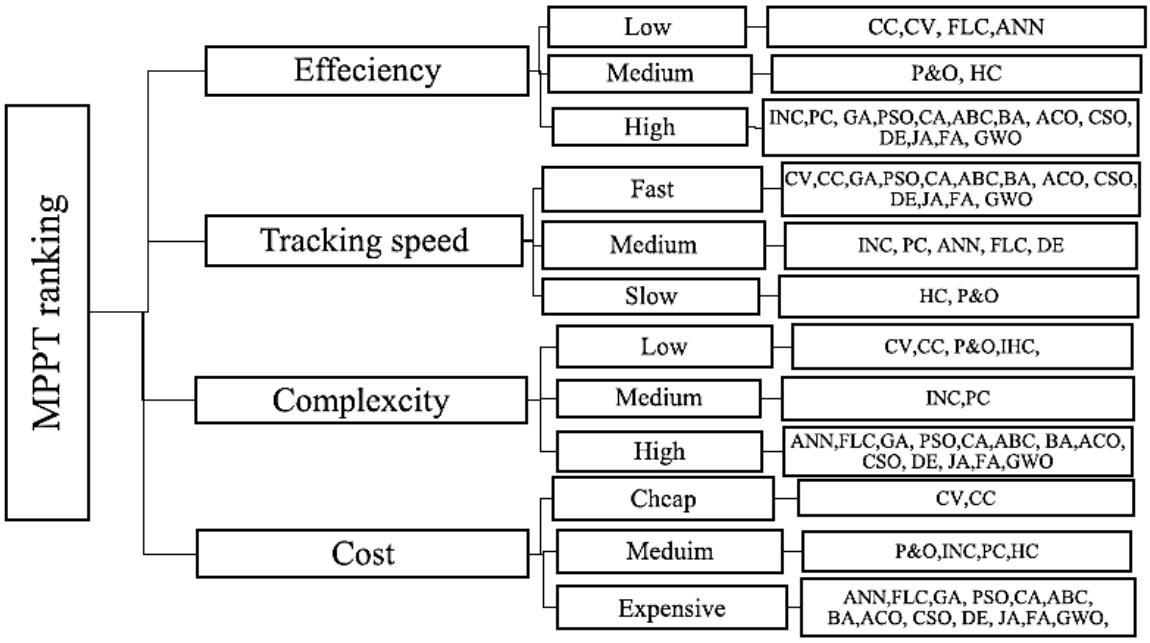


Figure 2.5: MPPT General Classification

voltage at the terminals of the PV arrays and then comparing the current power output P(k) with the previous one P(k-1) to decide the direction of the next adjustment. If a change leads to an increase in power from the PV array, the same direction of adjustment is continued; if not, the direction is reversed. This process iteratively guides the system towards a state of equilibrium around the Maximum Power Point (MPP), as depicted in the flowchart in Figure 2.6. The P&O algorithm is favored for its straightforward implementation and reliable tracking under stable irradiance conditions. Nonetheless, it may encounter difficulties in identifying the true MPP under variable shading, often settling at local maxima instead. The method also necessitates a balance between tracking accuracy and the magnitude of oscillation near the MPP. Smaller perturbation steps enhance precision but reduce tracking speed, whereas larger steps increase speed at the expense of causing significant oscillations around the MPP. To refine both tracking speed and precision, several adaptations of the P&O method have been developed, including versions with variable step sizes and the dP&O method. These adaptations generally involve adjusting the perturbation

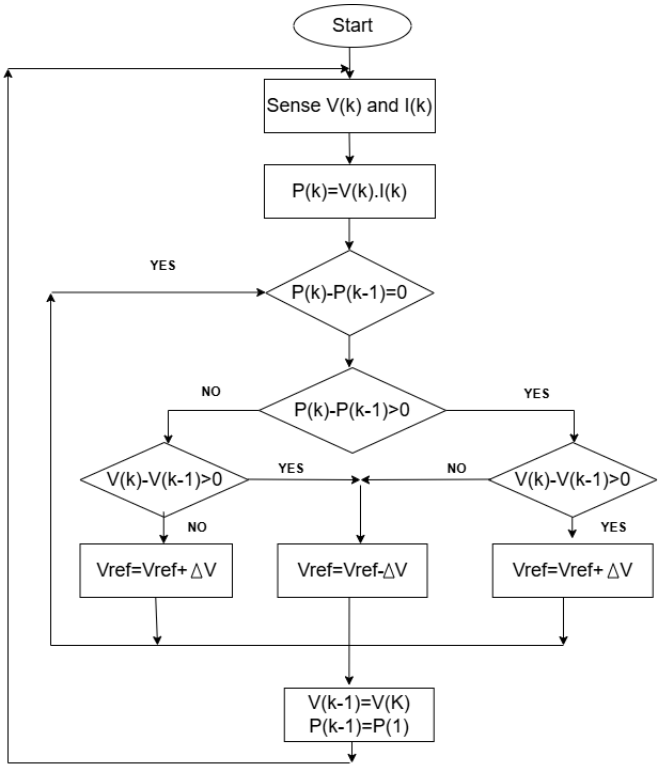


Figure 2.6: flowchart of Perturb & Observe (P&O)

step size dynamically throughout the tracking process: larger steps are used to quickly approach the MPP from a distance, while smaller steps are employed near the MPP to minimize oscillations, allowing the step size to be adjusted based on the slope of the P-V curve and the proximity to the MPP.[65]

$$D(k) = D(k-1) \pm N \cdot \Delta\delta \tag{2.3}$$

Where:

- N represents a scaling factor crucial for defining the MPPT (Maximum Power Point Tracking) system's efficiency, established through the system's tuning phase.
- $\Delta\delta$ denotes the variable component of the duty ratio, which may take forms such as $\frac{\Delta P}{\Delta V}$, $\frac{\Delta P}{\Delta I}$, $\frac{\Delta P}{\Delta D}$, or simply ΔP, where:
  - ΔP is the variation in power,

- ΔI is the change in current,
- ΔV is the alteration in voltage,
- ΔD is the shift in the duty ratio.

These parameters are measured during the preceding sampling interval.

1. 2. Incremental Conductance (INC) : The Incremental Conductance (INC) MPPT technique operates on the principle that at the Maximum Power Point (MPP), the rate of change of output power, P, with respect to voltage, V, equals zero (i.e., $\frac{dP}{dV} = 0$). Consequently, differentiating the power equation $P = IV$ yields the foundational formula for this method.[66]

$$\frac{dP}{dV} = V\frac{dI}{dV} + I = 0 \quad \text{(At the MPP)} \tag{2.4}$$

Hence, within one sampling period, this becomes:

$$\frac{\Delta I}{\Delta V} = -\frac{I}{V} \tag{2.5}$$

By comparing the incremental conductance $\frac{\Delta I}{\Delta V}$ to the instantaneous conductance $-\frac{I}{V}$, the direction for the next perturbation is established in the Incremental Conductance (INC) MPPT method. If $\frac{\Delta I}{\Delta V} > -\frac{I}{V}$, then the reference voltage V_{ref} is increased; if $\frac{\Delta I}{\Delta V} < -\frac{I}{V}$, V_{ref} is decreased. When neither condition applies, the Maximum Power Point (MPP) has been reached. Different from the Perturb & Observe (P&O) method, INC remains stable and does not deviate from the MPP with sudden changes in irradiance. Nonetheless, because INC relies on the slope of the current versus voltage (I-V) curve to inform its next perturbation direction, it demands highly accurate current and voltage sensors. Inaccuracies could lead to misdirection in the perturbation process, especially due to the flatness of the I-V curve on the MPP's left side. Similar to the P&O method, the concept of variable step size tracking can enhance INC's efficiency

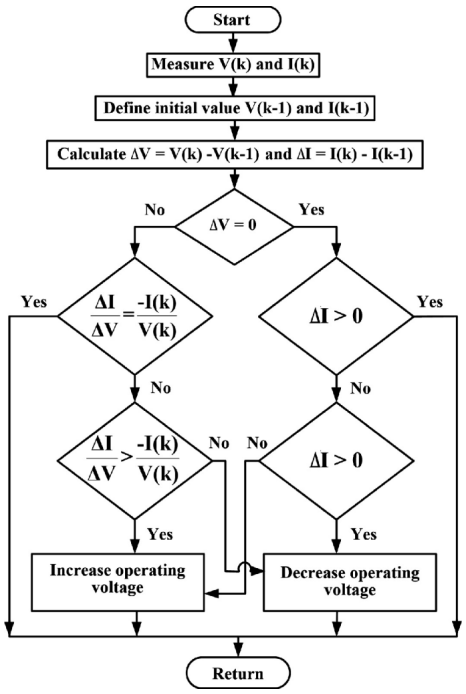


Figure 2.7: flowchart of Incremental Conductance (INC)

as depicted in the flowchart in Figure 2.7.

Intelligent MPPT Method

The traditional MPPT techniques mentioned earlier, along with their variations, perform well in uniform irradiance environments. Yet, they often struggle to identify the global MPP in situations of non-uniform irradiance. Global optimization strategies, particularly Artificial Intelligence (AI) algorithms, excel in addressing complex, nonlinear real-world challenges, surpassing the capabilities of basic mathematical approaches. These include computational techniques inspired by natural phenomena, such as swarm intelligence, neural networks, evolutionary algorithms, fuzzy logic, etc. The subsequent section will explore various AI-based MPPT strategies, providing concise explanations of each method to help readers grasp their operational principles swiftly.[67]

1. Artificial Neural Network (ANN): are employed for a wide range of applications including system modeling, optimization, simulation, and performance prediction. Their

popularity has surged in recent years, attributed to their rapid processing capabilities and high levels of accuracy. ANNs mimic the data processing mechanisms of the human brain, utilizing neurons as the fundamental units of computation, much like the biological networks found in nature. In these networks, dendrites act as receivers of input signals, the cell body functions akin to a processor, synapses serve as connections, and axons transmit output signals to subsequent neurons, facilitating non-linear computations. The architecture of an ANN is composed of numerous neurons, or processing units. Similar to the cognitive processes of the human brain, ANNs operate by learning and memorizing through a network of interconnected links known as weights. Each neuron aggregates inputs from others based on these weights, applies a non-linear activation function to these inputs, and produces an output.[68]This output can be relayed to other neurons, with the process continuing across layers in the network. Within the realm of solar energy collection systems, the predominant Artificial Neural Network (ANN) models employed are: Multi-Layer Feedforward Neural Network (MLFFNN) and Artificial Neuro-Fuzzy Inference System (ANFIS).

1.1 Multi-Layer Feedforward Neural Network (MLFFNN): A Multi-Layer Feedforward Neural Network (MLFFNN) see figure 2.8 , showcasing its foundational architecture. This model primarily encompasses three types of layers: an input layer, one or several hidden layers, and an output layer. Within this structure, each neuron processes input data received from preceding neurons, conveys it through the hidden layers, and directs it towards the output layer. These neurons, acting as interconnected processing nodes, collectively constitute an ANN. The output generated by each neuron derives from a weighted combination of its inputs, with the aggregated sum of these weighted inputs being formulated by the neurons is given as:[69]

$$X = \sum_{i=1}^{n} (w_{ij} a_i + b_j) \tag{2.6}$$

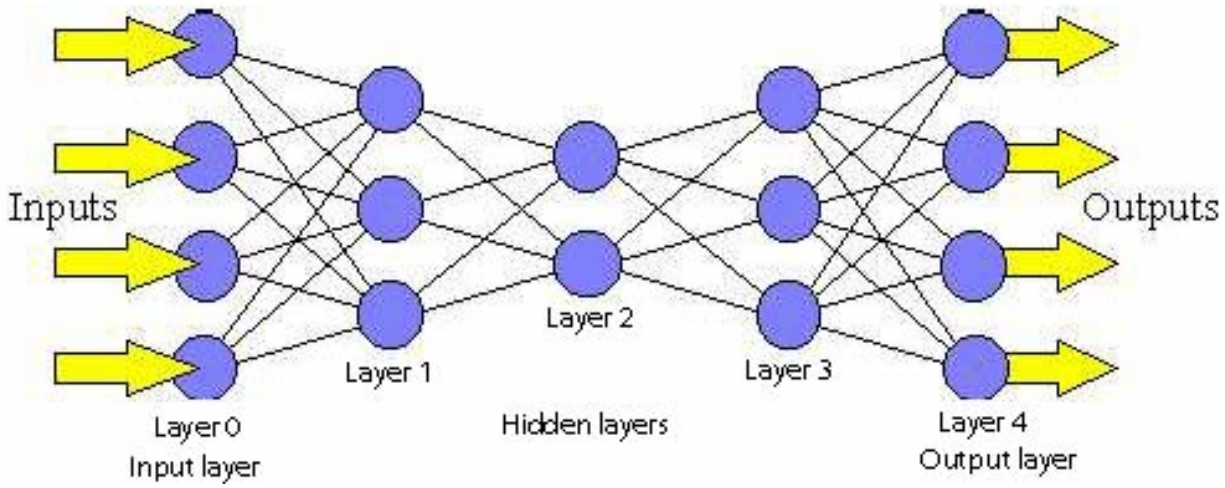


Figure 2.8: Basic structure of MLFFNN

In this context, n represents the total number of input data $i = 0, 1, 2, 3, \ldots, n$, where w_{ij} denotes the interconnecting weights associated with each input data a_i, and b_j signifies the bias allocated to the neuron. The knowledge within the network is encapsulated in the configuration of these connection weights and biases. The inputs, after being weighted and combined with the bias, are processed through a transfer function F, as illustrated in Figure 7. The output of this operation is then articulated by Equation 2.7:

$$Y = F(X) = F\left[\sum_{i=1}^{n} (w_{ij}a_i + b_j)\right] \tag{2.7}$$

Typically, both hidden and output layers incorporate an activation or transfer function, which can be either linear or non-linear. A variety of learning algorithms exist to establish the relationships between inputs and outputs, with the feedforward backpropagation learning algorithm being among the most prevalent. A commonly employed non-linear activation function is the sigmoid function, which constrains its output to a range between 0 and 1. The equation for the sigmoid transfer function is provided as follows:

$$F(X) = \frac{1}{1 + e^{-x}} \tag{2.8}$$

For instances where negative values are encountered at the input or output layer, the

hyperbolic tangent sigmoid (tansig) transfer function is utilized. The formula for the tansig transfer function is expressed as:

$$F(X) = \frac{1 - e^{-2X}}{1 + e^{-2X}} \tag{2.9}$$

The model undergoes training with a predefined number of neurons in the hidden layer, alongside specified learning rate, momentum factor, and transfer function settings. The Multi-Layer Feedforward Neural Network (MLFFNN) stands as the most prevalent neural model for predicting the performance of solar collector systems.[70]

1.2 Artificial Neuro-Fuzzy Inference System (ANFIS):ANFIS represents a computational framework that merges the principles of neural networks and fuzzy logic to create a hybrid intelligent system. Figure 2.9. illustrates the fundamental structure of ANFIS. It employs a neural network's learning algorithms alongside fuzzy logic to map input variables to their corresponding target values [71]. ANFIS is structured into five distinct layers:

- Fuzzy Layer (Layer 1): This initial layer features adjustable nodes, denoted by square symbols and labeled as A1, A2, B1, and B2, which receive inputs x and y.
- Product Layer (Layer 2): Known as the product layer, where each node is a fixed node represented by a circle symbol and labeled M. The output from these nodes, w1 and w2, serve as the weight functions for the nodes in the subsequent layer.
- Normalizing Layer (Layer 3): In this layer, all nodes are fixed and labeled N. These nodes normalize the firing strengths by calculating the ratio of an individual node's firing strength to the sum of all firing strengths.
- De-Fuzzy Layer (Layer 4): Represented by square nodes, this layer's function is to defuzzify the inputs received from the normalizing layer into specific outputs.
- Summation Layer (Layer 5): The final layer consists of a single fixed node that

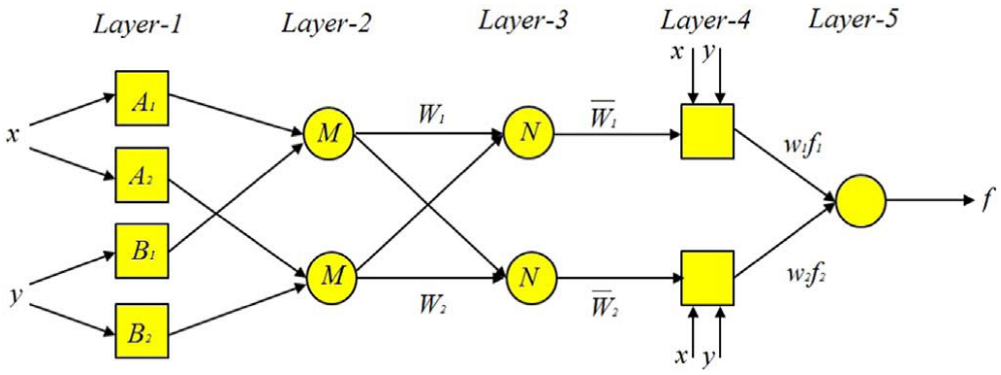


Figure 2.9: Basic structure of ANFIS

aggregates all inputs from the previous layer to produce the system's overall output.

This structured approach allows ANFIS to effectively handle complex modeling and prediction tasks, especially in systems like solar collectors, by leveraging the strengths of both neural networks and fuzzy logic.[72]

1.3 Model performance evaluation criteria: The evaluation of an Artificial Neural Network (ANN) model's performance involves specific criteria aimed at minimizing error metrics and optimizing the fit between the model's predictions and actual observed data. These criteria include the Root Mean Square Error (RMSE), Mean Absolute Error (MAE), Coefficient of Variation (COV), and the coefficient of determination R^2, which assesses the fit quality of ANN-predicted data against actual data.[73]

- Root Mean Square Error (RMSE):

$$\text{RMSE} = \sqrt{\frac{1}{n}\sum_{i=1}^{n}\left(X_A - X_P\right)^2} \tag{2.10}$$

- Mean Absolute Error (MAE):

$$\text{MAE} = \frac{1}{n}\sum_{i=1}^{n}\left|X_A - X_P\right| \tag{2.11}$$

- Coefficient of Variation (COV):

$$\text{COV} = \frac{\text{RMSE}}{\frac{1}{n}\sum_{i=1}^{n} X_P} \times 100 \tag{2.12}$$

Where:

- X_A represents the actual observed data,
- X_P represents the predicted data from the ANN model,
- n is the number of observations.

Numerous ANN-based MPPT approaches have been introduced, featuring variations in neural network architectures, control mechanisms, and the selection of inputs and outputs. Incorporating ANN into MPPT systems can enhance their efficiency through several strategies, including:

(a) Enhancing the MPPT or controller by leveraging ANN for optimization, such as applying ANN to refine Fuzzy Logic Controllers (FLC) or to enhance the Perturb & Observe (P&O) method;

(b) Integrating ANN with other MPPT methodologies to bolster tracking precision and speed, such as combinations like ANN with P&O or ANN with the three-point tracking method;

(c) Employing ANN in conjunction with advanced control systems to achieve superior control over transient behaviors;

(d) Considering different inputs and outputs for the ANN;

(e) Preprocessing the inputs before feeding them into the ANN.

2. Fuzzy Logic: A Fuzzy Logic Controller (FLC) operates on the principle of "degrees of truth" rather than the boolean logic that underpins conventional computing. The

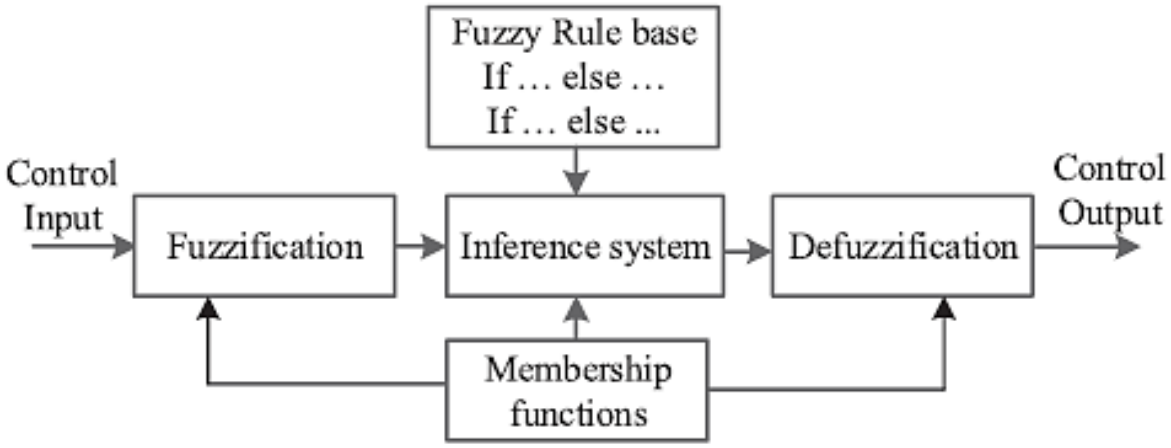


Figure 2.10: A typical structure of the fuzzy system

functioning of an FLC is segmented into three primary phases: fuzzification, inference via a rule base, and defuzzification, as depicted in Figure 2.10. In the initial fuzzification stage, crisp input values are converted into fuzzy sets based on predefined membership functions. The user-defined membership function and rule base serve as the foundation for the subsequent inference process. Following inference, the defuzzification stage is responsible for translating fuzzy set outputs back into crisp values, employing methods such as the center of singletons, a center of gravity, or maximum methods. Given its capacity to handle partial or imprecise data and deliver proximate solutions to complex problems that are challenging for other methodologies, FLC is particularly suited for implementing MPPT. The efficacy of FLC-based MPPT systems can be affected by various factors, including the choice of input/output variables, the selection of membership functions, the approach to defining fuzzy rules (whether fixed or adaptive), and the strategy for integrating with other MPPT methods.[74]

3. Genetic Algorithm (GA): Inspired by Darwin's theory of evolution through natural selection, Genetic Algorithms (GA) are employed to derive high-quality solutions for nonlinear optimization challenges. Solutions within GA are represented as binary arrays, known as chromosomes, and the set of these solutions forms a population that

evolves over generations to enhance their fitness values. GA operates through four primary mechanisms: selection, crossover, mutation, and acceptance, structured into the following steps:[75]

(a) **Initialization:** Begin by generating a random population of n chromosomes.

(b) **Evaluation:** Determine the fitness value for each chromosome in the population.

(c) **Solution Generation:** Create new solutions via:

- **Selection:** Select two parent chromosomes based on fitness values.
- **Crossover:** Generate offspring from parents based on a predefined crossover probability, while non-crossed parents proceed to the next generation.
- **Mutation:** Introduce mutations to the offspring at a certain probability to diversify the population.
- **Acceptance:** Combine the new offspring to form the updated population.

(d) **Termination:** End the process if a specific termination criterion is met.

(e) **Iteration:** If not terminated, evaluate the new population's fitness and repeat the generation process.

Although GA's inherent slow tracking speed makes it less directly applicable to MPPT issues, it is often utilized to optimize other MPPT strategies, enhancing both tracking speed and precision. For instance, GA has been applied to refine the parameters of Fuzzy Logic Controller (FLC) based MPPTs for photovoltaic (PV) systems, as well as to train Radial Basis Function Network (RBFN) models for predicting optimal MPP voltage and current in Grid-connected PV systems, using irradiance and temperature data as inputs.

These GA-optimized MPPT methods outperform their non-optimized counterparts in tracking accuracy. Additionally, GA has been proposed for the economical design of

Grid-connected PV systems with multiple inverters, optimizing system size and configuration by focusing on maximizing the net present value and adhering to electrical constraints.[76]

4. Evaluation and Ranking of MPPT Methods: The assessment of MPPT methods in the literature involves various factors, often used to provide a general evaluation, with some being approximate measures due to their imprecision. There is no definitive ranking for MPPT methods, as their suitability can vary depending on application needs, tracking speed, efficiency, complexity, and cost. However, Figure **??** serves as a summarized visual guide, providing an at-a-glance overview of MPPT methods ranked according to the discussed factors. The validity of these comparisons is based on an aggregation of results from multiple studies, acknowledging that some are simulation-based while others are experimental. This leads to the understanding that the rankings presented are approximations representing a consensus from the literature. This ranking intends to streamline the selection process, offering a straightforward reference based on commonly understood and clear parameters. This aids in choosing the most appropriate MPPT method tailored to specific system requirements and constraints.[77]

2.3 Global modeling of the variable speed wind system

Wind turbine systems with variable speed capabilities typically incorporate different generators tailored to specific operational requirements. The Doubly Fed Induction Generator (DFIG) and the Permanent Magnet Synchronous Generator (PMSG) are among the most prevalent choices in such systems. DFIGs and PMSGs are favored for their distinct benefits and are chosen based on a balance of factors, including cost-effectiveness, energy efficiency, the intricacy of control systems, and the frequency of maintenance. For an in-depth comparison of their respective advantages and trade-offs. Table 2.1summarizes the general characteristics of both DFIGs and PMSGs in variable-speed wind systems. It should be noted that

specific models and implementations can vary, and technological advancements continue to evolve the capabilities and features of both generator types. This ongoing development can lead to a broadening of the applications and performance enhancements of these generators in wind energy systems.[78]

Table 2.1: Comparative Table of DFIGs and PMSGs

Feature	**DFIG**	**PMSG**
Power Electronics	Partial-scale converters (25-30% of power rating)	Full-scale converters (100% of power rating)
Operational Speed	Variable speed operation with good efficiency	Variable speed operation with high efficiency
Complexity	More complex due to control of both rotor and grid-side converters	Simpler, especially in direct-drive applications
Maintenance	Higher, due to brushes and slip rings	Lower, often no gearbox and no brushes
Cost	Lower power converter costs, but overall system can be expensive	Higher due to permanent magnets and full-scale converters, but reduced mechanical complexity
Grid Services	Reactive power support and other services	Reactive power capability, dependent on converter design
Efficiency	Efficient over a range of wind speeds	Highly efficient across a wide range of operating conditions
Reliability	Less reliable due to gearbox and brushes	More reliable, especially in direct-drive applications
Cooling Requirements	Typically, standard cooling systems	May require advanced cooling systems due to heat generation

2.4 Description of the wind turbine system

The system is a variable-speed wind turbine that harnesses wind energy to produce electrical power, integrating a PMSG with a power electronic converter and a control mechanism to effectively transform wind energy into electrical power for a load. Wind causes the turbine blades to spin, creating rotational mechanical energy omegam, which in turn powers the PMSG to produce three-phase AC electricity. This AC is then rectified to DC by a PWM rectifier, with the resultant DC stored in a capacitor before delivery to the load. Control

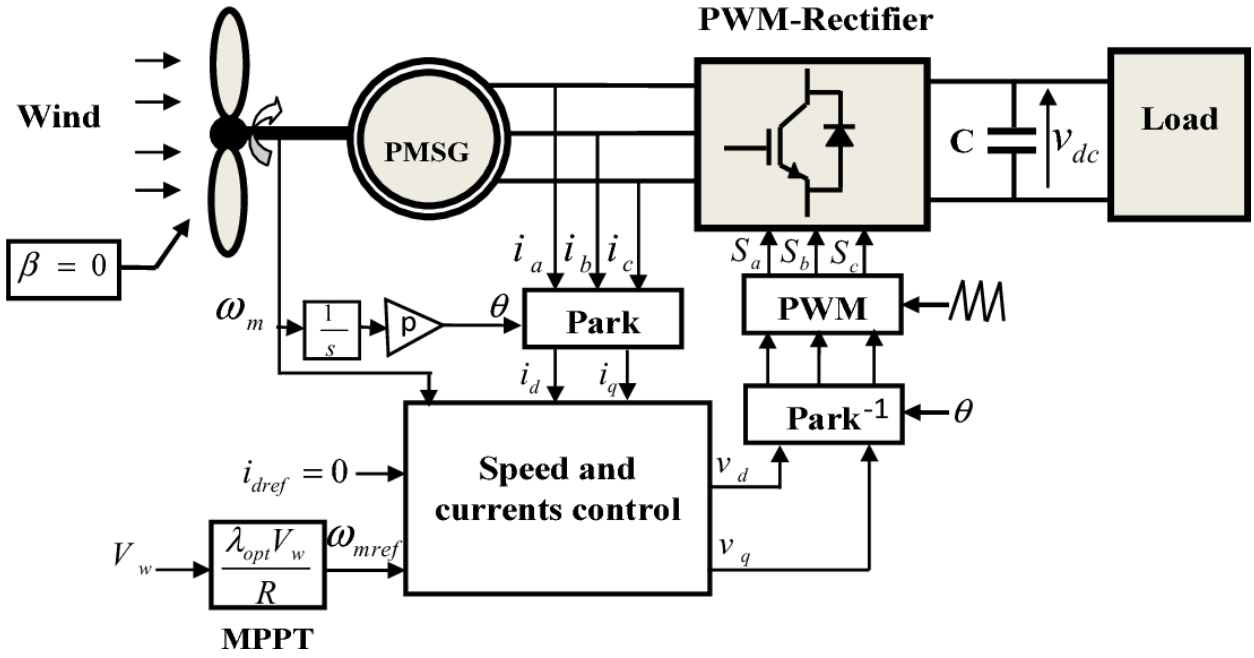


Figure 2.11: wind turbine system Description

systems employing Park's transformation manage the PMSG's output by adjusting its speed and current for optimal performance. Additionally, MPPT ensures the generator operates at maximum efficiency, factoring in wind speed and optimal rotational speed. Finally, the DC power is provided to the load, showcasing the system's capacity to harness wind kinetic energy, convert it efficiently, and control the output for an effective power supply.[79] (see Figure 2.11)

2.4.1 Wind Modeling

Wind is the primary energy source for wind turbines because the kinetic energy contained in the wind is partly transformed into mechanical energy by the turbine, and then into electrical power by the generator. It is appropriate to model wind variation, as the accuracy of the simulations will depend on the quality of the model. Air is modeled by several methods, but in general, the most used is Van Der Hoven's spectral characteristic: The magnitude of the instantaneous wind speed can be expressed as the sum of an average speed and a random

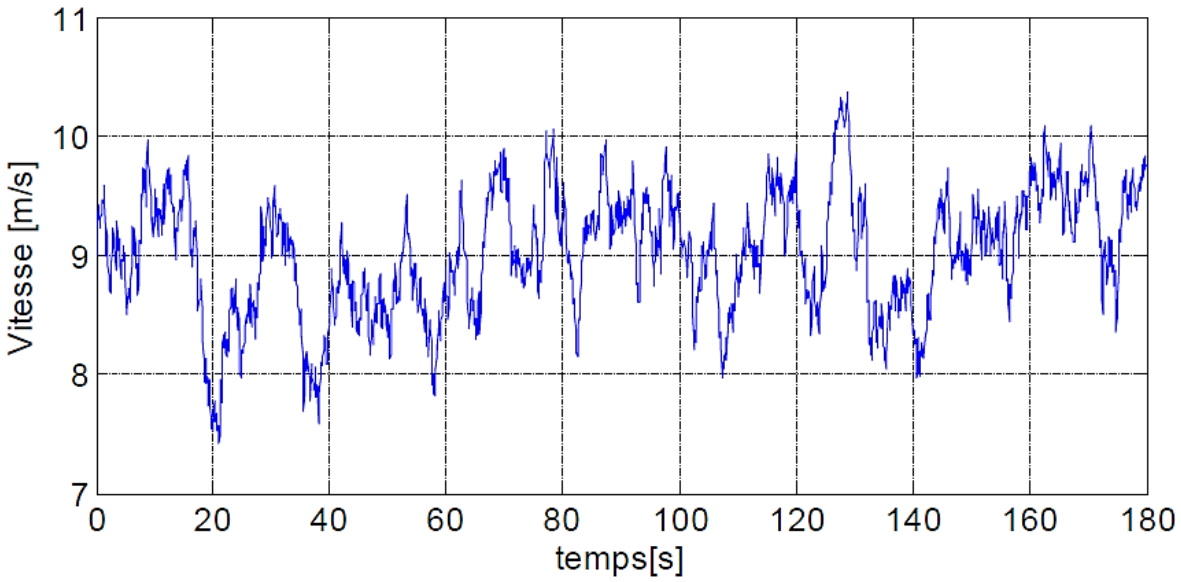


Figure 2.12: wind speed curve

speed [80]. (See figure Figure 2.12)

$$V(t) = V_0 + V_T(t) \tag{2.13}$$

Where:

- $V_T(t)$: The wind perturbation speed or (Gaussian white noise), which is a stationary random process (does not vary with the average wind speed).
- V_0: The average wind speed, which varies regularly over longer periods at a given site.

2.4.2 Wind System Modeling

Three factors determine the relationship between wind energy and the mechanical energy recovered by the rotor: air density, the area swept by the rotor, and wind speed. Air density and wind speed are climatological parameters that depend on the site .[81] The mechanism studied here is composed of a wind turbine with blades of length R driving a generator through a speed multiplier with a gain of G, as shown in Figure 2.13. The wind power or

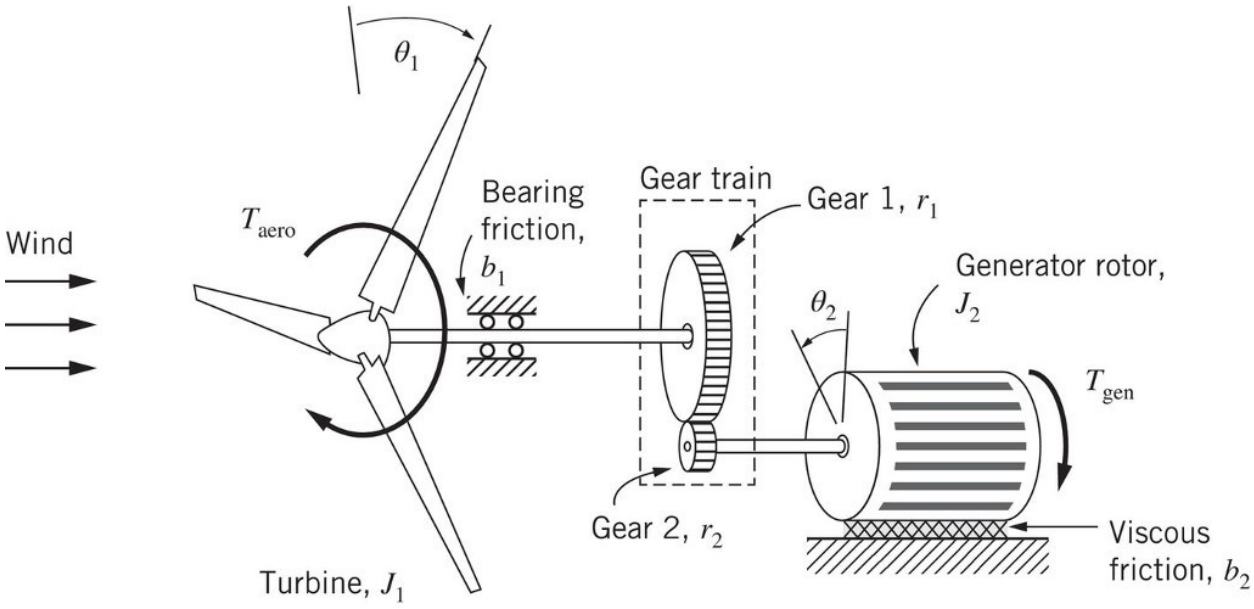


Figure 2.13: Wind System Modeling

wind energy is defined by the following mathematical equation :

$$P_{\text{vent}} = \frac{1}{2}\pi\rho R^2 V^3 \tag{2.14}$$

Where:

- $\rho = 1.25\,\text{kg/m}^3$: The air density or air volume mass under normal conditions of temperature and pressure.
- V: The wind speed.
- R: The blade length.

The aerodynamic power, which is converted by a wind turbine, P_{turbine}, depends on the power coefficient C_P.

$$P_{\text{aer}} = \frac{1}{2}C_P(\beta,\lambda)\pi\rho R^2 V^3 \tag{2.15}$$

And

$$\lambda = \frac{\Omega_t R}{V} \tag{2.16}$$

Where:

- λ: The relative speed representing the ratio between the linear speed at the end of the wind turbine blades and the wind speed.
- Ω_t: The rotation speed of the turbine.

The power coefficient C_P represents the aerodynamic efficiency of the wind turbine. It depends on the turbine's characteristics. Figure 2.14 shows the variation of this coefficient as a function of the speed ratio λ and the blade orientation angle β [82, 83, 84].

Knowing the aerodynamic energy of the wind that is converted by the turbine, one can calculate the aerodynamic torque C_{aer} in (N.m) by the expression:

$$C_{\text{aer}} = \frac{P_{\text{aer}}}{\Omega_t} \tag{2.17}$$

In the context of this thesis, we use an approximation of the power coefficient by analytical functions based on the relative speed λ and the pitch angle of the blades β, whose expression is :

$$C_P = f(\beta, \lambda) = C_1 \left(\frac{C_2}{\lambda_i} - C_3\beta - C_4 \right) \exp\left(\frac{-C_5}{\lambda_i} \right) + C_6\lambda \tag{2.18}$$

With:

$$\frac{1}{\lambda_i} = \frac{1}{\lambda + 0.08\beta} - \frac{0.035}{\beta^3 + 1} \tag{2.19}$$

Where the constants are defined as:

$$C_1 = 0.5176, \quad C_2 = 116, \quad C_3 = 0.4, \quad C_4 = 5, \quad C_5 = 21, \quad C_6 = 0.0068$$

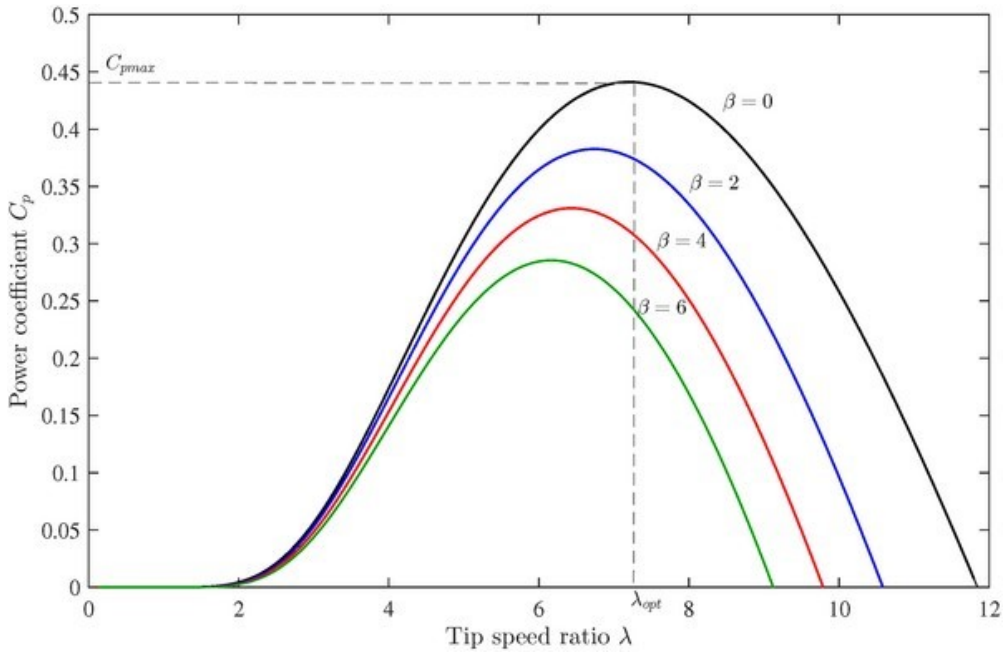


Figure 2.14: The Power Coefficient for Different Pitch Angles

Equation (22) shows that to maintain λ at its nominal or optimal value, and thus maximize the power of the wind turbine, it is necessary to vary the rotation speed Ω_t linearly with the wind speed V. In this case, the optimal nominal rotation speed Ω_t^{nom} for the maximum mechanical transmission of the wind turbine is given by:

$$\Omega_t^{\text{nom}} = \frac{\lambda_{\text{nom}}}{R} V \tag{2.20}$$

Where:

- λ_{nom}: The nominal or optimal tip speed ratio.
- R: The blade length.
- V: The wind speed.

This leads us to plot the characteristics of the optimal aerodynamic power of our variable-speed wind turbine, based on the generator's rotation speed and for different wind speeds according to equation (23), which will become:

$$P_{\text{turbine}}^{\text{nom}} = \frac{1}{2}\pi\rho R^2 V^3 C_P^{\max}(\lambda_{\text{nom}}, \beta_{\text{nom}}) \tag{2.21}$$

Where:

- $C_P^{\max}$: The maximum value of the power coefficient, dependent on the optimal tip speed ratio λ_{nom} and the optimal pitch angle β_{nom}.
- ρ: The air density.
- R: The blade length.
- V: The wind speed.

Modeling of the Gearbox

The gearbox acts as an intermediary between the turbine and the generator. Its purpose is to adjust the turbine's speed Ω_t, which is quite slow, to the generator's speed Ω_{mec}. It is assumed to be rigid and modeled by a simple gain. The elasticity and friction of the gearbox are neglected. Energy losses in the gearbox are considered to be zero. It is a very complex device that we have modeled very simply by the following two equations:[85]

$$C_g = \frac{1}{K} C_{\text{aer}} \tag{2.22}$$

$$\Omega_{\text{mec}} = K\Omega_t \tag{2.23}$$

Where:

- K: Gear ratio.
- C_g: Gearbox torque.
- Ω_{mec}: Generator speed [rad/s].

- C_{aer}: Aerodynamic torque from the turbine.
- Ω_t: Turbine speed [rad/s].

Modeling of Transmission Shaft Dynamic

The fundamental equation of dynamics allows for the determination of the evolution of the mechanical speed from the total mechanical torque T_m applied to the wind turbine rotor:

$$\frac{d\Omega_t}{dt} = \frac{1}{J_t}T_e + \frac{D_G}{J_t}\Omega_t - \frac{1}{J_t}T_m \tag{2.24}$$

Where:

- J_t: The turbine's moment of inertia.
- T_e: The electromagnetic torque.
- D_G: The damping coefficient.
- Ω_t: The turbine speed [rad/s].
- T_m: The total mechanical torque applied to the rotor.

In generator operation, the electromagnetic torque T_e has a negative sign. The block diagram below represents the modeling of the wind turbine shaft associated with the generator model (see Figure 2.15).[86]

Modeling of the Permanent Magnet Synchronous Machine

Synchronous machines represent a significant portion of the electromechanical energy converter market and cover a very wide power range extending up to several MW. Traditionally, high power remains the domain reserved for electricity production.

Before developing the mathematical model of the PMSG (Permanent Magnet Synchronous Generator), several important assumptions must be taken into account [87]:

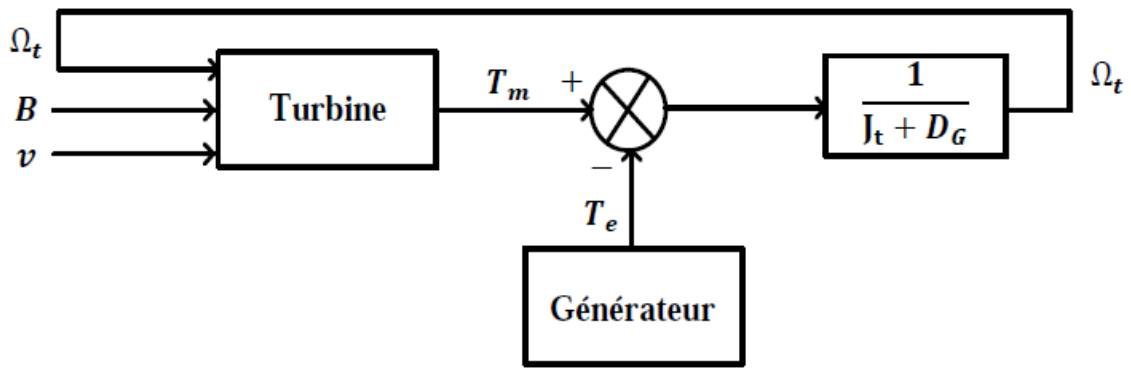


Figure 2.15: Wind Turbine Shaft Model

- The damping effect in the magnets and the rotor are negligible;
- The effects of magnetic saturation are neglected;
- The losses due to eddy currents and hysteresis are neglected;
- The electromotive force (EMF) induced in the stator windings is sinusoidal.

The electrical equation of the PMSG on the stator side in three-phase is:

$$V_a = Ri_a + \frac{d\phi_a}{dt} \tag{2.25}$$

$$V_b = Ri_b + \frac{d\phi_b}{dt} \tag{2.26}$$

$$V_c = Ri_c + \frac{d\phi_c}{dt} \tag{2.27}$$

In matrix form:

$$[V_s] = R_s[I_s] + \frac{d}{dt}[\phi_s]$$

Where:

- V_s: Vector notation for the stator phase voltages (V),

- I_s: Vector notation for the stator phase currents (I),
- ϕ_s: Vector notation for the stator phase fluxes,
- R_s: Stator resistance.

The flux induced on the stator windings for phase a, the total flux ϕ_a, represents the sum of four terms:

$$\phi_a = \phi_{aa} + \phi_{ba} + \phi_{ca} + \phi_{fa} = L_s i_a + M_s(i_b + i_c) + \phi_{fa}$$

Assuming $i_b + i_c = -i_a$, this relationship becomes:

$$\phi_a = (L_s - M_s)i_a + \phi_{fa} = L_c i_a + \phi_{fa} \tag{2.28}$$

Similarly, for the other two phases:

$$\phi_b = (L_s - M_s)i_b + \phi_{fb} = L_c i_b + \phi_{fb} \tag{2.29}$$

$$\phi_c = (L_s - M_s)i_c + \phi_{fc} = L_c i_c + \phi_{fc} \tag{2.30}$$

With:

$$\phi_{fc} = \phi_f \cos(\theta_e + 2\pi/3) \quad \text{and} \quad \phi_{fb} = \phi_f \cos(\theta_e - 2\pi/3)$$

Where ϕ_f is the flux of the permanent magnet.

To simplify the dynamic model of the PMSG, which involves independent relationships and reduces the order of the machine equations, a frame change (Park transformation [88]) is applied. This transforms the three fixed stator coils, phase-shifted by $2\pi/3$, into two equivalent fictitious coils, phase-shifted by π.

The Park transformation matrix is defined as:

$$P(\theta_r) = \frac{2}{3}\begin{bmatrix} \cos(\theta_r) & \cos(\theta_r - 2\pi/3) & \cos(\theta_r - 4\pi/3) \\ -\sin(\theta_r) & -\sin(\theta_r - 2\pi/3) & -\sin(\theta_r - 4\pi/3) \\ 1/2 & 1/2 & 1/2 \end{bmatrix}$$

The equation that translates the transition from the three-phase system to the two-phase (d, q) system is given by:

$$X_{dq0} = P(\theta_r) X_{abc}^T \tag{2.31}$$

To perform the inverse operation, transitioning from the two-phase (d, q) system back to the three-phase system, the following equation is used:

$$X_{abc} = P(\theta_r)^{-1} X_{dq0}^T \tag{2.32}$$

With the inverse Park transformation matrix:

$$P(\theta_r)^{-1} = \frac{2}{3}\begin{bmatrix} \cos(\theta_r) & -\sin(\theta_r) & 1 \\ \cos(\theta_r - 2\pi/3) & -\sin(\theta_r - 2\pi/3) & 1 \\ \cos(\theta_r - 4\pi/3) & -\sin(\theta_r - 4\pi/3) & 1 \end{bmatrix}$$

The model of the machine after the Park transformation in a reference frame linked to the rotating field is given by:

$$u_{sd} = R_s i_{sd} + \frac{d\phi_{sd}}{dt} - P\Omega_{\text{mec}}\phi_{sq} \tag{2.33}$$

$$u_{sq} = R_s i_{sq} + \frac{d\phi_{sq}}{dt} - P\Omega_{\text{mec}}\phi_{sd} \tag{2.34}$$

With the direct and quadrature axis fluxes as follows:

$$\phi_{sd} = L_d i_{sd} + \phi_f \tag{2.35}$$

$$\phi_{sq} = L_q i_{sq} \tag{2.36}$$

The electromagnetic torque of the motor can be expressed as:

$$C_{\text{em}} = \frac{3}{2} P \left[\phi_f i_{sq} + (L_d - L_q) i_{sd} i_{sd}\right] \tag{2.37}$$

Where:

- Ω_{mec}: The rotational speed of the PMSG [rad/s],
- P: Number of pole pairs,
- J: Total rotor moment of inertia,
- f: Friction coefficient [N.m.s/rad],
- C_r: Load resisting torque [N.m],
- L_d: Direct-axis inductance,
- L_q: Quadrature-axis inductance,
- R_s: Stator winding resistance,
- ϕ_f: Flux induced by permanent magnets.

From equations (2.33), (2.34), (2.35), and (2.36), we obtain the mathematical model of the PMSG in the form of a state equation:

$$\begin{bmatrix} \frac{di_{sd}}{dt} \\ \frac{di_{sq}}{dt} \end{bmatrix} = \begin{bmatrix} -\frac{R_s}{L_d} i_{sd} + \frac{PL_q}{L_d} i_{sq} \omega_r \\ -\frac{R_s}{L_q} i_{sq} - \frac{PL_d}{L_q} i_{sd} \omega_r - \frac{P\phi_f}{L_q} \omega_r \end{bmatrix} + \begin{bmatrix} \frac{1}{L_d} & 0 \\ 0 & \frac{1}{L_q} \end{bmatrix} \begin{bmatrix} u_{sd} \\ u_{sq} \end{bmatrix}$$

Using the dq transformation, the active and reactive power is given by:

$$P = \frac{3}{2} \left(u_{sd} i_{sd} + u_{sq} i_{sq}\right) \tag{2.38}$$

$$Q = \frac{3}{2}\left(u_{sd}i_{sq} - u_{sq}i_{sd}\right) \tag{2.39}$$

If the reference frame is such that $u_{qs} = 0$ and $u_{ds} = |V|$, the equations for active and reactive power become:

$$P = \frac{3}{2}u_{sd}i_{sd} \tag{2.40}$$

$$Q = \frac{3}{2}u_{sd}i_{sq} \tag{2.41}$$

As a result, active and reactive power can be controlled by controlling the direct and quadrature current components, respectively.[89]

2.4.3 MPPT control of variable speed wind turbines

The output power of a Wind Energy Conversion System (WECS) depends on the accuracy with which the peak power points are tracked by the system's MPPT (Maximum Power Point Tracking) controller, regardless of the type of generator used [90, 91]. A large number of MPPT techniques for wind turbines have been studied and reported in the literature. These methods are broadly categorized into two main types: Indirect Power Controllers (IPC) and Direct Power Controllers (DPC).

[label=**0**]**Indirect Power Controllers (IPC)**

1.
   - Tip Speed Ratio (TSR) Algorithm
   - Power Signal Feedback (PSF)
   - Optimal Torque (OT) MPPT Algorithm

2. **Direct Power Controllers (DPC)**

   - Hill Climbing Search (HCS) / Perturb and Observe (P&O)

- Incremental Conductance (INC)
- Optimum Relation Based (ORB) MPPT Algorithms
- Hybrid Algorithms
- Adaptive MPPT Algorithm
- Multivariable Perturb and Observe (MVPO)
- Soft computing techniques or intelligent technologies, such as fuzzy logic and neural networks, used independently or in conjunction with other methods to refine MPP tracking.

Each of the above methods has its advantages and disadvantages. The blade pitch control method is applied for strong winds, whereas the other approaches are used for light winds.

2.4.4 Wind turbine operating zones

The wind turbine's output power can be optimized within a defined range of wind speeds, limited by the minimum (cut-in) and maximum (cut-out) operational speeds. Operating the turbine outside this range is discouraged to ensure both turbine and generator safety. The turbine achieves its designated rated power at a certain wind speed. Accordingly, there are four principal operational zones. The first and last zones fall below the cut-in speed and above the cut-out speed, respectively, where it's advised to halt the turbine and disconnect it from the electrical grid to avoid being powered by the generator. The intermediary second zone, lying between the cut-in speed and the rated speed, is where the turbine controller engages the MPPT algorithm to maximize energy extraction. In the third zone, between the rated speed and the cut-out speed, power generation must be controlled to not exceed the turbine's rated capacity, preventing potential damage. Therefore, the MPPT algorithm's primary focus is on optimizing performance in the second zone. See Figure 2.16 In this chapter, we used the optimal torque MPPT method, designed to be effective in both low-wind and high-wind conditions. In this algorithm, as referenced in studies [92, 93], the generator's

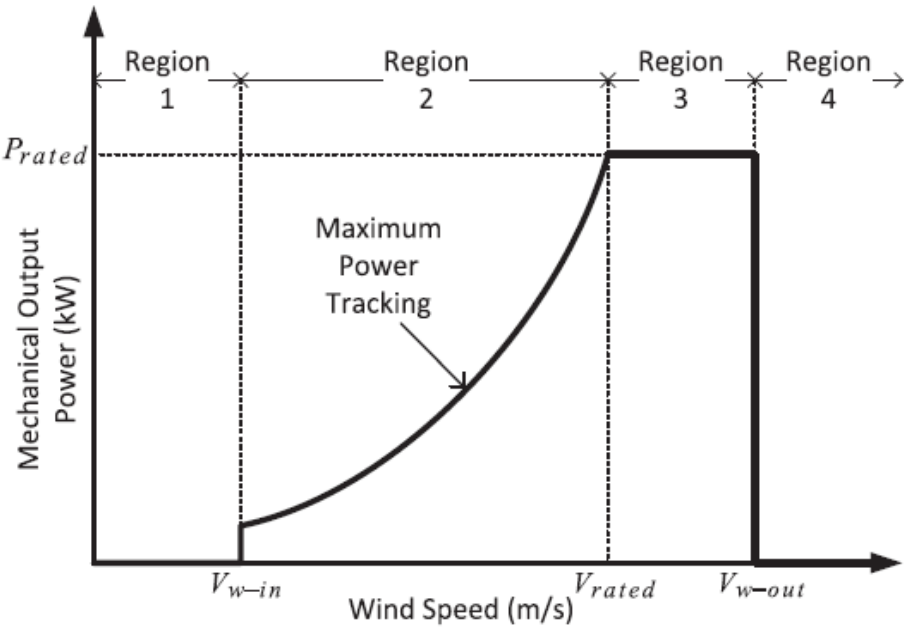


Figure 2.16: Strategy for Controlling Wind Turbines Across Four Wind Speed Zones

torque is regulated to match the optimum torque reference curve, which aligns with the wind turbine's maximum power output for any specific wind speed. According to Equations (17), (20), and (21), the mechanical torque produced by the turbine is calculated based on the variables λ (tip speed ratio) and ω_m (rotational speed). When the rotor operates at the optimal tip speed ratio ($\lambda = \lambda_{\text{opt}}$), it achieves the maximum power coefficient ($C_P = C_P^{\max}$). Consequently, the formula for the turbine's optimum mechanical torque is derived:

$$T_m^{\text{opt}} = \frac{1}{2}\rho\pi R^5 \frac{C_P^{\max}}{\lambda_{\text{opt}}^3}\omega_m^2 = K_{\text{opt}}\omega_m^2 \tag{2.42}$$

Where:

- T_m^{opt}: The turbine's optimum mechanical torque.
- ρ: Air density.
- R: Blade radius.
- $C_P^{\max}$: Maximum power coefficient.

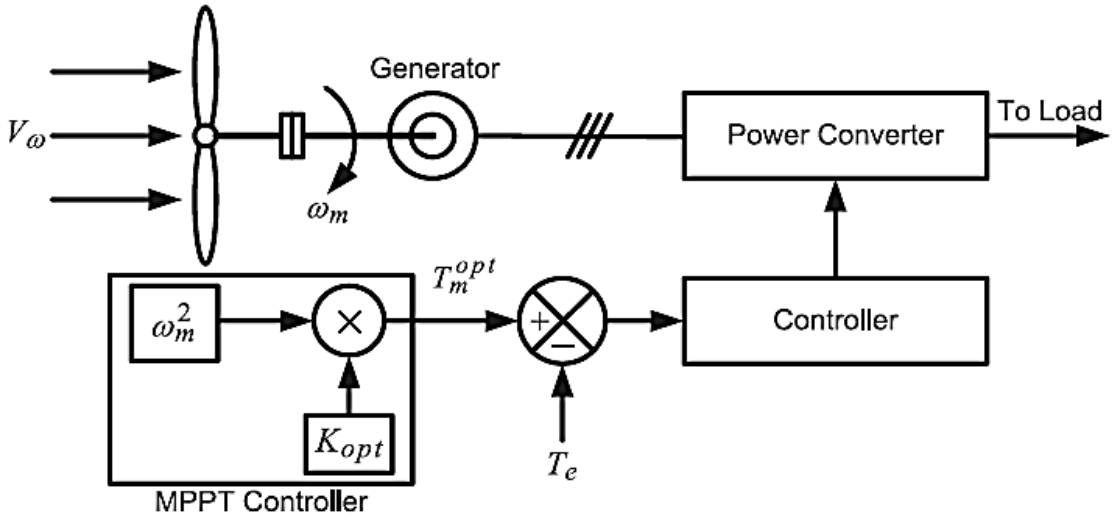


Figure 2.17: Optimal Torque MPPT Algorithm for Wind Energy Conversion Systems

- λ_{opt}: Optimal tip speed ratio.
- ω_m: Rotational speed of the turbine.
- K_{opt}: Optimal constant derived from the physical characteristics of the wind turbine.

Figure 2.17 illustrates the optimum torque curve's characteristics. The formula for optimum torque, detailed in Equation (2.42), serves as the reference torque for the MPPT controller linked to the wind turbine, as cited in references [94]. This reference torque is deducted from the actual torque to generate a control signal for the controller, aiming to reduce the discrepancy between the two.

2.5 Battery modeling

Battery modeling is a sophisticated process that establishes a mathematical framework to replicate and predict the behaviors and performance metrics of a battery under diverse operational scenarios. The core objective of battery modeling encompasses the anticipation of performance parameters, such as capacity, energy efficiency, and life span, which are instrumental in optimizing battery designs to meet specific application requisites. Moreover,

it facilitates precise state-of-charge (SoC) and state-of-health (SoH) estimations, critical for battery management systems to ensure reliability and safety. Modeling approaches range from simple electrical models, leveraging equivalent circuits to mirror the battery's electrical characteristics, to intricate electrochemical models that delve into the internal chemical processes, providing a granular view of ion transport and reaction dynamics. Additionally, thermal models are pivotal, addressing the heat generation and dissipation within batteries, a vital aspect for maintaining operational integrity and prolonging lifespan.[95]

2.5.1 Thevenin model

In The Thevenin model, presented in Figure 2.18 model, Cb denotes a controlled voltage source that emulates the battery's electromotive force (EMF), and its value is influenced by the battery's state of charge (SoC), discharge current Ib, and state of health (SoH). This voltage source is indicative of the open-circuit voltage (OCV) of the battery, which is the voltage measured when the battery is not supplying any current, and it varies with the SoC and temperature. Adjacent to the voltage source is Rint, a resistor symbolizing the internal resistance of the battery. This resistance accounts for the instantaneous voltage drop experienced when the battery delivers or receives current, reflecting the inherent opposition to current flow within the battery's materials.

When a load is connected to the battery, the current ib flows through it. The direction of ib indicates whether the battery is being discharged (positive current) or charged (negative current). The terminal voltage Vt, which is the voltage available across the battery terminals, can be calculated using Ohm's law by subtracting the voltage drop across the internal resistance from the open-circuit voltage, mathematically expressed as:

$$V_t = V_{OC} - R_{\text{int}} i_b \tag{2.43}$$

Furthermore, the state of charge (SoC) is a dynamic parameter that changes with battery

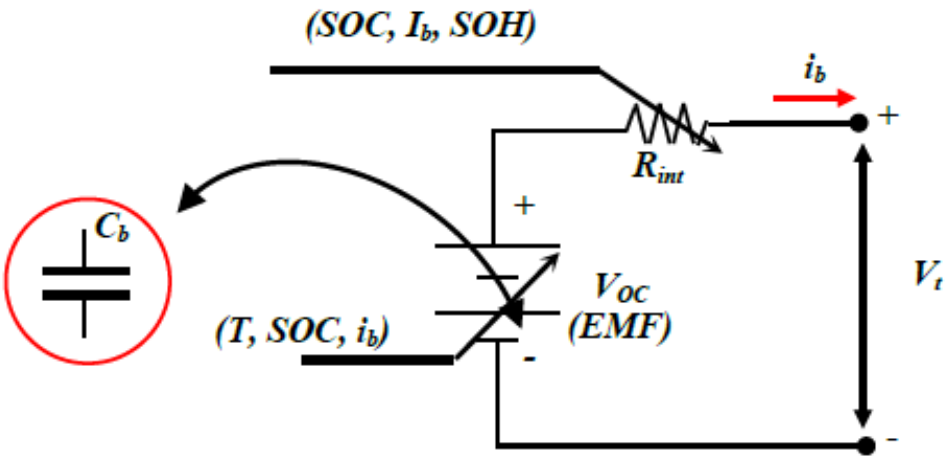


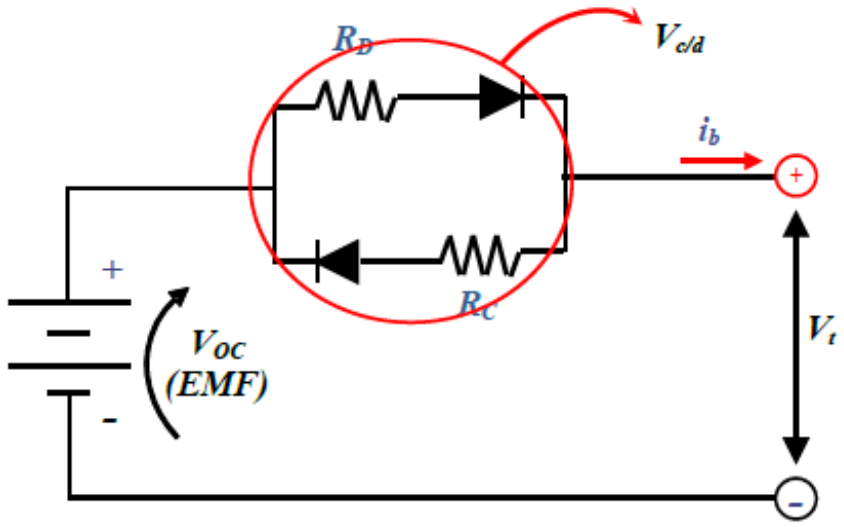
Figure 2.18: Thevenin's electric model for battery

usage, decreasing during discharge and increasing during charging. It is updated over time based on the current i_b using the integral of the current with respect to time, factoring in the rated capacity of the battery. This model serves as a fundamental tool in battery management systems, enabling the monitoring and control of battery performance. To ensure accuracy, the parameters V_{OC} and R_{int} are often derived from experimental data, reflecting their dependency on SoC, temperature, and other conditions. The precision of this model makes it widely applicable in various scenarios, from small-scale electronics to large energy storage solutions.

In this model, the open-circuit voltage V_{OC} encompasses the voltage generated by the theoretical free Gibbs energy, overpotentials (η), and losses due to defects.

2.5.2 Thevenin Model Including Hysteresis Effect

Figure 2.19 explain With two resistances R_D and R_C, this electrical model differentiates between the ions in mobility during charging and those during discharging. This resistance difference affects the trajectory taken by the battery voltage V_t during charging and/or discharging, according to Equation (52):



h!

Figure 2.19: Thevenin model including the charge/discharge hysteresis effect

$$V_t = V_{OC} - R_{c/D} i_b \tag{2.44}$$

Where:

$$R_{C/D} = (\alpha R_D - \alpha R_C), \quad \alpha = 1 \text{ during discharge and } \alpha = 0 \text{ during charging.}$$

The diodes in the model do not have a physical or mathematical significance; their use implies that only one resistance R_D is functional during the battery's discharge and R_C during charging.

2.5.3 Dynamic model including the polarization effect

To include the phenomenon of diffusion at the electrode-electrolyte interface, identified as the Electric Double Layer (EDL), and based on the Gouy-Chapman model, a polarized capacitor (C_p) is integrated,see Figure 2.20. This model also considers the effect of transient currents observed in various applications (e.g., EV and/or HEV in urban traffic) during changes in regime (C-rate) or phase (charge/discharge). The model is formulated and expressed by the

following equations:

$$\dot{V_p} = \frac{dV_p}{dt} = -V_p \frac{1}{R_{C/D} C_p} + V_{OC} \frac{1}{R_{C/D} C_p} - i_p \frac{1}{C_p} \tag{2.45}$$

And:

$$V_t = V_p - R_b i_b \tag{2.46}$$

Where:

- V_p: The voltage across the polarized capacitor C_p.
- V_{OC}: The open-circuit voltage.
- $R_{C/D}$: The resistance during charging/discharging.
- C_p: The capacitance of the polarized capacitor.
- i_p: The current through the polarized capacitor.
- R_b: The battery's internal resistance.
- i_b: The current through the battery.
- V_t: The terminal voltage of the battery.

2.5.4 2nd Thevenin model including the polarization effect

The polarization effect is represented differently in this model by adding a pair of elements (R_{pc}) in series to reproduce the gradual drop or overvoltage (ΔV) caused by transient fluctuations (start and end of phase in charging and/or discharging). The following equations express this model:

$$i_b = \frac{V_p}{R_p} + C_p \frac{dV_p}{dt} \tag{2.47}$$

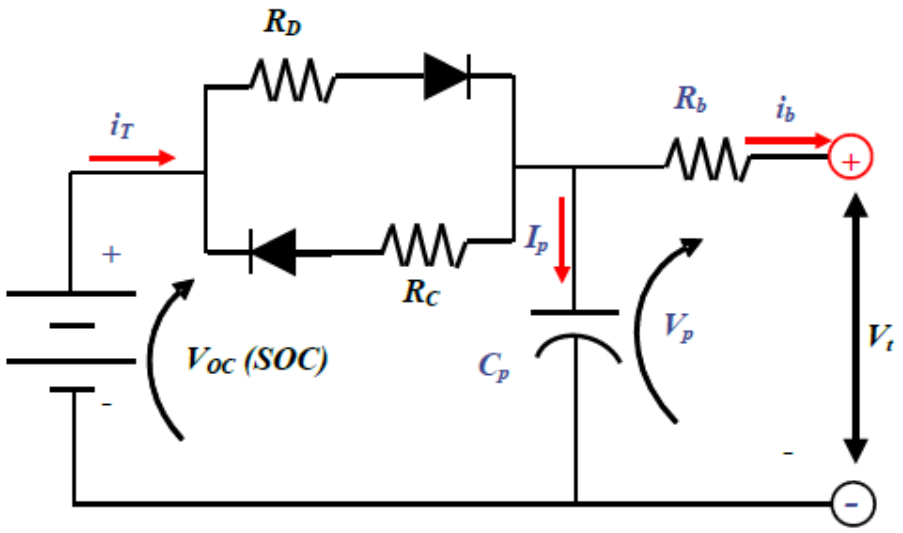


Figure 2.20: Dynamic Model

$$\dot{V_p} = \frac{dV_p}{dt} = -\frac{V_p}{R_{C/D}C_p} + \frac{i_p}{C_p} \tag{2.48}$$

$$V_t = V_{OC} - V_p - R_b i_b \tag{2.49}$$

Where:

- i_b: Battery current.
- V_p: Voltage across the polarized capacitor C_p.
- R_p: Resistance associated with the polarized capacitor.
- C_p: Capacitance of the polarized capacitor.
- $R_{C/D}$: Resistance during charging/discharging.
- i_p: Current through the polarized capacitor.
- V_{OC}: Open-circuit voltage.
- R_b: Battery internal resistance.

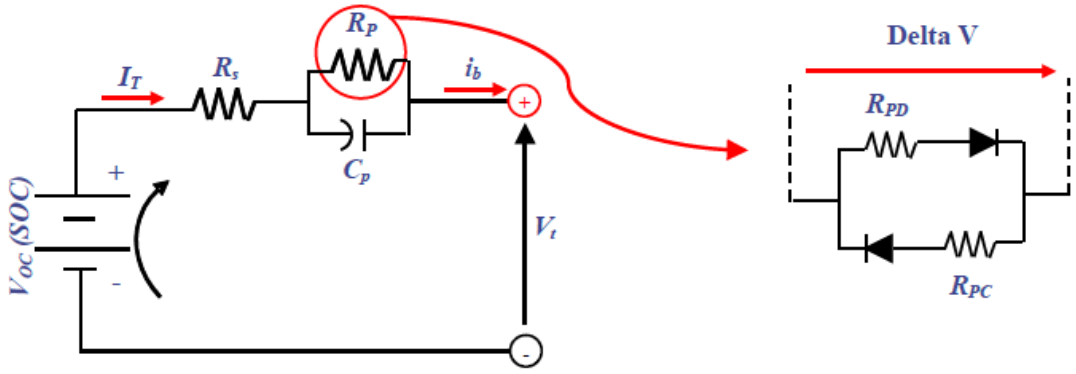


Figure 2.21: Model "2" representing the polarization effect

- V_t: Terminal voltage of the battery.

For applications where the cyclic (and micro-cyclic) rhythm is more frequently solicited, it is possible to add the hysteresis effect to this model to reduce the error introduced by ΔV (see Figure 2.21)

2.5.5 Model including the "EDL" electrical double layer phenomenon

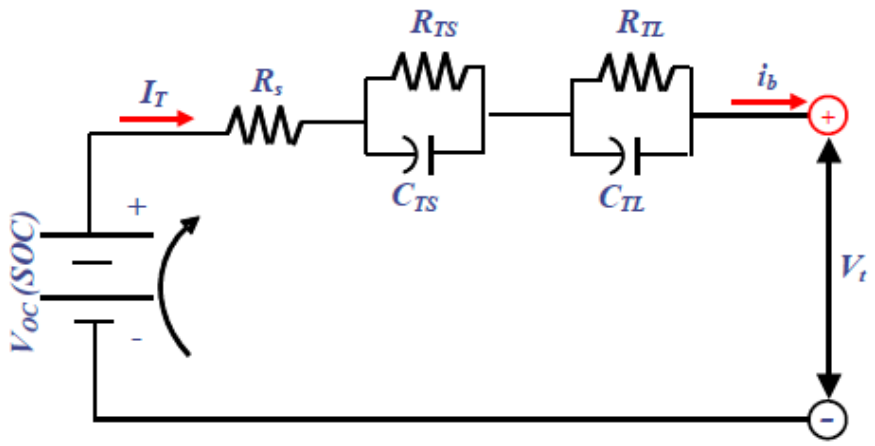
The model described above accounts for the transient response of the voltage (V_t) related to the phenomenon of the electric double-layer polarization (EDL) and dynamic polarization. The two networks (R_{TS}/C_{TS}, R_{TL}/C_{TL}) respond with two different time constants, τ_{TS} (fast) and τ_{TL} (slow) . The model is expressed by the following equations:

$$\dot{V}_{TS} = \frac{dV_{TS}}{dt} = -\frac{V_{TS}}{R_{TS}C_{TS}} + \frac{i_p}{C_{TS}} \tag{2.50}$$

$$\dot{V}_{TL} = \frac{dV_{TL}}{dt} = -\frac{V_{TL}}{R_{TL}C_{TL}} + \frac{i_p}{C_{TL}} \tag{2.51}$$

$$V_t = V_{OC} - V_{TS} - R_b i_b - V_{TL} \tag{2.52}$$

Where:



h

Figure 2.22: Model including the double electrical layer EDL

- V_{TS}: Fast transient response voltage across the R_{TS}/C_{TS} network.
- V_{TL}: Slow transient response voltage across the R_{TL}/C_{TL} network.
- R_{TS}, C_{TS}: Resistance and capacitance of the fast transient network.
- R_{TL}, C_{TL}: Resistance and capacitance of the slow transient network.
- i_p: Current through the network.
- V_{OC}: Open-circuit voltage.
- R_b: Battery internal resistance.
- i_b: Battery current.
- V_t: Terminal voltage of the battery.

It is possible to have a model with only one (R/C) network or a more complex one with several networks (3 or more). The choice can be made based on experimental trials and specific profiles related to the application. Given the precision sought, the choice of two networks is a widely adapted compromise.(see Figure 2.22)

2.6 Deferent Types of batteries

Rechargeable batteries, also known as secondary batteries, come in various chemical compositions, each with distinct characteristics. The differences between these rechargeable battery types can be summarized in terms of capacity, cost, weight, size, and safety. This table provides a quick overview of the characteristics of each rechargeable battery type. It is important to note that advancements in technology may lead to improvements and changes in these properties over time. The choice of a battery for a specific application will depend on a balance of these factors in the context of the intended use.[96, 97, 98, 99]

Table 2.2: Comparative Table of Rechargeable Batteries

Feature	**Nickel-Cadmium (NiCd)**	**Nickel-Metal Hydride (NiMH)**	**Lead-Acid**	**Lithium-Ion (Li-ion)**	**Lithium-Polymer (LiPo)**
Energy Density	Low to moderate	Moderate	Low	High	High
Cost	Low	Moderate	Low	High	Moderate to high
Weight	Moderate	Moderate	Heavy	Light	Light
Maintenance	High	Moderate	High	Low	Low
Lifespan	Long (with proper care)	Moderate to long	Moderate (with maintenance)	Moderate to long	Moderate
Memory Effect	Yes	Less than NiCd	No	No	No
Environmental Impact	High (toxic cadmium)	Lower (no toxic metals)	High (lead acid)	Moderate	Moderate
Safety	Stable	Stable	Risk of acid spill	Requires protection circuit	Requires protection circuit
Self-Discharge Rate	Low	High	Moderate	Low	Low
Versatility	Good	Good	Poor	Excellent	Excellent

2.7 Conclusion

In summary, the chapter has addressed the complex task of modeling and optimizing a multi-source energy system that combines the variable powers of wind and solar, augmented by the reliability of storage systems. The implementation of MPPT techniques has been emphasized as a critical component in the optimization process, ensuring that each source operates at its maximum efficiency despite the inherent unpredictability of natural resources.

Chapter 3

Management and Sizing of Multi-Source Systems

3.1 Introduction

This chapter examines the key principles of sizing and managing renewable multi-source energy systems, focusing on optimizing the configuration of energy sources and storage components to ensure reliable and efficient power delivery. Sizing involves determining the ideal capacity for each energy source and storage unit to achieve a balanced and cost-effective system. Effective management strategies are crucial for coordinating system operations, adapting to real-time conditions, and maximizing overall performance. Advanced techniques, such as Artificial Neural Networks (ANN) and other intelligent control algorithms, play a vital role in enhancing the flexibility and efficiency of these systems. By accurately predicting energy generation and consumption, these methods enable dynamic adjustments that optimize energy utilization and extend storage system lifespan. This chapter provides a detailed overview of the methodologies and technologies used in the sizing and management of renewable multi-source systems, highlighting both current practices and emerging trends that are shaping the future of sustainable energy management.

3.2 Sizing Methodologies

The sizing of multi-source systems for photovoltaic (PV) and wind power generation with storage involves determining the optimal size of the PV and wind power sources, as well as the storage capacity, to meet the energy demand of the system while minimizing costs and maximizing efficiency. This is a complex problem due to the variability of renewable energy sources and the need to balance energy supply and demand [100].

3.2.1 Criteria for Sizing

The sizing of components in a multi-source system, such as a hybrid PV-Wind system with energy storage, is crucial for the overall performance of the system [101]. The criteria used for sizing these components include:

- **Cost:** The cost of the system is a crucial factor in determining the optimal size of the components. This includes the initial investment cost, operational and maintenance costs, and the cost of energy storage.
- **Efficiency:** The efficiency of the system is another important criterion for sizing. This includes the efficiency of the PV panels, wind turbines, and energy storage systems.
- **Reliability:** The reliability of the system is also crucial, as it determines the ability of the system to meet the energy demand. This includes the availability of the PV panels, wind turbines, and energy storage systems.
- **Environmental impact:** The environmental impact of the system is also an important criterion. This includes the carbon footprint of the system, the use of renewable energy sources, and the reduction of greenhouse gas emissions.

In addition to these criteria, the sizing of the components should also consider the energy balance, grid independence factors, and thermal comfort. The optimal sizing of the com-

ponents should be determined using mathematical optimization techniques, such as genetic algorithms or linear programming.

3.2.2 Sizing Methods

The methods for sizing multi-source renewable energy systems involve a blend of classical and advanced techniques. These methods consider demand profiles, resource availability, and technical constraints to optimize the design and functionality of systems combining photovoltaics (PV), wind turbines, and storage solutions [102].

1. Classical Methods for Sizing

    - **Monthly Average Method:** This method involves calculating the average monthly energy consumption and production to ensure the system can meet the demands across varying seasons. For both solar PV and wind systems, historical irradiance and wind speed data are averaged for each month to predict the typical output. This helps in designing a system that can handle the month-to-month variability in energy production and demand.
    - **Peak Sun Hours Method:**
        - Used specifically for sizing PV systems, this method calculates the effective number of hours per day the sunlight is strong enough to be considered equivalent to peak conditions. This figure helps in determining the required size of the PV array to meet daily energy requirements based on the average daily peak sun hours over the year.
    - **Bin Method:**
        - Often used in HVAC systems but applicable in renewable energy, the bin method involves sorting data (like temperature or wind speed) into bins. Each bin represents a range of values, and the frequency of occurrence in each bin

is calculated. This method can help in determining how often certain levels of solar irradiance or wind speeds occur, informing expected output ranges.

- **Diversity Factor:**
  - This method accounts for the fact that not all components in a system will peak at the same time. The diversity factor is the ratio of the sum of the individual maximum demands to the maximum demand of the whole system. This ensures that the system is not oversized unnecessarily, reducing costs and improving efficiency [103].
- **Utilization Factor:**
  - This factor measures the proportion of time that equipment (such as a wind turbine or solar panel) operates at full capacity over a specific period. It helps determine the efficiency and effectiveness of each component, guiding sizing decisions to optimize overall system performance.

These classical methods provide a solid foundation for designing and sizing multi-source renewable energy systems using reliable data and established mathematical approaches to predict and meet energy demands. They are particularly useful for straightforward scenarios and initial planning phases, where complexity and computational costs need to be minimized.

2. Advanced Methods for Sizing:

   Advanced methods for sizing multi-source renewable energy systems involve sophisticated techniques that leverage computational models, optimization algorithms, and data analytics to achieve highly efficient and reliable system designs [104]. Here are some of the key advanced methods used:

   - **Optimization Algorithms:**
     - **Genetic Algorithms (GA):** These are used to solve complex optimization problems by mimicking the process of natural selection. GA is particularly

effective in optimizing the component sizes and configurations of hybrid renewable energy systems where multiple objectives, such as cost, efficiency, and reliability, must be balanced.

  - **Particle Swarm Optimization (PSO):** This method optimizes a problem by iteratively improving a candidate solution with regard to a given measure of quality. PSO is used for its speed and efficiency in finding the optimal sizes of system components based on the system's performance criteria.
  - **Simulated Annealing (SA):** SA is a probabilistic technique for approximating the global optimum of a given function. It is particularly useful for handling discrete sizing decisions, like the number of panels or turbines, under multiple constraints and varying scenarios.

- **Stochastic Models:**
  - **Monte Carlo Simulations:** These simulations model the probability of different outcomes in processes that cannot easily be predicted due to the intervention of random variables. This is crucial for assessing the reliability and performance of renewable energy systems under uncertain weather conditions and variable load demands.
  - **Markov Chains:** Applied in modeling the state changes within a system, such as battery charge levels, based on transition probabilities. This helps in predicting energy availability and optimizing storage capacity to enhance system reliability.

- **Artificial Intelligence and Machine Learning:**
  - **Artificial Neural Networks (ANN):** ANNs are used for forecasting and pattern recognition, such as predicting solar irradiance and wind speed from historical data. This predictive capability is essential for accurately sizing energy production units to match forecasted energy demands.

- **Reinforcement Learning (RL):** In RL, algorithms learn to make sequences of decisions by interacting with a dynamic environment. It is used to dynamically adjust the operation and sizing of system components in real-time to maximize performance under changing conditions.

These advanced methods provide a robust framework for accurately and efficiently sizing multi-source renewable energy systems. They enable designers to incorporate complex system dynamics, multiple performance criteria, and uncertain environmental conditions into the decision-making process.

When sizing multi-source renewable energy systems incorporating photovoltaics (PV), wind turbines, and storage, both classical and advanced analytical methods draw on essential data and analyses to ensure optimal configuration and performance. Key to both approaches is the analysis of historical energy consumption data, forming the basis for understanding daily, monthly, and seasonal demand profiles. This data is used to establish the minimum, average, and peak energy requirements, essential for all sizing calculations. Additionally, the Load Duration Curve (LDC) is crucial for evaluating the variability and continuity of energy demand, informing decisions on storage and generation capacities. Resource assessment is also fundamental, where historical weather data are analyzed to calculate solar irradiance and wind speeds, aiding in the creation of probability distributions for energy availability. Both methods assess the feasibility of hybrid systems to determine if PV and wind can provide complementary outputs, enhancing reliability. Furthermore, ensuring that the energy output matches the load profile across various timescales is critical to maintaining energy balance and meeting demands consistently [105, 106]. System redundancy is also considered to increase reliability, especially in critical load scenarios, ensuring the system has backup resources to minimize outages. These comprehensive evaluations are pivotal, whether using traditional or cutting-edge techniques, to design efficient, cost-effective, and robust renewable energy systems capable of handling the variability of renewable resources.

3.2.3 Simulation Tools for Sizing Multi-Source Renewable Energy Systems

Table 3.1: Tool Comparison for Renewable Energy System Design

Tool Name	Capabilities	Limitations
HOMER Pro	- Models hybrid renewable systems - Analyzes economic and technical viability - Simulates energy balances and financial projections	- May oversimplify interactions - Accuracy depends on user-provided data - Licensing cost
RETScreen	- Evaluates energy production, savings, and financial viability - Extensive database of climate data	- Focuses more on feasibility than detailed technical design - Generic models may require adjustments
PVsyst	- Specialized in solar PV system design and analysis - Provides shading analysis, system layout, and performance analysis	- Primarily for solar PV, not integrated with other renewable sources - Complex, steep learning curve
Hybrid2	- Models performance of hybrid power systems - Useful for technical and economic performance analysis	- Less user-friendly interface - Less frequent updates and support
SAM (System Advisor Model)	- Models a variety of renewable and conventional energy systems - Supports detailed financial and economic analysis	- Complex setup, requiring time to learn

3.3 Energy Management Systems (EMS)

Energy Management Systems (EMS) are integral to optimizing the generation, distribution, and consumption of energy, particularly within systems that incorporate renewable sources like solar, wind, and hydroelectric power. The primary purpose of an EMS is to enhance the efficiency, reliability, and sustainability of energy systems while minimizing costs and environmental impact. As the integration of renewable energy sources grows, EMS play a

crucial role in ensuring that energy systems operate smoothly, efficiently, and adaptively to varying conditions.

3.3.1 Key Techniques and Technologies in EMS

One of the fundamental aspects of an EMS is data acquisition and monitoring. This involves the use of smart meters, sensors, and data acquisition systems to collect real-time data on energy production, consumption, and system performance. These technologies allow for detailed tracking of operational parameters, which is essential for informed decision-making and system optimization [107]. Advanced control systems are another critical component of EMS. These systems manage and automate the operation of various components such as generators and inverters based on the data received. Technologies like Programmable Logic Controllers (PLCs), Supervisory Control and Data Acquisition (SCADA) systems, and Distributed Control Systems (DCS) are commonly employed to execute these tasks. These control systems ensure that energy generation and distribution are adjusted in real-time to match demand and optimize performanceData analytics and optimization algorithms are at the heart of EMS functionality. These tools analyze the vast amounts of data collected to optimize system operations, improve efficiency, and reduce costs. Machine learning algorithms, for instance, are employed for predictive maintenance, load forecasting, and anomaly detection. Optimization models, such as linear and quadratic programming, are used to optimize energy distribution and storage, ensuring that the system operates at its best possible efficiency [108, 109]. Demand response management is another critical technique within EMS. It involves adjusting the energy load in real-time based on consumption patterns and grid demands. Automated Demand Response (ADR) systems can automatically reduce power usage during peak periods, while dynamic pricing models encourage consumers to shift their energy usage to off-peak times, thereby reducing overall energy costs and strain on the grid [110]. Energy storage management is also a key focus of EMS, particularly in systems that incorporate renewable energy sources. Effective management of energy storage systems, such

as batteries, involves algorithms that determine the optimal times to charge and discharge energy. This balance between supply and demand is crucial for maintaining system stability and maximizing economic benefits. The integration of renewable energy sources within an EMS framework requires sophisticated management techniques. Hybrid inverters and grid intertie configurations are used to manage the intermittent nature of renewable energy sources like solar and wind. These technologies ensure that renewable energy is effectively harnessed and integrated into the broader energy system, contributing to a more sustainable and reliable energy supply [111].

3.3.2 Management Strategies for Hybrid Renewable Energy Systems

Involve the coordinated operation and optimization of multiple energy sources—typically a combination of renewable energy sources such as solar, wind, and energy storage systems like batteries. The primary goal of these strategies is to ensure a reliable, efficient, and sustainable energy supply by effectively managing the variability and intermittency inherent in renewable energy sources. By integrating advanced control algorithms, predictive analytics, and real-time monitoring, these strategies allow hybrid systems to balance energy supply and demand, minimize costs, and enhance overall system resilience. These strategies are crucial in maximizing the potential of renewable energy systems, particularly in off-grid and remote areas, where reliable energy supply is vital [112].

1. Integration Techniques

   Integration techniques are essential for seamlessly incorporating multiple renewable energy sources into hybrid systems. These techniques aim to enhance system reliability and grid integration by leveraging the strengths of each energy source while mitigating their weaknesses. They are particularly important for managing the fluctuating outputs from renewable sources, which can vary from minute-to-minute or day by day

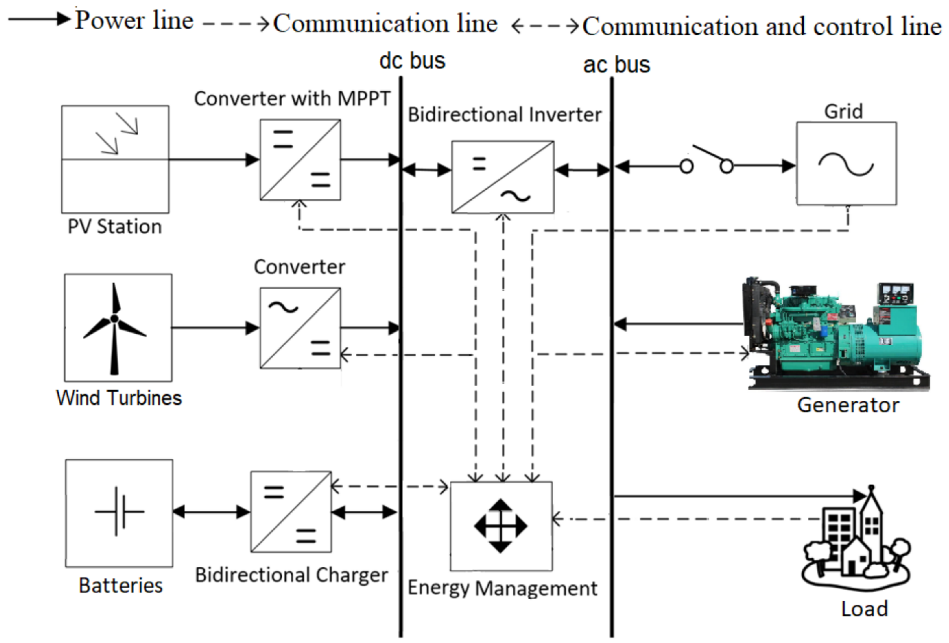


Figure 3.1: Schematic representation of a hybrid renewable energy system with energy management

[113, 114].

- **Intermittency Management:** Use of energy storage systems like batteries and flywheels to buffer and balance the variability of renewable sources such as wind and solar.
- **Hybrid Configuration:** Designing system configurations that complement the strengths and weaknesses of each energy source. For example, combining solar (which peaks during the day) with wind (which can be stronger at night or during different seasons) to provide a more constant energy flow.
- **Grid Interfacing:** Developing advanced inverters and converters that can efficiently connect and synchronize different renewable sources to the power grid or standalone systems.
- **Energy Routing:** Implementing smart switches and energy routers that dynamically direct energy flow based on source availability and load demand.

The figure 3.1illustrates a hybrid strategy that incorporates all previously mentioned strategies: intermittency management, hybrid configuration, grid interfacing, and energy routing. This table has a representation of contrasts in the different methods, highlighting how each addresses the challenges of integrating renewable energy sources into a cohesive hybrid system.

Table 3.2: Compact Comparison of Hybrid System Integration Techniques

Technique	**Pros**	**Cons**
Intermittency Management	- Stable supply - Good power quality - Scalable	- High initial costs - Limited lifespan - Environmental issues
Hybrid Configuration	- Balanced energy - Less storage needed - Customizable	- Complex management - Resource-intensive setup - Multi-tech dependence
Grid Interfacing	- Grid stability - Easier integration - Lower losses	- Infrastructure cost - Technical complexity - Regulatory compliance
Energy Routing	- Optimized usage - Quick adaptability - Less waste	- Complex controls - Technology reliance - Vulnerability risks

2. Control Algorithms

Control Algorithms are essential for managing the output from multi-source systems to optimize performance and ensure stability. Various algorithms, including PID controllers, fuzzy logic controllers, and machine learning algorithms, are utilized to regulate energy production and consumption efficiently PID controllers are known for their simplicity and effectiveness in predictable systems, as they offer a straightforward approach to controlling the output of energy systems. They are widely used in industrial applications and can be found in various energy systems, including heating, ventilation, and air conditioning (HVAC) systems [115]. Fuzzy logic controllers and machine learning algorithms, on the other hand, excel in handling uncertainties and non-linearities that are common in renewable energy systems [116]. These algorithms

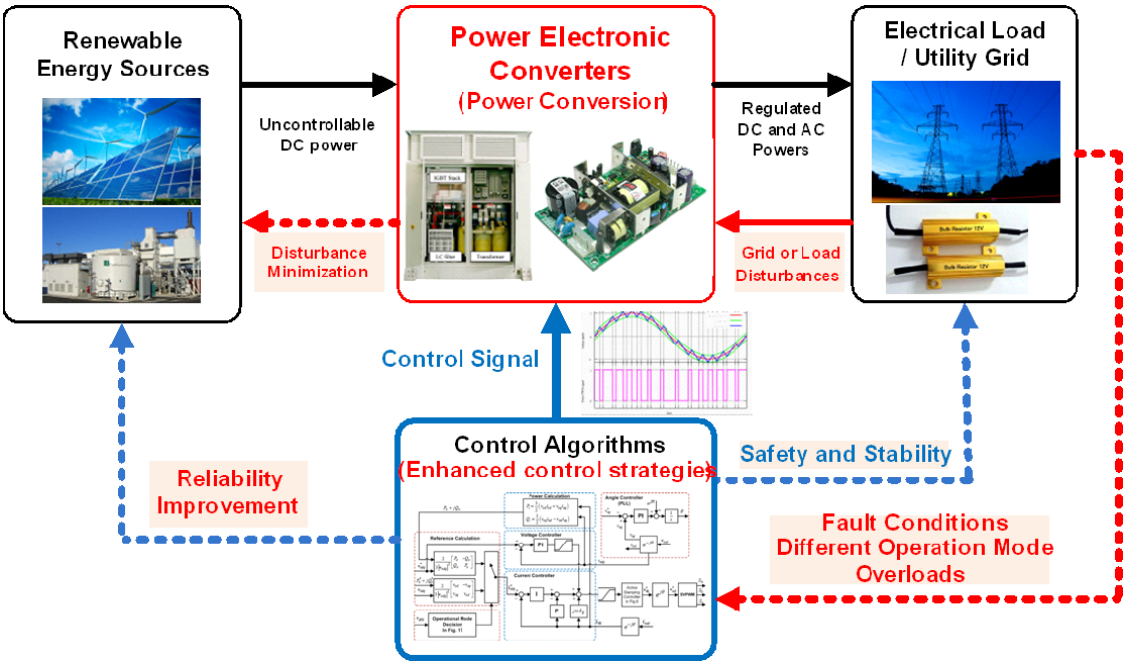


Figure 3.2: Renewable energy system with power converters and control algorithms for enhanced reliability and stability

are particularly useful in managing the variable and intermittent nature of renewable energy sources, such as solar and wind power. In recent years, there has been a growing interest in the application of advanced control algorithms, such as model predictive control and reinforcement learning, for the optimal control of renewable energy communities (RECs) [117]. These algorithms are designed to minimize the sum of individual electricity bills, taking into account the costs related to power peaks and the energy exchanges with retailers.(see Figure 3.3)

3.4 Case Studies and Applications

Standalone systems that combine photovoltaic (PV) panels, wind turbines, and battery storage are increasingly vital for providing reliable and sustainable power in remote or off-grid areas. These systems harness the complementary nature of solar and wind resources to ensure a continuous energy supply, while batteries serve as an essential storage component to balance supply and demand over time. Effective sizing and management of these en-

Table 3.3: Comparison of Control Algorithms for Renewable Energy Systems

Control Algorithm	**Purpose**	**Operation**	**Applications**
PID Controllers	Simple, effective control in predictable systems	Continuously calculates error value as the difference between a desired setpoint and a measured process variable. Adjusts based on proportional, integral, and derivative terms.	Widely used in industrial applications, including HVAC systems and stable energy systems.
Fuzzy Logic Controllers (FLC)	Handle uncertainties and non-linearities in systems	Uses fuzzy logic to interpret input data with degrees of truth, making dynamic adjustments to system operation.	Renewable energy systems like wind and solar power, where input conditions are highly variable.
Machine Learning Algorithms	Learn from data to optimize system performance	Analyzes historical and real-time data to predict system behavior and optimize control strategies.	Load forecasting, predictive maintenance, real-time optimization in renewable energy systems.
Model Predictive Control (MPC)	Optimize complex energy systems by predicting future states	Uses a model of the system to predict future states and optimize control actions over a specified time horizon, handling multiple inputs and constraints.	Management of microgrids and Renewable Energy Communities (RECs), optimizing energy production and consumption.
Reinforcement Learning (RL)	Learn optimal control strategies in dynamic environments	Learns by interacting with the environment, receiving feedback, and optimizing strategies to maximize long-term benefits.	Renewable Energy Communities (RECs), energy usage optimization, storage management, grid interactions.

ergy components are critical to maximizing system efficiency, reducing costs, and ensuring long-term reliability. Traditional methods of system management often struggle to handle the inherent variability and intermittency of renewable resources. However, the application

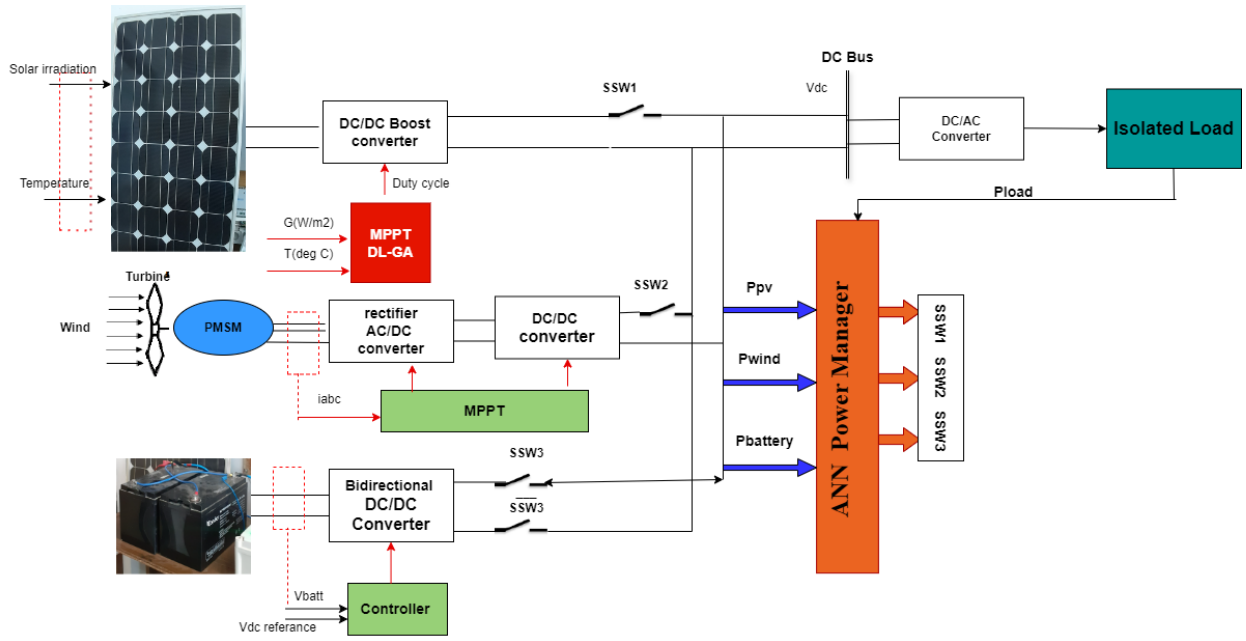


Figure 3.3: System components and description.

of Artificial Neural Networks (ANN) offers a powerful alternative by providing advanced predictive capabilities and adaptive control strategies. In this case, study, we focus on a stand-alone hybrid energy system that integrates PV panels, wind turbines, and batteries. The objective is to optimize the sizing of each component and manage the system's operation effectively using ANN. This approach not only enhances the system's ability to respond dynamically to changes in energy availability and demand but also improves overall performance by learning from past data and making informed decisions in real-time. The components of a standard isolated system powered by a combination of solar and wind energy, complemented with battery storage, are explained through mathematical models. This system is depicted as a stand-alone setup in Figure 3.3.

3.4.1 Sizing hybrid system based on Monthly average method

The effective and dependable functioning of an Autonomous Wind Turbine/Photovoltaic/-Battery System relies heavily on accurate sizing. Sizing this hybrid system utilizing monthly average data entails establishing the suitable capacities for the PV panels, wind turbines, and

energy storage elements, all of which are crucial in fulfilling the load demands proficiently.

The general load, wind, PV, and energy produced are given by the following equations:

$$E_{\text{load}} = E_{\text{PV}} S_{\text{PV}} + E_{\text{Wind}} S_{\text{wind}} \tag{3.1}$$

$$E_{\text{wind}} = \frac{1}{2} C_p \rho S V_{\text{wind}}^3 \Delta t = P_{\text{wind}} \Delta t \tag{3.2}$$

$$E_{\text{PV}} = S_{\text{PV}} E_{\text{irr}} \eta_{\text{PV}} \tag{3.3}$$

With:

$$\eta_{\text{PV}} = \eta_{\text{PV-STC}} [1 - \beta_{oc} (T_j - T_{\text{j-STC}})] \tag{3.4}$$

Through rigorous computations of monthly energy yield for each generator and corresponding load demand, distinct surface areas for photovoltaic panels and wind turbine generators are discerned. These quantifications are deduced using the following formulas for PV and wind turbine generators:

$$S_{\text{wind}} = \max \left(\frac{E_{\text{Load},m}}{E_{\text{wind},m}} \right) \tag{3.5}$$

$$S_{\text{PV}} = \max \left(\frac{E_{\text{Load},m}}{E_{\text{PV},m}} \right) \tag{3.6}$$

The monthly energies produced by PV and Wind turbines are:

$$\begin{cases} E_{\text{PV},m} = \frac{\sum_{m=1}^{12} E_{\text{PV}}}{12} \\ E_{\text{wind},m} = \frac{\sum_{m=1}^{12} E_{\text{wind}}}{12} \\ E_{\text{Load},m} = \frac{\sum_{m=1}^{12} E_{\text{Load}}}{12} \end{cases} \tag{3.7}$$

Here, K_{perc} represents the proportion of the load supplied by the PV source, while $(1-K_{\text{perc}})$ designates the fraction of the load met by the wind source. Consequently, we derive the following result:

$$\begin{cases} S_{\text{wind}} = (1 - K_{\text{perc}}) \left(\frac{E_{\text{Load,ave}}}{E_{\text{wind,ave}}} \right) \\ S_{\text{PV}} = K_{\text{perc}} \left(\frac{E_{\text{Load,ave}}}{E_{\text{PV,ave}}} \right) \end{cases} \tag{3.8}$$

The subsequent equations establish the quantities of PV panels and wind turbines required:

$$\begin{cases} S_{\text{wind,final}} = N_{\text{wind}} S_{\text{wind,unit}} \\ S_{\text{PV,final}} = N_{\text{PV}} S_{\text{PV,unit}} \end{cases} \tag{3.9}$$

The mean energy consumption is expressed as:

$$E_{\text{load-ave}} = E_{\text{wind,ave}} S_{\text{wind,unit}} + E_{\text{PV,ave}} S_{\text{PV,unit}} \tag{3.10}$$

The sizing parameters for the hybrid system are determined based on the previously outlined relationships. Table 3 provides a breakdown of the monthly energy production from the various components of the hybrid system, including the wind power system integrated with the solar systems. The average photovoltaic energy output is approximately 13.42 kWh/m^2, while the average wind energy output is around 63.015 kWh/m^2. Given that the average load energy demand is 338.5 kWh, the system configuration of 16 panels and 1 wind turbine comes closest to meeting the required load energy of 523.47 kWh. This is further elaborated in Table 4.

Battery capacity is calculated using the annual monthly average method with a day of autonomy:

$$C_{\text{batt}} = \frac{d_{\text{aut}} E_{\text{load,m}}}{U_{\text{batt}} \cdot \text{PDP} \cdot \eta_{\text{batt}} \cdot N_m} \tag{3.11}$$

Where $E_{\text{load,m}}$ is the monthly load consumed (kWh/d), and N_m is the number of days in the month that presents the maximum load (31 days). PDP stands for Percentage Depth of

Discharge, and η_{batt} is the efficiency of the battery.

The number of batteries used is calculated by the following relationship:

$$N_{\text{batt}} = \left\lceil \frac{C_{\text{batt}}}{C_{\text{batt-u}}} \right\rceil \tag{3.12}$$

Where $C_{\text{batt-u}}$ represents the selected battery capacity. Table 5 offers a comprehensive summary of all the necessary components [118].

To summarize, the total maximum power output of the photovoltaic panels is determined as $P_{\text{PV}} = 16 \times 80 = 1.280\,\text{kW}$, and the maximum power output of the wind turbine is approximately $1 \times 900\,\text{W} = 900\,\text{W}$. Moreover, the system utilizes two batteries with specifications of (12 V, 100 Ah).

Table 3.4: Compact Comparison Table for KPERC and Energy Parameters

KPE	SPV (m^2)	SWIND (m^2)	NPV	NWIN	SPV, FINAL (m^2)	SWIND, FINAL (m^2)	ELMEAN (kWh)
0.0	0.0	8.77	0	3	0.0	10.38	654.09
0.1	4.28	5.19	7	2	4.52	6.92	496.74
0.2	7.50	2.87	12	1	7.75	3.46	321.98
0.3	7.76	2.43	12	1	7.75	3.46	321.98
0.4	8.40	2.02	13	1	8.39	3.46	330.62
0.5	8.64	2.27	13	1	8.40	3.46	331.00
0.6	10.04	2.23	16	1	10.34	3.46	356.65
0.7	11.17	1.07	17	1	10.98	3.46	365.38
0.8	14.12	0.77	23	0	14.86	0.00	199.28
0.9	19.83	0.57	31	0	20.02	0.00	268.66
1.0	26.38	0.00	41	0	26.48	0.00	355.36

The hybrid energy system consists of 16 photovoltaic (PV) panels, which serve as the primary source of solar energy. Additionally, the system includes one wind turbine, contributing to energy generation by harnessing wind power. To ensure energy storage and supply stability, the system is equipped with two batteries, which store excess energy produced by the PV panels and wind turbine, making it available for later use when energy demand exceeds production.

Table 3.5: The Number of Wind Turbines and Panels Determined Through Calculation

Month	EIRR (kWh/m	T (°C)	NPV	V_{WIND} (m/s)	E_{PV} (kWh/m	E_{WIND} (kWh/m	E_{LOAD} (kWh)
January	85.5	10.1	0.1410	3.70	7.78	38.00	333.60
February	98.6	11.5	0.1419	4.10	9.03	52.17	339.00
March	143.6	16.1	0.1446	4.59	13.41	96.70	347.00
April	174.2	19.8	0.1468	5.09	16.51	99.82	347.04
May	201.5	24.5	0.1497	5.19	19.48	100.00	336.72
June	207.3	28.7	0.1486	5.10	19.89	76.27	332.88
July	218.2	32.3	0.1539	4.70	21.74	59.69	347.04
August	197.1	31.6	0.1512	4.40	19.59	64.48	345.84
Septembe	156.4	27.1	0.1512	4.31	15.27	60.60	336.48
October	127.9	22.7	0.1485	3.80	12.26	41.53	323.52
Novembe	95.0	15.5	0.1443	3.59	8.85	35.02	343.44
Decembe	79.6	11.1	0.1416	3.48	7.28	31.90	329.52

3.4.2 Energy Management System Based on ANN Model

Utilizing an Artificial Neural Network (ANN) for system management involves training the ANN with specific datasets. Hidden layers utilize the sigmoid activation function to introduce non-linearity, enabling the model to capture complex data relationships. Using a mathematical equation to train the data is a fundamental step in building an effective ANN. This equation serves as the foundation for establishing the relationships between various variables, constants, and the desired outcome or Target.

Within the system under consideration the power available from the photovoltaic subsystem is denoted by equation (11), while the power available from the wind turbine subsystem is represented by equation (7). The limited battery power is denoted by:

$$P_b^{\lim}(t) = V_b(t) I_b^{\lim}(t)$$

When managing this system, we adhere to the principles outlined in the first equation. By incorporating equations (11), (7), and $P_b^{\lim}(t)$, we arrive at the following expression:

$$P_L(t) = \eta_{DA}\left(\frac{1}{2}C_P(\lambda,\beta)\rho_a A v^3(t)\right) + \eta_{DD}\left(A_{\text{pv}}G(t)n_{\text{pv}}(1 + B_{\text{pv}}(T(t) - T_{\text{ref}}))\right) \pm \eta_{DD}\left(V_b(t)I_b^{\text{lim}}(t)\right) \tag{3.13}$$

Indeed, this equation encompasses four variables influenced by temperature, wind speed, solar irradiance, and the state of charge (SOC) of the battery, all while accommodating a variable load. The proposed Energy Management System (EMS) prioritizes the solar subsystem for primary power generation, while the wind subsystem assumes a secondary role. This decision stems from the fact that the system is designed for deployment in an area abundant in solar resources.

The architecture of the ANN is designed with three hidden layers, each containing 10 neurons. This configuration allows the network to process and learn intricate relationships between the input parameters. With multiple layers and neurons, the ANN can capture complex patterns in the data, enabling it to adapt to changing conditions and make precise control decisions, as shown in Figure 3.4. Output nodes correspond to control signals dictating actions for the PV, WT, and battery components. During training, the network learns to map input data to desired output control signals through backpropagation, iteratively adjusting weights and biases to minimize prediction errors.

A separate validation set refines hyperparameters and assesses the network's performance. As we see in Figure 3.5, the best validation performance of 0.024457 at epoch 33 signifies a significant achievement in neural network training. It means that after 33 complete iterations through the training data, the model demonstrated exceptional proficiency on a separate validation dataset, yielding a low validation error of 0.024457. This indicates that the neural network has learned to make accurate predictions on new, unseen data, a crucial indicator of its effectiveness. Once validated, the model undergoes testing on an independent dataset to ensure its generalization capabilities. The trained ANN is integrated into the standalone system, processing real-time data as inputs and generating control signals for the PV,

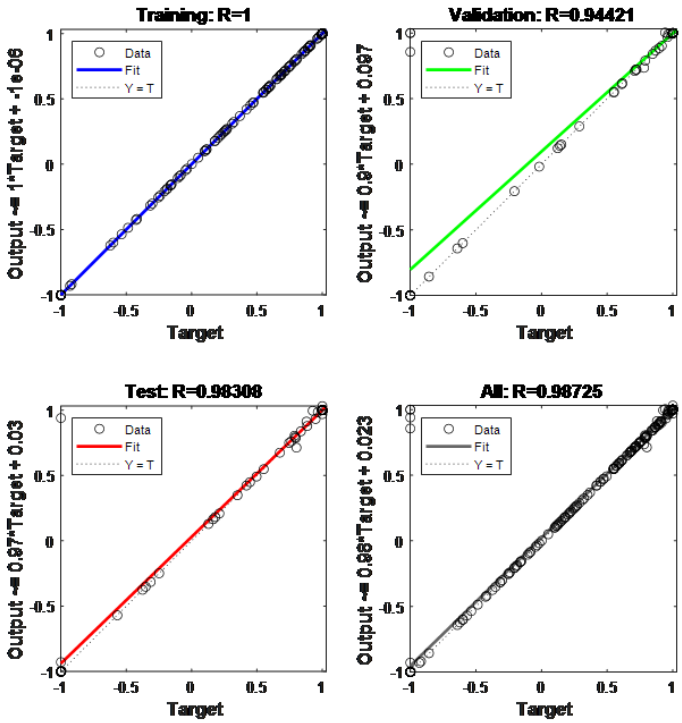


Figure 3.4: Performance of ANN, training, tasting, and validation

WT, and battery. Ongoing monitoring of the system's actual performance compared to the ANN's predictions allows for adjustments and retraining if discrepancies arise. This approach harnesses the ANN's capabilities to dynamically manage a diverse energy system, adapting seamlessly to varying load demands for optimal energy utilization. The intelligent energy management system based on ANN follows a structured process. It starts with data collection, defining inputs such as solar irradiance (G), temperature (T), wind speed (v), and target output. The network is configured with 10 neurons, 3 hidden layers, and a sigmoid transfer function. The data set is then divided into training (70%), validation (15%) and testing (15%). After random initialization of the weights and biases, the model undergoes validation with up to 1000 epochs and a minimum gradient of 10^1. The ANN training and optimization process begins, where the system checks if the gradient has converged. If so, the network is validated and the test is stopped. If not, the weights and biases are updated and the process continues until convergence is achieved. This approach ensures an optimized

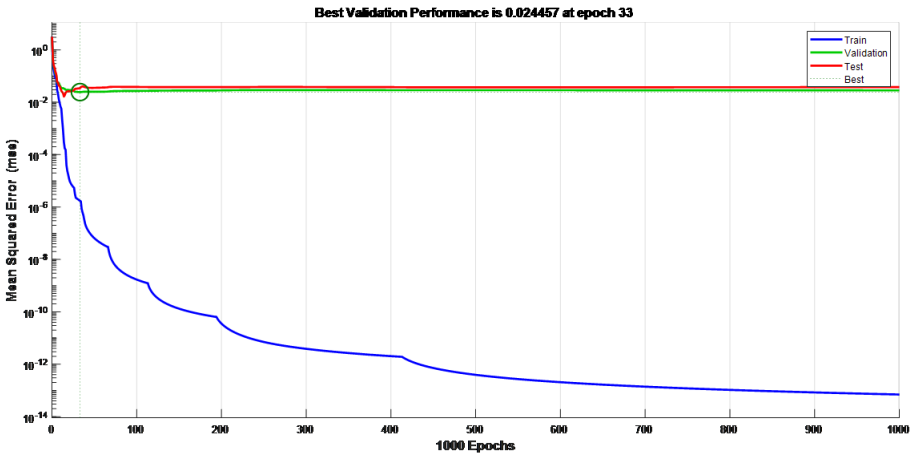


Figure 3.5: The Best validation Perfermance

and efficient energy management system.

3.5 Challenges and Future Perspectives

The management and sizing of multi-source renewable energy systems face several technical challenges, primarily due to the variability and intermittency of renewable energy sources like solar and wind. This variability complicates the task of ensuring a consistent energy supply, particularly in systems without grid backup. Additionally, energy storage remains a critical bottleneck, with current battery technologies facing limitations in capacity, lifespan, and cost. The integration of multiple energy sources also poses challenges in system control and coordination. To address these issues, advanced control strategies such as Artificial Neural Networks (ANN) are emerging as effective solutions. These strategies can dynamically manage energy resources by learning from historical data and adapting to real-time conditions. Innovations in next-generation storage technologies, such as solid-state and flow batteries, offer the potential for improved performance and cost-effectiveness. Hybrid storage solutions are also being explored to optimize energy management. Looking to the future, continued advancements in AI, machine learning, and predictive analytics will enhance the efficiency and reliability of multi-source systems. The integration of these systems into smart

grids and broader energy networks will provide greater flexibility and coordination. Supportive policies that encourage the adoption of renewable technologies and the development of advanced storage solutions will be key to overcoming current challenges and realizing the full potential of multi-source renewable energy systems.

Chapter 4

Results, Analysis, and Discussion

4.1 Introduction

This chapter focuses on the analysis and discussion of the results obtained from implementing advanced techniques for managing hybrid renewable energy systems. The chapter presents a detailed evaluation of Maximum Power Point Tracking (MPPT) strategies, particularly the innovative combination of Deep Learning with Genetic Algorithms (DL-GA) and the intelligent management approach using Artificial Neural Networks (ANN). The DL-GA technique is examined for its ability to optimize energy extraction from photovoltaic (PV) systems, ensuring maximum efficiency under varying environmental conditions. This method is compared against conventional and other advanced MPPT techniques, demonstrating its superiority in maintaining higher stability, efficiency, and peak power outputs. In addition to MPPT optimization, the chapter explores the intelligent management of the hybrid system through ANN, which is crucial for effectively handling the variability and unpredictability of renewable energy sources. This management strategy is evaluated for its performance in regulating battery charge and discharge cycles, maintaining system stability, and improving the overall efficiency of energy storage and distribution. The analysis is supported by simulations and real-world data, providing insights into the strengths and

weaknesses of each approach. The findings presented in this chapter contribute to the development of more reliable and efficient renewable energy systems, highlighting the potential of integrating advanced machine learning algorithms in the optimization and management of hybrid systems.

4.2 Evaluation of DL-GA Based MPPT Technique

In this section, we explore the efficacy of various Maximum Power Point Tracking (MPPT) techniques aimed at optimizing a photovoltaic (PV) system under diverse environmental conditions. The study utilized a DC-DC boost converter paired with a stable load to simulate the real world functioning of these systems. The MPPT techniques analyzed ranged from conventional methods such as Perturb and Observe (P&O) to more advanced strategies, including Artificial Neural Networks (ANN), Deep Learning (DL), and an innovative combination of Deep Learning with Genetic Algorithms (DL-GA). These techniques were tested across varying solar irradiations and temperatures to comprehensively evaluate their performance. This comparative analysis not only highlights the strengths and weaknesses of each technique but also identifies the best-performing method. The findings from this investigation are critical as they inform the optimal choice of MPPT technique to be implemented in a more complex hybrid system, integrating PV panels, wind turbines, and battery storage with variable loads. This approach ensures that the selected MPPT technique enhances overall system efficiency and reliability, thereby aligning with the overarching goal of improving renewable energy system performance under fluctuating environmental conditions.

4.2.1 Methodology and results

The application of ANN in MPP Tracking is particularly essential due to solar energy's inherently variable nature, which is affected by a range of environmental conditions, including the intensity of sunlight, temperature, and shadow impacts. For precise identification of the

MPP, these weights associated with the neurons must be meticulously calculated via an extensive training process. Once this training is complete, the ANN can serve as an estimator for the MPP, providing the reference value (VMP or IMP) to the MPPT controller. The training of an ANN involves a systematic adjustment of weights and biases, often utilizing the sigmoid activation function. Initially, weights and biases are randomly assigned to set the starting point for the learning process. During forward propagation, inputs pass through the network, with each neuron calculating a weighted sum and adding a bias, subsequently passed through an activation function like sigmoid. The sigmoid function, mapping values between 0 and 1, is favored for its ability to convert numbers into probabilities and handle non-linear data relationships. Following this, the back propagation phase begins where the network's output error is calculated and propagated backward, adjusting weights and biases. This adjustment is based on the error's partial derivatives concerning each weight and bias, guided by a learning rate parameter.

This cycle of forward propagation, back propagation, and weight and bias adjustments repeats over multiple iterations, gradually refining the network to minimize prediction errors. The training process also includes evaluating and adjusting the model with a validation set to prevent overfitting or underfitting, ensuring the ANN effectively generalizes to new data. In ANNs, an increase in the number of hidden layers can lead to enhanced tracking efficiency and improved performance in adapting to power fluctuations in the array, though it may also result in slower tracking speed The integration GA with DL for the optimization of ANN architectures has been a focus of various researchers. This approach aims to enhance the performance of multi-layer perceptron networks.

Given the computational complexity and extended training duration inherent in deep learning, evolutionary algorithms like GA are employed to optimize network performance. GA is particularly noted for its robust optimization capabilities. This method effectively reduces computational complexity and increases overall system flexibility through parameter tuning, thereby augmenting the performance of DL. DL is utilized to determine the optimal duty

cycle value, ensuring maximum power extraction. The neural network undergoes training with a dataset, which is then optimized using GA for improved effic. The steps involved in implementing the genetic algorithm are outlined as follows:

- Step I: Assess the fitness function and pinpoint the design parameters.
- Step II: Generate a population, representing potential solutions to the problem.
- Step III: Evaluate this population using an objective function.
- Step IV: From the population, select two parents based on their fitness levels. Higher fitness increases the likelihood of selection.
- Step V: Create a new population by repeatedly executing Selection, Crossover, and Mutation, until the new population is complete.
- Step VI: Form a new generation and return to Step III.
- Step VII: If the end condition (minimization of MSE) is met, conclude the process and identify the best solution as the target.

The Figure 4.1 presents the training dynamics of various ANN architectures (specifically, ANN with 10 neurons, ANN with 100 neurons, DL, and DLGA) labeled as A, B, C, and D respectively, alongside their Mean Squared Error (MSE) over multiple iterations. Figure D emerges as the most successful, showing remarkable convergence with training, validation, and test errors rapidly declining to a low MSE, indicative of a model that is both well-adjusted and highly generalizable to new data. In contrast, Figure A demonstrates promising initial learning, which then reaches a plateau, suggesting limited further improvement, possibly due to reaching an optimization plateau or constraints within the data. Figure B reveals signs of overfitting, characterized by an increase in validation error after an initial decline, indicating that the model starts to memorize the training data rather than generalize. Similarly, Figure C, akin to Figure A, displays a decent model fit but with a

slight divergence between training and validation errors, signaling the onset of overfitting or misalignment with the data's intricacies. Out of these, Figure D showcases the most robust learning process, free from overfitting issues, positioning its corresponding model as the preferable choice for real-world applications, thanks to its superior predictive accuracy and ability to generalize effectively. In addition to the training dynamics illustrated in the Figure 4.1, a comprehensive comparison of the different ANN architectures is also presented in an accompanying table 6, focusing on key performance metrics such as epoch, training time, overall performance, and gradient behavior. This comparison is crucial for understanding the efficiency and effectiveness of each architecture, which includes ANN with 10 neurons, ANN with 100 neurons, DL, and DLGA, corresponding to Figures A, B, C, and D respectively. The epoch range for all models is set from 0 to 1000, providing a substantial period for observing the learning progression of each architecture. The training time is another critical factor, offering insights into the computational efficiency of each model. Performance metrics in the table highlight the effectiveness of each model in achieving the desired output. Additionally, the gradient, a significant indicator of the learning rate and convergence efficiency of the model, is closely monitored, with a target value set at 1e-16. This target is indicative of a high degree of precision in the learning process. The Figure 4.2 presents

Table 4.1: Comparison of ANN Architectures' Performance

Architectu	Epochs	Time (s)	Performan	Gradient
ANN 10N	1000	4	1.44e-14	9.45e-14
ANN 100N	1000	8	1.33e-14	7.32e-11
DL	1000	15	4.09e-12	9.68e-9
DL GA	14	877	3.47e-32	5.16e-17

the comparative performance profile of a PV power in the 12 hours by using four MPPT techniques: DLGA, DL, ANN, and P&O. During the initial ramp-up, the DLGA and identically performing ANN/DL techniques exhibit a swift and stable rise to peak power, with the DLGA showing superior stability by maintaining peak levels with minimal fluctuation. As the solar irradiance changes around the 6-hour mark, the DLGA method exhibits a slight dip

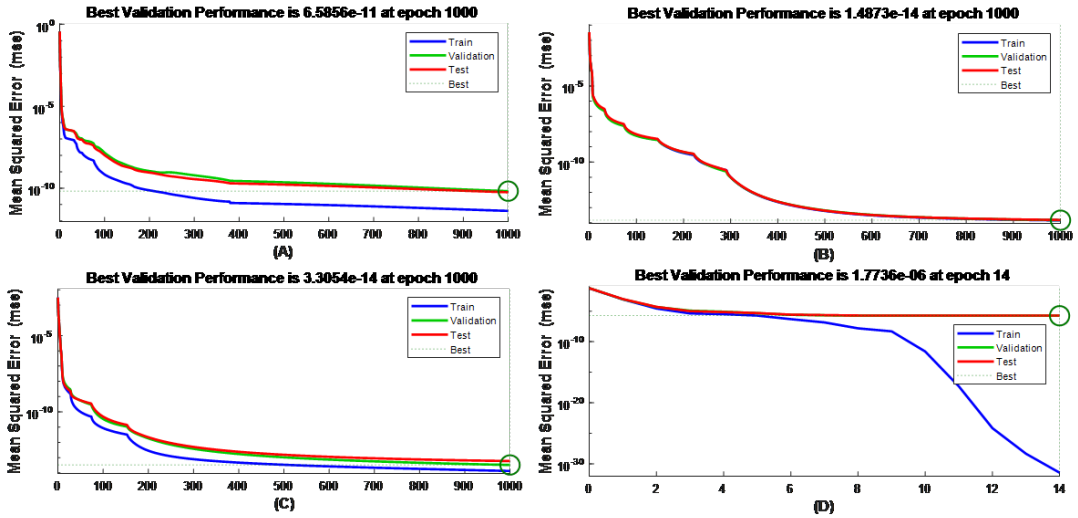


Figure 4.1: The Dynamic training of varions ANN architectures

but still operates close to its optimal power level of about 880W, suggesting its capability to adapt to transient changes in weather effectively. In contrast, the P&O method experiences a more pronounced drop to approximately 780 W, indicating a less stable response to these environmental shifts. During midday, when the irradiance is usually at its peak, the DLGA method maintains power levels around 1550W, whereas the P&O fluctuates and settles near 1500W. The ANN and DL, with their identical performance curves, match the 1350W output of DLGA but again show a less dynamic response to the initial increase in irradiance. In the late afternoon, as irradiance levels fall, the DLGA's output gradually decreases, maintaining the highest output of all methods at about 850 W before the sunsets, affirming its superior efficiency. The P&O's output also declines but does so more erratically, ending up slightly lower than the DLGA's output. The ANN and DL methods, while initially matching the DLGA's output, drop more sharply as they respond to the decreased sunlight. Throughout the day, the DLGA method outperforms others by consistently holding near-maximum output, suggesting its robust adaptability to varying solar conditions. As daylight wanes, the ANN/DL methods mirror each other closely, indicating a binary approach to sunlight availability, while the DLGA reveals a gradual descent, underscoring its nuanced response to diminishing irradiance. The P&O's performance, although reliable, is overshadowed by the

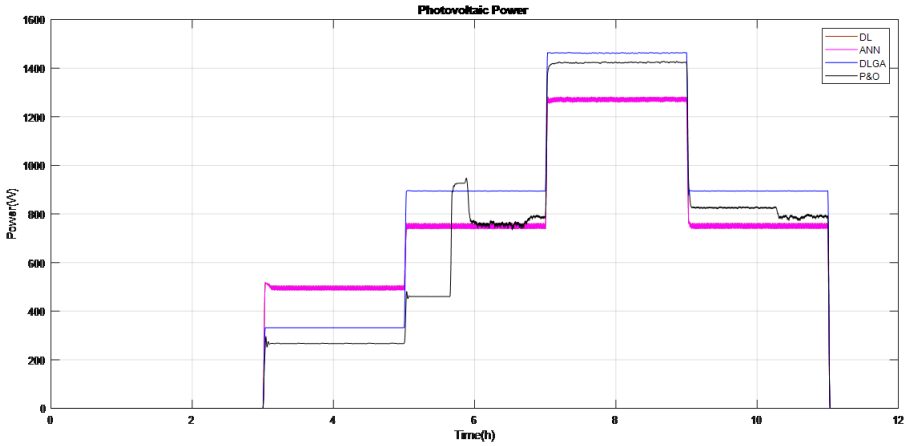


Figure 4.2: profile of a PV power in the 12 hours

machine learning-based methods, which show promise for enhancing efficiency and stability in stand-alone solar systems. The Figure 4.3 depicting the battery power output across 12 hours show cases the distinct performance characteristics of four MPPT methods: DLGA, DL, ANN, and P&O. At the onset, the DLGA technique rapidly stabilizes to an optimal charging power level, signifying an efficient charging process. As the day progresses, the DLGA maintains a consistent power output with minimal fluctuation, indicative of its superior charge regulation and adaptability to varying charging conditions. This contrasts with the P&O method, which exhibits more pronounced fluctuations, suggesting less efficient battery charge management and potential stress on the battery system. In the evening, as the system shifts from charging to discharging, the DLGA's power output reduces in a controlled manner, highlighting its effective energy management in transitioning states. The ANN and DL methods display remarkably synchronized performance, maintaining an identical power output profile throughout the day, which underscores the similarities in their algorithmic approaches to battery charging and discharging. Overall, the DLGA method stands out for its robustness and reliability, ensuring maximum battery efficiency and stability regardless of solar irradiance changes, thereby optimizing the system's energy availability.

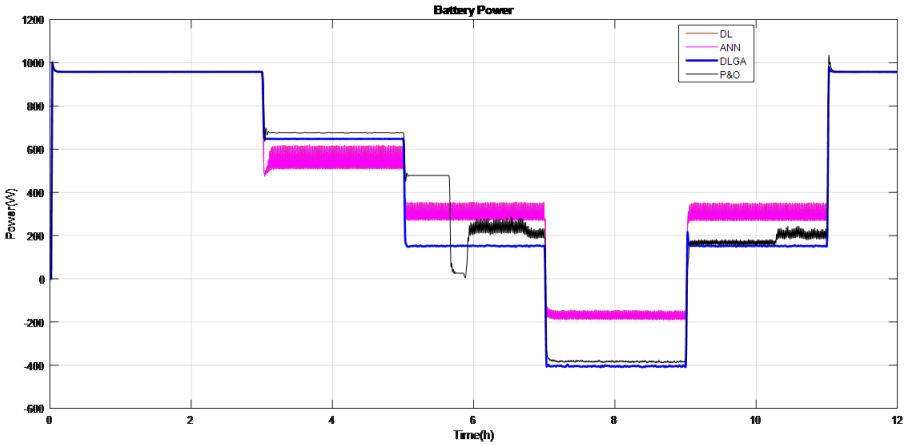


Figure 4.3: profile of a Battery power in the 12 hours

4.3 Power Curve Analysis of the Standalone System

This section presents the validation of the proposed intelligent energy management system through the utilization of a newly acquired historical dataset on atmospheric conditions (solar irradiation, temperature, and wind speed) from 2012, originating from Negrine, a city in Algeria. These atmospheric data have been processed to calculate power outputs, which then serve as inputs for the FLC. Furthermore, the state of charge for the batteries, an essential variable in this system, is adjusted to range from 50% to 90% of the battery bank's full capacity.

The HRES, configured with various parameters as elaborated in Figure 4.4, undergoes simulation via the Matlab/Simulink environment. The 288-hour simulation duration provides a comprehensive assessment of the system's performance, capturing seasonal and daily variations in renewable resource availability. This process adheres to the modeling specifications previously described and leverages the historical data depicted in Figure 4.5. The graphical representation in Figure 4.6illustrates the power output from the photovoltaic (PV) panels and wind turbines about the consumption profile, facilitating a comprehensive evaluation of the system's performance. The renewable power is defined as shown in Figure 4.7. Plotting the combined power output of the hybrid PV and wind system (P_{Renew}) alongside the power

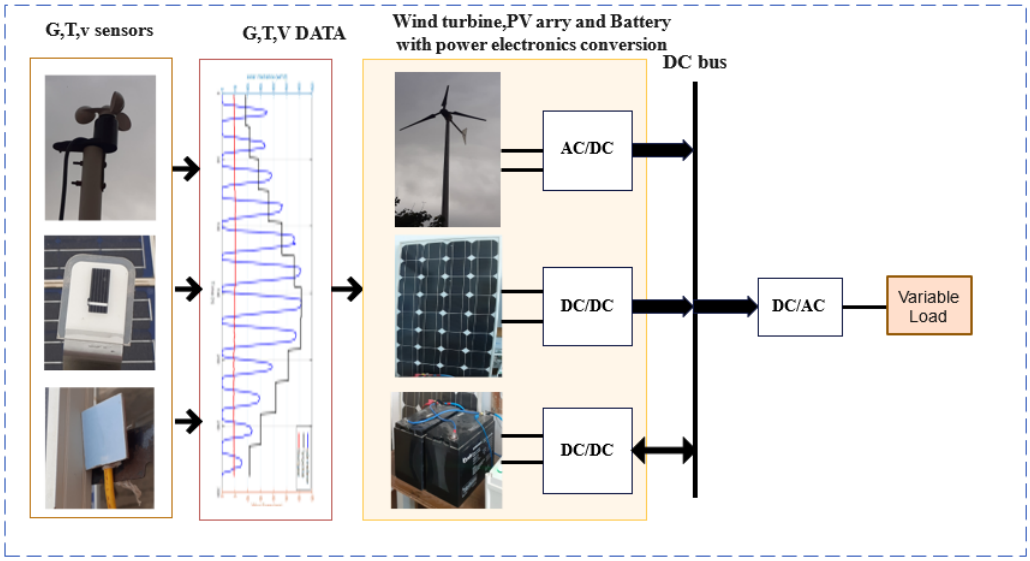


Figure 4.4: System components and description

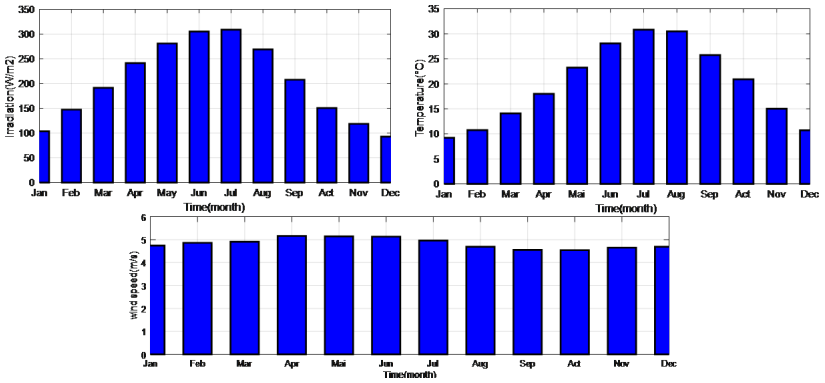


Figure 4.5: Historical data Wind speed, ambient temperature, and solar insolation in one year

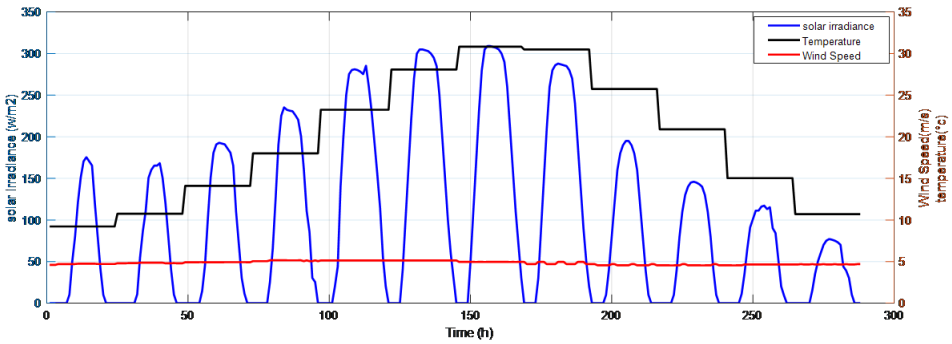


Figure 4.6: Profile of a typical day corresponding to each Month in year

h!

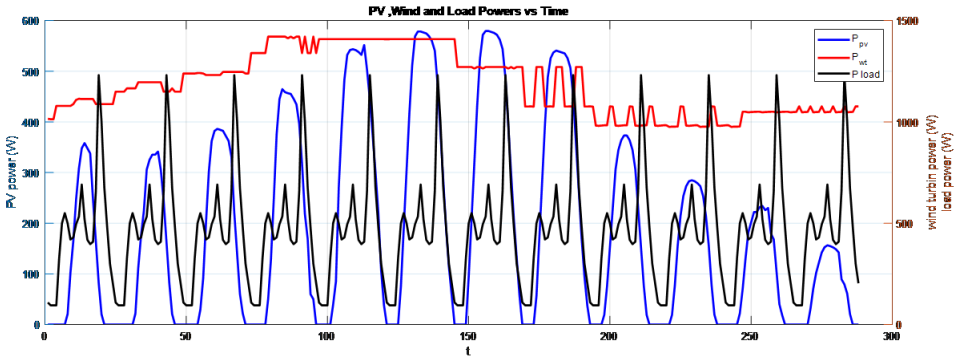


Figure 4.7: PV and Wind Load Powers Profile

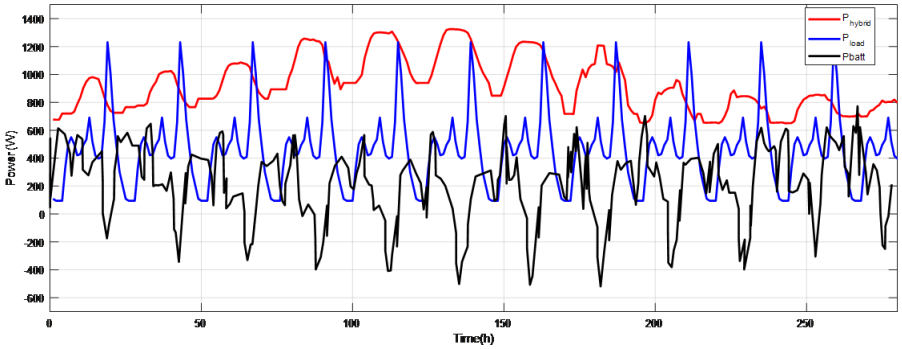


Figure 4.8: Various power outputs were obtained

demand (P_{Load}) and power of the battery (P_{battery}) over a 288-hour period offers valuable insights into the system's performance. It reveals instances of surplus renewable energy generation, where P_{Renew} exceeds P_{Load}, indicating the system's capacity to meet energy needs using these sources.

$$P_{\text{Renew}} = P_{\text{pv}} + P_{\text{wind}} \tag{4.1}$$

Fluctuations in P_{Renew} highlight the variability in solar irradiance and wind speeds, underscoring the impact of environmental conditions on power generation. Peaks in P_{Renew} signify optimal conditions for both solar and wind resources, aligning with high energy demand periods. Analyzing the State of Charge (SOC %) patterns over the extensive 288-hour simulation period reveals crucial insights into the energy storage dynamics, as illustrated in Figure 4.8. The SOC% trends depict the battery's dynamic charging and discharging cycles, effectively responding to fluctuations in renewable energy generation and load demand.

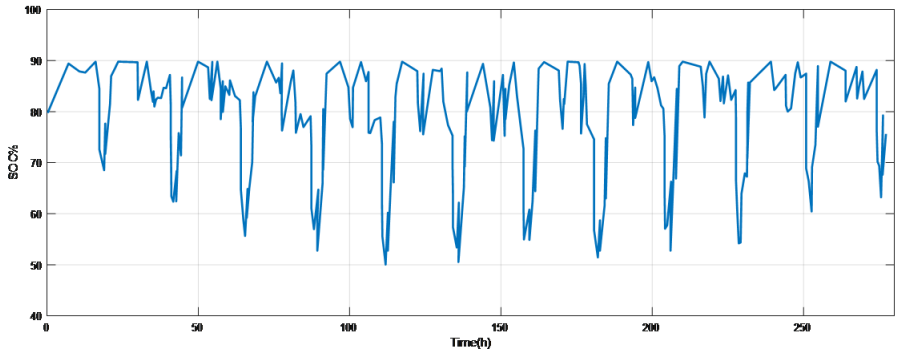


Figure 4.9: State of charge profile

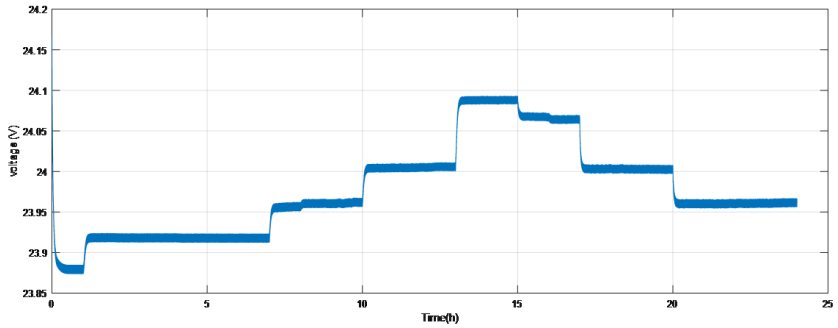


Figure 4.10: Voltage of battery in 24 h

Peaks in SOC% align with surplus renewable energy, indicating efficient charging, while troughs correspond to periods of heightened load demand, leading to controlled discharging. A thorough examination of the simulation results presented in Figure 4.9 and 4.10 reveals that the stability of the DC bus voltage over a 24-hour period underscores the efficiency and quick response of the FL control strategies applied. The ability of the system to keep the DC bus voltage (Vdc) closely aligned with the reference voltage (Vdcref) of 50 V demonstrates effective energy management and the protection of system components from potential damage due to voltage fluctuations. This significantly enhances the system's dependability and increases its service life. The pattern of battery voltage, which is closely linked to its state of charge, further highlights the complex relationship between these critical parameters. The observed complexity and the rapid adjustments made in the simulation emphasize the model's precision and effectiveness in simulating real-world conditions.(see Figure 4.11)

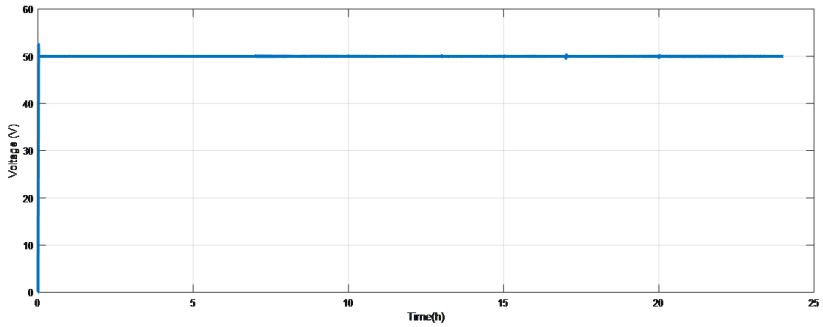


Figure 4.11: Profile of Voltage DC bus in 24 h

4.4 Overall System Performance and Efficiency

Table 3 highlights the analysis of the performance comparison of DLGA, DL, ANN, and P&O across various metrics related to PV and battery power profiles. The proposed DLGA method exhibits superior performance in multiple areas compared to the other methods. Both DLGA and DL show the highest stability in PV and battery power profiles, significantly outperforming ANN and P&O. Stability is crucial for maintaining a consistent and reliable power supply. DLGA demonstrates the highest efficiency, closely followed by DL, while ANN and P&O show lower efficiency levels. High efficiency indicates better energy utilization and system performance. In terms of responsiveness, DL and DLGA excel, far exceeding the capabilities of ANN and P&O. Responsiveness measures how quickly the system adapts to changing conditions, ensuring optimal performance. DLGA and DL achieve the highest peak power output for both PV and battery, while ANN and P&O fall short in this regard. Higher peak power output translates to better performance under varying load conditions. Additionally, DLGA and DL prove to be the most effective in regulating battery charge and discharge, while ANN and P&O are less efficient. Effective regulation is essential for extending battery life and maintaining system reliability. DLGA and DL show significantly better adaptability compared to ANN and P&O. Adaptability indicates the system's ability to handle different scenarios and changing conditions efficiently. DLGA is the top performer in predictive accuracy, followed by ANN, DL, and P&O. High predictive accuracy enables

the system to anticipate and respond to future conditions effectively. Key performance

Table 4.2: the performance comparison of DLGA, DL, ANN, and P&O

Metric	DL	ANN	DLGA	P&O
PV Power Profile				
Stability	90%	75%	90%	50%
Efficiency	90%	85%	95%	70%
Responsiveness	90%	70%	90%	50%
Power Output (Peak)	1600W	1400W	1600W	1000W
Battery Power Profile				
Stability	90%	75%	90%	50%
Efficiency	90%	85%	95%	70%
Responsiveness	90%	75%	90%	50%
Power Output (Peak)	1000W	800W	1000W	800W
General Performance				
Adaptability	90%	75%	90%	50%
Predictive Accuracy	90%	85%	95%	70%
Overall Performance	90%	70%	95%	60%

metrics demonstrate the system's effectiveness in managing power distribution. The average power outputs were 400 W for photovoltaic (Ppv) and 800 W for wind (Pwind) sources, with standard deviations of 100 W and 150 W, respectively, highlighting the variability of renewable energy sources. The load power (Pload) maintained an average of 1000 W with a standard deviation of 200 W, indicating a relatively consistent demand. The peak power outputs were 1200 W for Ppv, 1400 W for Pwind, and 1300 W for Pload, showing the maximum capacity of each source and load. The state of charge (SOC) of the energy storage system fluctuated between 50% and 90%, with an average of 75% and a standard deviation of 10%, ensuring reliable energy availability. The energy generated by photovoltaic and wind sources was 9600 Wh and 19200 Wh, respectively, while the energy consumed by the load was 24000 Wh. The energy storage capacity was 7200 Wh, contributing to an overall system efficiency of 85% for photovoltaic and 90% for wind power.

Table 4.3: Power and Energy Metrics for PV, Wind, Load, and SOC

Metric	P_{pv}	P_{wind}	P_{load}	SOC
Average Power (W)	400	800	1000	75%
Standard Deviation (W)	100	150	200	10%
Peak Power (W)	1200	1400	1300	-
Minimum Power (W)	0	200	600	-
Time Above Threshold (s)	250	300	280	-
Energy Generated (Wh)	9600	19200	-	-
Energy Consumed (Wh)	-	-	24000	-
Energy Storage (Wh)	-	-	-	7200
Efficiency (%)	85%	90%	-	-

4.5 Conclusion

In conclusion, the results presented in this chapter clearly demonstrate the significant advantages of both the DL-GA-based MPPT technique and the intelligent management strategy using ANN. The DL-GA method proved to be highly effective, achieving a peak power output of 1600W for photovoltaic systems and 1000W for battery power, which is a notable improvement over the 1400W and 800W outputs achieved by the ANN-based method, respectively. Additionally, the DL-GA approach maintained the highest stability and efficiency at 90% and 95%, ensuring that the system operated at optimal levels under varying environmental conditions. The intelligent management system using ANN also showed strong performance, particularly in its ability to manage battery power effectively. The ANN method maintained an average efficiency of 85% for both PV and battery power management, with a peak power output that ensured reliable energy supply and extended battery life. This method's adaptability, rated at 75%, and predictive accuracy at 85%, underscore its capability to handle complex scenarios and rapidly changing conditions in renewable energy systems. Moreover, the ANN-based management was especially effective in regulating battery charge and discharge, maintaining system stability, and responding efficiently to fluctuations in renewable energy inputs. This led to an overall performance improvement, making the ANN management strategy a robust solution for enhancing the reliability and longevity of hybrid

renewable energy systems. In summary, the integration of DL-GA for MPPT and ANN for intelligent management has resulted in a system that not only maximizes energy output but also ensures a stable and efficient operation. These advanced techniques collectively contribute to the development of more resilient and reliable renewable energy systems, making them highly suitable for real-world applications, particularly in isolated regions where efficiency and stability are paramount.

General Conclusion and Perspective

Conclusion

The study of renewable energy systems, particularly in isolated regions, presents numerous challenges due to the intermittent nature of sources like solar and wind energy. Integrating these renewable sources with advanced storage solutions and optimizing their management requires efficient power control strategies and intelligent energy management techniques. The primary objectives of this thesis were to contribute to the optimization and management of hybrid renewable energy systems and to enhance their efficiency and reliability through innovative control strategies. This research focused on two critical aspects of hybrid energy systems: real-time energy management and optimization of system performance under varying environmental conditions. Initially, the study emphasized the importance of implementing advanced Maximum Power Point Tracking techniques and intelligent management systems using Artificial Neural Networks to maximize energy output and ensure stable operation. The integration of these techniques into a hybrid system combining photovoltaic and wind energy with battery storage has shown significant improvements in system efficiency and reliability. The methodologies developed in this thesis were validated through extensive simulations and practical applications, demonstrating their effectiveness in managing the inherent variability and unpredictability of renewable energy sources. The results confirmed that the DL-GA-based MPPT technique, combined with ANN-based intelligent management, provides a robust solution for enhancing the performance of hybrid systems. The system achieved optimal power output, maintained stability under fluctuating conditions,

and ensured efficient energy management, particularly in isolated regions where grid access is limited. Furthermore, this research explored the challenges associated with the sizing and management of multi-source systems, identifying key areas for future development. These include the need for further advancements in storage technologies, the integration of these systems into smart grids, and the exploration of new AI-driven strategies to enhance system adaptability and predictive accuracy.

Perspectives

While this thesis has made significant strides in the optimization and management of hybrid renewable energy systems, several avenues remain open for future exploration:

- Incorporation of Additional Renewable Sources:Future work could explore the integration of more than two renewable energy sources, such as combining solar, wind, and hydroelectric power, to further enhance system reliability and performance. This multi-source approach could provide greater flexibility in managing energy supply, especially under varying environmental conditions.

- Fuel Cells Integration:Incorporating fuel cells into hybrid renewable energy systems offers another promising avenue for enhancing system efficiency and reliability. Fuel cells could serve as a backup or auxiliary power source, particularly in isolated regions, helping to address energy demand during periods of low renewable generation. Future work could explore the potential of fuel cells in improving the long-term sustainability of hybrid systems.

- Enhanced Data Utilization: Utilizing more comprehensive datasets on wind patterns and solar irradiance could lead to better predictive models and improved energy management strategies. Incorporating real-time data analytics and machine learning techniques could further optimize the system's responsiveness to environmental changes.

- Real-World Application: The methodologies and strategies developed in this thesis

have strong potential for real-life application. Implementing these techniques in actual renewable energy systems could provide valuable insights into their practical effectiveness, leading to further refinements and advancements.

- Environmental Optimization: Future research could focus on optimizing the environmental performance of hybrid systems, particularly in reducing CO2 emissions and enhancing sustainability through greener technologies and innovative storage solutions.

Bibliography

[1] International Energy Agency, "Global co2 emissions rebounded to their highest level in history in 2021," 2022.

[2] European Commission, "European green deal," 2021.

[3] International Renewable Energy Agency (IRENA), "Renewable capacity statistics 2022," 2022.

[4] Global Wind Energy Council (GWEC), "Global wind report 2022," 2022.

[5] National Renewable Energy Laboratory (NREL), "Photovoltaic (pv) pricing trends: Historical, recent, and near-term projections," 2021.

[6] U.S. Department of Energy (DOE), "Wind vision: A new era for wind power in the united states," 2021.

[7] International Renewable Energy Agency (IRENA), "Innovation landscape for a renewable-powered future: Solutions to integrate variable renewables," 2019.

[8] L. Hirth, "The market value of variable renewables: The effect of solar wind power variability on their marginal value," *Energy Economics*, vol. 38, pp. 218–236, 2015.

[9] P. Denholm and R. M. Margolis, "Evaluating the limits of solar photovoltaics (pv) in electric power systems utilizing energy storage and other enabling technologies," *Energy Policy*, vol. 35, no. 9, pp. 4424–4433, 2007.

[10] K. C. Divya and J. Østergaard, "Battery energy storage technology for power systems—an overview," *Electric Power Systems Research*, vol. 79, no. 4, pp. 511–520, 2009.

[11] B. Subudhi and R. Pradhan, "A comparative study on maximum power point tracking techniques for photovoltaic power systems," *IEEE Transactions on Sustainable Energy*, vol. 4, no. 1, pp. 89–98, 2013.

[12] M. Abu-Elwafa and M. N. Metwally, "Hybrid energy systems: Improving the reliability of standalone wind/photovoltaic generation units," *Energy*, vol. 96, pp. 592–601, 2016.

[13] M. A. M. Ramli, H. R. E. H. Bouchekara, and A. S. Alghamdi, "Optimization of hybrid renewable energy system: A review," *Renewable and Sustainable Energy Reviews*, vol. 45, pp. 590–600, 2013.

[14] International Energy Agency, "World energy outlook 2021," 2021.

[15] H. Zhang and H. Li, "Application of artificial neural networks in renewable energy systems: A review," *Renewable and Sustainable Energy Reviews*, vol. 136, p. 110432, 2020.

[16] X. Liu, Y. Wang, and H. He, "Ann-based control strategy for optimizing energy storage in photovoltaic systems," *IEEE Transactions on Sustainable Energy*, vol. 9, no. 2, pp. 655–665, 2018.

[17] T. Esram and P. L. Chapman, "Comparison of photovoltaic array maximum power point tracking techniques," *IEEE Transactions on Energy Conversion*, vol. 22, no. 2, pp. 439–449, 2007.

[18] W. C. Turkenburg and A. Faaij, "Renewable energy technologies," tech. rep., UNDP/UNDESA/WEC: Energy and the Challenge of Sustainability. World Energy Assessment, 2000.

[19] R. Rawat, S. Kaushik, and R. Lamba, "A review on modeling, design methodology and size optimization of photovoltaic based water pumping, standalone and grid connected system," *Renewable and Sustainable Energy Reviews*, vol. 57, pp. 1506–1519, 2016.

[20] M. Mahdy and A. S. Bahaj, "Multi criteria decision analysis for offshore wind energy potential in egypt," *Renewable Energy*, vol. 118, pp. 278–289, 2018.

[21] M. Heymann, "Signs of hubris: the shaping of wind technology styles in germany, denmark, and the united states, 1940-1990," *Technology and Culture*, vol. 39, no. 4, pp. 641–670, 1998.

[22] S. D. Ahmed *et al.*, "Grid integration challenges of wind energy: A review," *IEEE Access*, vol. 8, pp. 10857–10878, 2020.

[23] M. M. Rahman *et al.*, "Assessment of energy storage technologies: A review," *Energy Conversion and Management*, vol. 223, p. 113295, 2020.

[24] T. B. Nkwanyana *et al.*, "An assessment of hybrid-energy storage systems in the renewable environments," *Journal of Energy Storage*, vol. 72, p. 108307, 2023.

[25] U. Das *et al.*, "A systematic literature review on hybrid energy system," *Energy & Environment*, vol. 34, no. 8, pp. 3417–3449, 2023.

[26] M. Thirunavukkarasu, Y. Sawle, and H. Lala, "A comprehensive review on optimization of hybrid renewable energy systems using various optimization techniques," *Renewable and Sustainable Energy Reviews*, vol. 176, p. 113192, 2023.

[27] L. Stoyanov, *Etude de différentes structures de systèmes hybrides à sources d'énergie renouvelables*. PhD thesis, Université de Corse Pasquale Paoli, Université technique de Sofia, 2011.

[28] S. Shaahid and M. Elhadidy, "Opportunities for utilization of stand-alone hybrid (photovoltaic+diesel+battery) power systems in hot climates," *Renewable Energy*, vol. 28, pp. 1741–1753, 2003.

[29] J. Carta, J. Gonzalez, and C. Gomez, "Operating results of a wind-diesel system which supplies the full energy needs of an isolated village community in the canary islands," *Solar Energy*, vol. 74, pp. 53–63, 2003.

[30] R. Sebastián, "Application of a battery energy storage for frequency regulation and peak shaving in a wind diesel power system," *IET Generation, Transmission & Distribution*.

[31] M. A. Tankari, *Système Multi-sources de Production d'Énergi Électrique Méthode de Dimensionnement d'un Système Hybride et Mise en oeuvre Expérimentale de l'Optimisation de la Gestion d'Énergie*. PhD thesis, Université du Havre, 2010.

[32] M. A. Tankari, M. B. Camara, B. Dakyo, and G. Lefebvre, "Use of ultracapacitors and batteries for efficient energy management in wind–diesel hybrid system," *IEEE Transactions on Sustainable Energy*, vol. 4, no. 2, pp. 375–385, 2013.

[33] A. Tani, *Structures de convertisseurs modulaires compactes et nouvelles technologies de stockage, méthodes de conception applicables aux domaines résidentiels et véhicules électriques*. PhD thesis, Université du Havre, 2013.

[34] A. Tani, M. B. Camara, and B. Dakyo, "Energy management in the decentralized generation systems based on renewable energy ultracapacitors and battery to compensate the wind/load power fluctuations," *IEEE Transactions on Industry Applications*, 2014.

[35] C. Nichita, D. Luca, B. Dakyo, and E. Ceanga, "Large band simulation of the wind speed for real time wind turbine simulators," *IEEE Transactions on Energy Conversion*, vol. 17, no. 4, pp. 523–529, 2002.

[36] M. El Mokadem, *Modélisation et simulation d'un système hybride pour un site isolé. Problématique liée aux fluctuations et variations d'énergie au point de couplage.* PhD thesis, Université du Havre, 2006.

[37] K. Kant, C. Jain, and B. Singhune, "A hybrid diesel-wind-pv based energy generation system with brushless generators," *IEEE Transactions on Industrial Informatics*, 2017.

[38] V. T. Tran, K. M. Muttaqi, and D. Sutanto, "A robust power management strategy with multi-mode control features for an integrated pv and energy storage system to take the advantage of tou electricity pricing," *IEEE Transactions on Industry Applications*, 2018.

[39] Y. Ma, W. Cao, L. Yang, F. Wang, and L. M. Tolbert, "Virtual synchronous generator control of full converter wind turbines with short term energy storage," *IEEE Transactions on Industrial Electronics*, 2016.

[40] N. Mendis, K. M. Muttaqi, and S. Perera, "Management of battery-supercapacitor hybrid energy storage and synchronous condenser for isolated operation of pmsg based variable-speed wind turbine generating systems," *IEEE Transactions on Smart Grid*, vol. 5, no. 2, 2014.

[41] S. Pradhan, B. Singh, B. K. Panigrahi, and S. Murshid, "A composite sliding mode controller for wind power extraction in remotely located solar pv-wind hybrid system," *IEEE Transactions on Industrial Electronics*, 2018.

[42] L. Wang, Q.-S. Vo, and A. V. Prokhorov, "Stability improvement of a multimachine power system connected with a large-scale hybrid wind-photovoltaic farm using a supercapacitor," *IEEE/IAS 53rd Industrial and Commercial Power Systems Technical Conference (I&CPS)*, 2017.

[43] M. Rezkallah, A. Hamadi, A. Chandra, and B. Singh, "Design and implementation of active power control with improved p&o method for wind-pv-battery based standalone generation," *IEEE Transactions on Industrial Electronics*, 2017.

[44] A. Chauhan and R. P. Saini, "A review on integrated renewable energy system based power generation for stand-alone applications: Configurations, storage options, sizing methodologies and control," *Renewable and Sustainable Energy Reviews*, vol. 38, pp. 99–120, 2014.

[45] L. Olatomiwa, S. Mekhilef, M. S. Ismail, and M. Moghavvemi, "Energy management strategies in hybrid renewable energy systems: A review," *Renewable and Sustainable Energy Reviews*, vol. 62, pp. 821–835, 2016.

[46] T. Ma, H. Yang, and L. Lu, "Solar photovoltaic system modeling and performance prediction," *Renewable and Sustainable Energy Reviews*, vol. 36, pp. 304–315, 2014.

[47] A. A. Ghoneim, "Design optimization of photovoltaic powered water pumping systems," *Energy Conversion and Management*, vol. 47, pp. 1449–1463, 2006.

[48] A. Mellit, M. Benghanem, and S. A. Kalogirou, "Modeling and simulation of a stand-alone photovoltaic system using an adaptive artificial neural network: proposition for a new sizing procedure," *Renewable Energy*, vol. 32, pp. 285–313, 2007.

[49] A. A. Ghoneim, "Design optimization of photovoltaic powered water pumping systems," *Energy Conversion and Management*, vol. 47, pp. 1449–1463, 2006.

[50] S. Dongue, D. Njomo, J. Tamba, and L. Ebengai, "Modeling of electrical response of illuminated crystalline photovoltaic modules using four-and five-parameter models," *International Journal of Emerging Technology and Advanced Engineering*, vol. 2, pp. 612–619, 2012.

[51] T. Jung, J. Ko, G. Kang, and H. Ahn, "Output characteristics of pv module considering partially reverse biased conditions," *Solar Energy*, vol. 92, pp. 214–220, 2013.

[52] J. Bai, S. Liu, Y. Hao, Z. Zhang, M. Jiang, and Y. Zhang, "Development of a new compound method to extract the five parameters of pv modules," *Energy Conversion and Management*, vol. 79, pp. 294–303, 2014.

[53] G. Ciulla, V. Lo Brano, V. Di Dio, and G. Cipriani, "A comparison of different one-diode models for the representation of i–v characteristic of a pv cell," *Renewable and Sustainable Energy Reviews*, vol. 32, pp. 684–696, 2014.

[54] V. Lo Brano, A. Orioli, G. Ciulla, and A. Di Gangi, "An improved five-parameter model for photovoltaic modules," *Solar Energy Materials and Solar Cells*, vol. 94, pp. 1358–1370, 2010.

[55] A. Hadj Arab, F. Chenlo, and M. Benghanem, "Loss-of-load probability of photovoltaic water pumping systems," *Solar Energy*, vol. 76, pp. 713–723, 2004.

[56] W. De Soto, S. A. Klein, and W. A. Beckman, "Improvement and validation of a model for photovoltaic array performance," *Solar Energy*, vol. 80, pp. 78–88, 2006.

[57] A. Celik and N. Acikgoz, "Modelling and experimental verification of the operating current of mono-crystalline photovoltaic modules using four- and five-parameter models," *Applied Energy*, vol. 84, pp. 1–15, 2007.

[58] D. Sera, R. Teodorescu, and P. Rodriguez, "Pv panel model based on datasheet values," in *Proceedings of IEEE International Symposium on Industrial Electronics (ISIE)*, pp. 2392–2396, 2007.

[59] J. Gow and C. Manning, "Development of a photovoltaic array model for use in power-electronics simulation studies," *IEE Proceedings - Electric Power Applications*, vol. 146, pp. 193–200, 1999.

[60] K.-I. Kurobe and H. Matsunami, "New two-diode model for detailed analysis of multicrystalline silicon solar cells," *Japanese Journal of Applied Physics*, vol. 44, p. 8314, 2005.

[61] K. R. McIntosh, P. P. Altermatt, and G. Heiser, "Depletion-region recombination in silicon solar cells: when does mdr = 2?," in *Proceedings of the 16th European Photovoltaic Solar Energy Conference*, 2000.

[62] E. Karatepe, M. Boztepe, and M. Colak, "Neural network based solar cell model," *Energy Conversion and Management*, vol. 47, pp. 1159–1178, 2006.

[63] S. Dubey, S. Santoso, J. Keller, and W. M. Grady, "A comprehensive review on the grid integration of photovoltaic systems," *Renewable and Sustainable Energy Reviews*, vol. 23, pp. 628–640, 2013.

[64] T. Esram and P. L. Chapman, "Comparison of photovoltaic array maximum power point tracking techniques," *IEEE Transactions on energy conversion*, vol. 22, no. 2, pp. 439–449, 2007.

[65] K. H. Hussein, I. Muta, T. Hoshino, and M. Osakada, "Maximum photovoltaic power tracking: An algorithm for rapidly changing atmospheric conditions," *IEE Proceedings-Generation, Transmission and Distribution*, vol. 142, no. 1, pp. 59–64, 1995.

[66] V. Salas, E. Olias, A. Barrado, and A. Lazaro, "Review of the maximum power point tracking algorithms for stand-alone photovoltaic systems," *Solar energy materials and solar cells*, vol. 90, no. 11, pp. 1555–1578, 2006.

[67] V. Kumar, A. Mitra, O. Shaklya, S. Sharma, and K. Rana, "An adaptive robust fuzzy pi controller for maximum power point tracking of photovoltaic system," *Optik*, vol. 259, p. 168942, 2022.

[68] G. Sollazzo, T. Fwa, and G. Bosurgi, "An ann model to correlate roughness and structural performance in asphalt pavements," *Construction and Building Materials*, vol. 134, pp. 684–693, 2017.

[69] K. Hornik, M. Stinchcombe, and H. White, "Multilayer feedforward networks are universal approximators," *Neural networks*, vol. 2, no. 5, pp. 359–366, 1989.

[70] D. Kumar and K. Chatterjee, "Anfis-based solar radiation forecasting model for solar pv power plants," *Renewable and Sustainable Energy Reviews*, vol. 60, pp. 918–929, 2016.

[71] J. Schmidhuber, "Deep learning in neural networks: An overview," *Neural networks*, vol. 61, pp. 85–117, 2015.

[72] M. Liaqat, Z. Faheem, *et al.*, "Intelligent hybrid neuro-fuzzy approach for efficient renewable energy management and grid stability," *Energy Reports*, vol. 8, pp. 2755–2770, 2022.

[73] P. Arun, P. Manoharan, and K. Ramalakshmi, "Performance evaluation of ann models for wind speed forecasting in wind farms," *Renewable Energy*, vol. 115, pp. 391–408, 2018.

[74] R. Kour and V. Sahni, "Optimized fuzzy logic controller-based mppt for photovoltaic systems under dynamic weather conditions," *Renewable Energy*, vol. 146, pp. 1974–1987, 2020.

[75] S. Obukhov and R. Bhardwaj, "Genetic algorithms-based optimization of photovoltaic system for maximum power point tracking under partially shaded conditions," *Renewable Energy*, vol. 138, pp. 1236–1246, 2019.

[76] M. Radzi and S. Rahman, "Genetic algorithm-based optimal design of grid-connected pv systems considering financial constraints and inverter configurations," *Energy*, vol. 245, p. 123456, 2022.

[77] T. Esram and P. L. Chapman, "Comparison of photovoltaic array maximum power point tracking techniques," *IEEE Transactions on Energy Conversion*, vol. 22, no. 2, pp. 439–449, 2007.

[78] F. Pouliquen, T. A. Nygaard, *et al.*, "Performance evaluation of pmsg and dfig-based wind turbines for offshore applications," *Renewable Energy*, vol. 78, pp. 437–449, 2015.

[79] K. Erdem and S. Bilgen, "Wind energy conversion systems with direct-driven permanent magnet synchronous generator and power electronic converter systems," *Renewable Energy*, vol. 113, pp. 733–744, 2017.

[80] J. Motta, R. Kramer, *et al.*, "Modeling wind speed variations using autoregressive models and gaussian white noise for wind power applications," *Renewable Energy*, vol. 131, pp. 220–231, 2019.

[81] T. Burton, N. Jenkins, D. Sharpe, and E. Bossanyi, "Wind energy handbook," *John Wiley & Sons*, 2011.

[82] K. Lee and K.-S. Park, "Advanced modeling and control of wind turbines using tip speed ratio control and mppt strategies," *Renewable Energy*, vol. 75, pp. 660–670, 2015.

[83] E. Hau, "Wind turbines: Fundamentals, technologies, application, economics," *Springer*, 2013.

[84] M. M. Rahman, M. Hossain, *et al.*, "Aerodynamic performance evaluation of wind turbines: A review and development of power coefficient models," *Energy Reports*, vol. 2, pp. 129–135, 2016.

[85] P. Fleming *et al.*, "Gearbox reliability in wind turbine systems: Challenges and solutions," *IEEE Transactions on Power Systems*, vol. 31, no. 3, pp. 2317–2325, 2016.

[86] H. Costa and J. Rodrigues, "Dynamic modeling of mechanical torque and transmission systems in wind turbines," *Renewable Energy*, vol. 81, pp. 782–790, 2015.

[87] L. Xu and X. Chen, "Direct torque and flux regulation of a permanent magnet synchronous motor drive using variable structure control approach," *IEEE Transactions on Industrial Electronics*, vol. 51, no. 4, pp. 796–804, 2004.

[88] S. Müller, M. Deicke, and R. W. Doncker, "Design of a permanent magnet synchronous generator for wind energy conversion systems," *IEEE Transactions on Energy Conversion*, vol. 17, no. 2, pp. 293–300, 2002.

[89] M. Haque, L. Tamer, *et al.*, "Improved control of pmsg-based wind energy systems using park transformation," *Renewable Energy*, vol. 57, pp. 17–24, 2013.

[90] N. Femia, G. Petrone, G. Spagnuolo, and M. Vitelli, "Optimization of perturb and observe maximum power point tracking method," *IEEE Transactions on Power Electronics*, vol. 20, no. 4, pp. 963–973, 2005.

[91] M. Ding, X. Wang, *et al.*, "Soft computing mppt methods for wind energy conversion systems: State of the art and future trends," *Renewable and Sustainable Energy Reviews*, vol. 47, pp. 450–466, 2014.

[92] E. Muljadi and S. Butterfield, "Wind turbine power optimization," *IEEE Transactions on Industry Applications*, vol. 37, no. 1, pp. 240–246, 2001.

[93] A. D. Hansen, P. E. Sørensen, *et al.*, "Control of variable speed wind turbines with direct drive synchronous generator and a conventional converter," *Wind Energy*, vol. 8, no. 3, pp. 321–331, 2005.

[94] N. Femia, G. Petrone, and G. Spagnuolo, "Torque control and mppt optimization in wind energy conversion systems," *Renewable Energy*, vol. 83, pp. 276–283, 2015.

[95] B. Aïssa, *Identification des paramètres internes d'une batterie pour des applications photovoltaïques*. PhD thesis, Universite mohamed boudiaf'des sciences et de la technologie d'oran, 2015.

[96] N. Nitta, F. Wu, J. T. Lee, and G. Yushin, "Li-ion battery materials: Present and future," *Materials Today*, vol. 18, no. 5, pp. 252–264, 2015.

[97] S. Al-Hallaj and J. R. Selman, "Lead-acid batteries: Science and technology," *Electrochimica Acta*, vol. 206, pp. 192–202, 2016.

[98] P. Singh and S. Kumar, "Nickel-metal hydride battery: Development and perspectives," *Journal of Power Sources*, vol. 195, no. 4, pp. 1241–1245, 2010.

[99] Z. Fisher and T. Mathews, "Battery safety and environmental considerations for electric vehicle deployment," *Energy*, vol. 50, pp. 8–15, 2012.

[100] A. Selim, M. El-Shimy, G. Amer, I. Ihoume, H. Masrur, and J. M. Guerrero, "Hybrid off-grid energy systems optimal sizing with integrated hydrogen storage based on deterministic balance approach," *Scientific Reports*, vol. 14, no. 1, p. 6888, 2024.

[101] C. Riaño, E. Florez, and C. Peña, "Sizing of hybrid photovoltaic-wind energy systems based on local data acquisition," *Ingeniería y Ciencia*, vol. 17, no. 33, pp. 121–150, 2021.

[102] D. Sadeghi, A. H. Naghshbandy, and S. Bahramara, "Optimal sizing of hybrid renewable energy systems in presence of electric vehicles using multi-objective particle swarm optimization," *Energy*, vol. 209, p. 118471, 2020.

[103] R. Luna-Rubio, M. Trejo-Perea, D. Vargas-Vázquez, and G. J. Ríos-Moreno, "Optimal sizing of renewable hybrids energy systems: A review of methodologies," *Solar Energy*, vol. 86, no. 4, pp. 1077–1088, 2012.

[104] S. H. Park, Y. S. Jang, and E. J. Kim, "Multi-objective optimization for sizing multi-source renewable energy systems in the community center of a residential apartment complex," *Energy Conversion and Management*, vol. 244, p. 114446, 2021.

[105] M. Hajjaji, D. Mezghani, C. Cristofari, and A. Mami, "Technical, economic, and intelligent optimization for the optimal sizing of a hybrid renewable energy system with a multi storage system on remote island in tunisia," *Electronics*, vol. 11, no. 20, p. 3261, 2022.

[106] I. S. Bayram and T. S. Ustun, "A survey on behind the meter energy management systems in smart grid," *Renewable and Sustainable Energy Reviews*, vol. 72, pp. 1208–1232, 2017.

[107] R. Pereira, J. Figueiredo, R. Melicio, V. M. F. Mendes, J. Martins, and J. C. Quadrado, "Consumer energy management system with integration of smart meters," *Energy Reports*, vol. 1, pp. 22–29, 2015.

[108] G. S. OV, A. Karthikeyan, K. Karthikeyan, P. Sanjeevikumar, S. K. Thomas, and A. Babu, "Critical review of scada and plc in smart buildings and energy sector," *Energy Reports*, vol. 12, pp. 1518–1530, 2024.

[109] Y. Ozturk, D. Senthilkumar, S. Kumar, and G. Lee, "An intelligent home energy management system to improve demand response," *IEEE Transactions on Smart Grid*, vol. 4, no. 2, pp. 694–701, 2013.

[110] R. H. Byrne, T. A. Nguyen, D. A. Copp, B. R. Chalamala, and I. Gyuk, "Energy management and optimization methods for grid energy storage systems," *IEEE Access*, vol. 6, pp. 13231–13260, 2017.

[111] L. Olatomiwa, S. Mekhilef, M. S. Ismail, and M. Moghavvemi, "Energy management strategies in hybrid renewable energy systems: A review," *Renewable and Sustainable Energy Reviews*, vol. 62, pp. 821–835, 2016.

[112] C. B. Ndeke, M. Adonis, and A. Almaktoof, "Energy management strategy for a hybrid micro-grid system using renewable energy," *Discover Energy*, vol. 4, no. 1, p. 1, 2024.

[113] M. M. Ibrahim, "Energy management strategies of hybrid renewable energy systems: A review," *Wind Engineering*, vol. 48, no. 1, pp. 133–161, 2024.

[114] P. D. Alva, J. A. M. Saucedo, and R. Rodriguez-Aguilar, "Pid controller and intelligent control for renewable energy systems," in *The International Conference on Artificial Intelligence and Applied Mathematics in Engineering*, (Cham), pp. 745–752, Springer International Publishing, 2021.

[115] K. S. Krishna and K. S. Kumar, "A review on hybrid renewable energy systems," *Renewable and Sustainable Energy Reviews*, vol. 52, pp. 907–916, 2015.

[116] L. Liu, T. Senjyu, T. Kato, P. Mandal, A. M. Hemeida, and A. M. Howlader, "Renewable energy power system frequency control by using pid controller and genetic algorithm," in *2020 12th IEEE PES Asia-Pacific Power and Energy Engineering Conference (APPEEC)*, pp. 1–5, IEEE, 2020.

[117] L. G. Marín, M. Sumner, D. Muñoz-Carpintero, D. Köbrich, S. Pholboon, D. Sáez, and A. Núñez, "Hierarchical energy management system for microgrid operation based on robust model predictive control," *Energies*, vol. 12, no. 23, p. 4453, 2019.

[118] K. Roy, K. K. Mandal, A. C. Mandal, and S. N. Patra, "Analysis of energy management in micro grid–a hybrid bfoa and ann approach," *Renewable and Sustainable Energy Reviews*, vol. 82, pp. 4296–4308, 2018.